Contents

Contents ..... *i*

List of Figures ..... *iii*

List of Tables ..... *vii*

Nomenclature ..... *ix*

Introduction *1*

1 ..... *7*

Theoretical background *7*

1.1. Simple tank response to a step input **8**

1.2. Simple tank response to a constant heat flux exchange **9**

1.3. Multiple tank response to a step input **11**

1.4. Multiple tank response to constant heat flux exchange **13**

2 ..... *15*

Overview on groundwater thermal storage systems for HVAC *15*

3 ..... *25*

Matlab Simulation *25*

3.1. Purposes **25**

3.2. Complete Mixing, Multi-connected series pattern and piston flow models **26**

3.3. Initial Data **29**

3.4. Matlab Routine Structure **31**

3.5. Results **33**

3.5.1. Simulation of the summer critical day 34

3.5.2. Simulation of the winter critical day 39

3.6. Convergence between piston flow and multi connected tanks **42**

3.7. Thermal storage feasibility 52
3.8. All year long simulation 53
3.9. Model Validation 56
4 63
Exergy Analysis 63
4.1. Heat exchanger exergy model 63
4.2. Tank exergy model 64
4.3. Exergy model of return temperature control mixing node 65
4.4. Exergy analysis results 66
5 79
CFD Analysis 79
5.1. CFD Model Assumptions 79
5.2. Mesh, Solver and Boundary Conditions 83
5.3. User Defined Functions (UD) implementation 86
5.4. Results 89
Conclusions 107
References 111

List of Figures

Figure 1 - Typical thermal storage system for HVAC services 3
Figure 2 - – Nakahara regulation recommendations 4
Figure 3 – Simple tank storage process.....8
Figure 4 – Constant heat flux exchange layout 10
Figure 5 –Constant heat flux response at different temperature ratios a. 11
Figure 6 – Five sub-tanks multiple tank step response.....12
Figure 7 – Multiple connected tank subjected to constant heat flux exchange control. 13
Figure 8 – Office buildings complex cooling load pattern with respect to groundwater limited cooling capacity during the critical summer day. 16
Figure 9 – Groundwater thermal storage strategy for an office buildings cooling: HVAC operating phase 17
Figure 10 – Groundwater thermal storage strategy for office buildings cooling: temperature restoration phase 17
Figure 11 – Balance between heat to be stored and available energy absorption for thermal storage tank temperature restoration. 18
Figure 12 – Thermal storage system combined to VRV®. 20
Figure 13 – System regulation strategy. 21
Figure 14 – Initial cooling load is fulfilled by GW capability. 22
Figure 15 – Groundwater thermal storage normal duty. 23
Figure 16 – Restoration on duty. 23
Figure 17 – Restoration, fully heat exchange. 24
Figure 18 – Restoration, heat exchange saturated 24
Figure 19 – Piston flow model assumptions. 27
Figure 20 – Cooling loads. 29
Figure 21 – Heating loads. 30
Figure 22 – Matlab program structure. 32
Figure 23 – Sub tanks conventional numerical order. 33
Figure 24 –Tank average temperature time dependant profile: comparison between simple tank performance towards 20 multi connected sub tanks, under complete mixing assumption. 34
Figure 25 –Multi connected tank 20 sub-tanks temperature profiles and overlain storage cycle phases (see Figure 14to Figure 18): 35
Figure 26 – Comparison between simple tank and 20 multi connected sub tanks about heat flux exchanged either by the tank than by ground water during the operation phase. 36
Figure 27 – Comparison between simple tank and 20 multi connected sub tanks about heat rejection rates under same cooling load conditions. 37

Figure 28 – Comparison between simple tank and 20 multi connected sub tanks about electrical power consumption under same cooling load conditions. 37
Figure 29 – Comparison between simple tank and 20 multi connected sub tanks about flow rate through heat exchanger, crossing flow rate through the tank, by pass flow rate and GW flow rate directly entering the tank. 38
Figure 30 – Comparison between simple tank and 20 multi connected sub tanks about restoration phase. 39
Figure 31 – Comparison between simple tank and 10 multi connected sub tanks in the winter critical day. 40
Figure 32 – Comparison between simple tank and 10 multi connected sub tanks about flow rates through heat exchanger. 41
Figure 33 – Absorbed/Rejected heat fluxes against heating/cooling loads. 41
Figure 34 – Comparison between simple tank and 10 multi connected sub tanks about heat fluxes exchanged either by the tank than by groundwater during the system operation. 42
Figure 35 – Piston flow effects on storage efficiency. 43
Figure 36 – Convergence of the first sub tank temperature profile. 44
Figure 37 – Convergence of the second last sub tank temperature profile. 45
Figure 38 – Convergence of the last sub tank temperature profile. 45
Figure 39 – Flows chromatic correspondence between a piston flow tank system and a multi-connected tank one. 46
Figure 40 – Convergence between multi connected (dashed lines) and piston flow models: temperatures profiles (solid line) – operation phase. 47
Figure 41 – Convergence between multi connected and piston flow models: flow rates profiles - operation phase. 48
Figure 42 –Restoration period and average COP surfaces related to global volume V and sub-tanks number. 49
Figure 43 – Convergence between multi connected and piston flow models: restoration period 50
Figure 44 – Convergence between multi connected and piston flow models: daily average COP 50
Figure 45 – Convergence between multi connected and piston flow models: 51
Figure 46 – Feasibility field for an office building GW thermal storage system conditioned by VRV® - (2% tolerance restoration time) 53
Figure 47 – Typical weeks temperature profiles for simple tank systems summer months . 55
Figure 48 – Comparison between a 20 sub-tanks multi-connected system and a simple tank system: annual electrical energy consumption. 55
Figure 49 – Validation system. 57
Figure 50 – Validation exercise: cooling loads, generator capacity and schedule, significant temperature profiles –Nakahara results 58
Figure 51 – Validation exercise: cooling loads, generator capacity and schedule, significant temperature profiles –Matlab results 59
Figure 52 – Validation exercise: spatial temperature profiles at significant operation hours: Nakahara results. 60
Figure 53 – Validation exercise: spatial temperature profiles match at significant operation hours Matlab results. 61
Figure 54 – Validation exercise: sub tank hourly temperature profiles and collector supply temperature to HVAC. 61
Figure 55 Exergy balance: heat exchanger. 64
Figure 56 Exergy balance: i-th sub-tank. 65
Figure 57 Exergy balance: return temperature mixing node. 66
Figure 58 – Exergy destruction rate within heat exchanger: comparison between simple tank and multi-connected tank under complete mixing assumption 67

Figure 59 – Logarithmic mean temperature difference: comparison between simple tank and multi-connected tank under complete mixing assumption.....67
Figure 60 –20 sub tanks multi-connected tank: exergy destruction rate split for each sub tank.....68
Figure 61 – Total exergy destruction rate within the tank and at the mixing node for return temperature control: comparison between simple tank and multi-connected tank under complete mixing assumption.....69
Figure 62 – Total system exergy destruction rate and its singular contributions. 70
Figure 63 – Heat exchanger exergy destruction at different exchange surfaces. 71
Figure 64 – Multi connected tank exergy destruction at different exchange surfaces. 71
Figure 65 – Return temperature mixing node exergy destruction at different exchange surfaces. 72
Figure 66 – Total exergy destruction rate comparison between the design heat exchanger surface and the improved by 90% one. 73
Figure 67 – First tank and last tank temperature profiles at different exchange surfaces. 73
Figure 68 – Double parallel connected heat exchanger diagram.....74
Figure 69 – Double system total exergy destruction compared to baseline system total exergy destruction rate referred to a heat exchange surface improved by 90%. 75
Figure 70 – Double system HEX exergy destruction compared to baseline system total exergy destruction rate referred to a heat exchange surface improved by 90%. 76
Figure 71 – Double system tank and operation mixings exergy destruction compared to baseline system total exergy destruction rate referred to a heat exchange surface improved by 90%. 77
Figure 72 – Double system exergy destruction at the return temperature mixing node compared to baseline system total exergy destruction rate referred to a heat exchange surface improved by 90%.....77
Figure 73 – 2D tank geometrical model for the simple tank configuration (6m height).....81
Figure 74– CFD calculations carried out through FLUENT.....82
Figure 75 - Unstructured triangular mesh. Simple tank 6m height and multi-connected tank height 3m. 83
Figure 76 – CFD results describing the operation phase process within the tank for the multi-connected configuration 6m height in terms of temperature field. 90
Figure 77 – CFD results describing the typical velocity field during the operation phase process within sub-tanks. 90
Figure 78 – CFD results describing the restoration phase process within the tank for the multi-connected configuration 6m height in terms of temperature field. 91
Figure 79 – CFD results describing the typical velocity field during the restoration phase process within sub-tanks. 91
Figure 80 – CFD results describing the operation phase process within the tank for the multi-connected configuration 3m height in terms of temperature field.. 93
Figure 81 – CFD results describing the velocity field during the operation phase process within sub-tanks. 93
Figure 82 – CFD results describing the restoration phase process within the tank for the multi-connected configuration 3m height in terms of temperature field. 94
Figure 83 – CFD results describing velocity field during the restoration phase process within sub-tanks. 94
Figure 84 – CFD results describing the typical velocity field during the operation phase process within sub-tanks. 95
Figure 85 – Multi connected tank: 6m height, 15 sub-tank, oversized heat exchanger. Comparison between CFD results and one dimension Matlab model.....96
Figure 86 – Multi connected tank: 3m height, 20 sub-tank, design heat exchanger. Comparison between CFD results and one dimension Matlab model.....96

Figure 87 – CFD results describing the operation phase process within the tank for the simple-connected configuration 6m height in terms of temperature field. 98
Figure 88 – CFD results describing the typical velocity field during the operation phase process within the simple tank. 98
Figure 89 – CFD results describing the restoration phase process within the tank for the simple-connected configuration 6m height in terms of temperature field. 99
Figure 90 – CFD results describing the velocity field during the restoration phase process within the simple tank. 100
Figure 91 – CFD results describing the operation phase process within the tank for the simple tank configuration 3m height in terms of temperature field. 101
Figure 92 – CFD results describing the velocity field during the operation phase process within simple tank. 101
Figure 93 – CFD results : restoration phase process for the simple tank configuration 3m height: temperature field. 102
Figure 94 – CFD results describing the restoration phase process within the tank for the simple tank configuration 3m height in terms of velocity field. 103
Figure 95 – Simple tank: 6m height, oversized heat exchanger. Comparison between CFD results and one dimension Matlab model 104
Figure 96 – Simple tank: 3m height, design heat exchanger. Comparison between CFD results and one dimension Matlab model 105
Figure 97 – Comparison between all CFD models investigated. 105

List of Tables

Table 1 – Annual simulation assumptions 54
Table 2 – CFD analysis case studies. 80
Table 3 – Inlet and outlet connection pipes model (see Figure 73).....80
Table 4 – Water density and viscosity properties at the top and bottom temperatures of the operating range.....84
Table 5 Boundary condition assignments for operation phase.....84
Table 6 Boundary condition assignments for operation and restoration phase 85
Table 7 – UDF system for groundwater storage tank modeling and UDFs activation state at operation phase or restoration phase. 87
Table 8 – UDM description.....88

Nomenclature

Scope	Symbol	Unit
Temperature ratio	a	
By-pass	$_{bp}$	
Flow heat capacity	C	kW/K
Specific heat capacity	c	kJ/kg K
Chilled water	CHW	
Heating or cooling coefficient of performance	COP	
Crossing through the tank	$_{Cross}$	
Condenser water	CW	
Parallel double heat exchanger configuration	Double	
Storage efficiency	ε	
Internal Exergy	E	kJ
Exergy destruction rate	$\dot{E}$	kW
First tank	$_{ft}$	
Groundwater	GW	
Groundwater directly entering the tank	GW_d / Direct GW	
Heat exchanger	HEX / HEX - …	
Stored heat	H_{stored}	
Loop-side	$_{Loop}$	
Return temperature control mixing node	M.N.	
Number of sub-tanks	n	
Nusselt Number	Nu	
Piston Flow	P.F.	
Prandtl Number	Pr	
Time	θ	s
Constant delivery flow-rate to the tank	Q	m^3/s

Tank filling period	Θ	s
Heat flux	Φ	kW
Dimensionless time	θ'	
By-pass flow-rate	$Q_{by\text{-}pass}$	m^3/s
Flow-rate crossing through the tank	Q_{cross}	m^3/s
Available groundwater flow-rate	Q_{GW}	m^3/s
k-th inlet flow-rate	q_{in}	m^3/s
Limit temperature time	θ'_{lim}	s
z-th outlet flow-rate	q_{out}	m^3/s
Restoration time	θ_{res}	s
Volumic mass density	ρ	kg/m^3
Load ratio	R_c	
Reynolds Number	Re	
Volume ratio	R_v	
Internal Entropy	S	kJ/K
Sub-tanks	S.T.	
Simple tank	SIMPLE	
Entropy generation rate	$\dot{S}_{irr}$	kW/K
Temperature	t	℃
Dimensionless temperature	t'	
Initial temperature	t_0	℃
Temperature increased by 5% with respect to t_{lim}	$t_{5\%}$	℃
External environment absolute temperature	T_a	K
Tank-side	Tank	
By-pass fllow absolute temperature	T_{bp}	K
First tank absolute temperature	T_{ft}	K
Inlet temperature	t_{in}	℃
Inlet absolute temperature	T_{in}	K
Limit temperature	t_{lim}	℃
Limit absolute temperature	T_{lim}	K
Outlet absolute temperature	T_{out}	K
Outlet temperature	t_{out}	℃
Internal energy	U	kJ
User defined function	UDF	

User defined memory	UDM	
Global tank volume	V	m^3
Control valve	V - …	
Volume refrigerant volume system	VRV	
Average temperature difference thorugh the HVAC coils weighted on cooling loads along the time	Δt_0	
Aspect ratio	R	
Tank height	H	
Tank length	L	

Introduction

In order to provide thermal-hygrometric standard conditions, buildings HVAC systems have to cope with highly unsteady thermal loads. Several renewable energy sources, as well as heat sinks, are either of stochastic nature or limited due to environmental concerns, and this may be a limiting factor for their efficient use. Thermal storage philosophy allows to match energy sources availability with specific buildings demands. At low load hours, building energy requirement falls below the source availability, and energy overflows are stored into a tank. As peak hours occur, the stored amount is released to meet buildings demand.
Underground water basins represent an attractive thermal source for building heating and cooling purposes. As a matter of fact, it assures an almost constant temperature that could facilitate heat rejection for cooling purposes in summer and heat withdrawal for heating purposes in winter enabling the use of reversible water cooled heat pumps at high coefficients of performance.
However, groundwater utilization could imply a relevant menace to underground potable water basins. Therefore, local administrations provide strict regulation in order to grant a proper management of such a resource. Finally groundwater availability for HVAC purposes depends on local plans of managements and on environmental issues.
For example, the case of Milan will be treated in the current work. Because of the high first groundwater level in Milan, groundwater source heat pumps became quite popular. However, local regulations for hydric resources specify strict limits on suction flow-rates and return temperatures. Thermal storage tanks are, thus, needed to allow the use of groundwater for HVAC purposes.

Thermal energy storage systems (TES) are largely discussed in literature and widely applied all over the world.
Yau and Rismanchi [6], Dincer[7][9]and Rosen [7] and Hasnain [8] gave a wide overview on available TES technologies, on the related applications as well on the economic and environmental aspects.
A list of the main applied technology is presented below:

- Water thermal storage
    - Labyrinth
    - Baffle tanks
    - Membrane tanks
    - Series-connected tanks (i.e. multi-connected tanks)
    - Stratified tanks
- Ice storage (ITS)
    - Ice harvesters

  - Ice slurry
  - Encapsulated ice
  - internal/external melt ice-on coil
- Eutectic salts storage

TES are usually interfaced to systems to which they deliver heat or from which they withdraw heat.
The management strategy of the combination tank-system is also an important aspect that should be accurately treated. Yau and Rismanchi [6] and Hasnain [8] distinguished the main strategies of storage systems operation into full storage strategies and partial storage strategies. Nakahara [4] led several experiments on chilled water storage tanks at different HVAC configuration and chillers shifted periods of operation with respect to building demands. Yamaha [5] overviewed several thermal storage technologies for cooling purposes and pointed out some basic principles for control strategy.
Moreover, the most common field of application of such technologies is the building heating and cooling oriented to economically optimize the different electricity fees between night and day, to let it possible to arrange oscillating energy sources , such as solar heat, to the specific building demands as well to optimize chillers size faced to short peak periods of demand and reduce the environmental impact of refrigerant gas amounts within buildings.
TES technologies have been developed in the U.S.A and in Japan and have been deeply studied and described in several ASHRAE papers. Moreover they have been applied as well in several regions of the world as Saudi Arabia, Australia, China, Korea and Europe.
ITS allows the best cool capacity per volume however it could be used only for cooling purposes and could result in worse chillers COP than water storage systems [6].
In the current work, the ice storage strategy, as well as chilled water reservoir, have not been considered because thermal storage is necessary during winter too and the technical requirements for shifting the storage to the side of generator delivery could result in technical and economical concerns. Heat storage will be used at the dissipation side of reversible heat-pumps so that the storage will be fully heated during the summer and slightly cooled during the winter.
Choice, proper sizing and control strategies for thermal water storage are not trivial. As an example, in order to reduce the water tank architectural impact a daily storage and release strategy may be implemented, and a partial storage strategy should be followed.
Proper HVAC control systems, as well as proper tank volume and geometry, are required to obtain high storage performances.
Mixing turbulences have to be avoided.
For that reason, multi-connected storage tanks, as well as stratified tanks, are recommendable.
Stratified tanks have been largely investigated in literature ([10] to [16]) even if usually more attention is paid to the component optimization rather than to the proper sizing process depending on the system to which the tank is coupled. However, stratified tanks need remarkable high spaces to be installed and cannot be obtained from residual spaces rather than simultaneously used for different purposes as multi-connected tanks do. For that reason the multi-connected solution will be investigated in the current treatment.
Thermal storage tanks for HVAC systems have been applying in Japan since 1952 thanks to Yanagimachi [1], who can be named the pioneer of water thermal storage.
He proved economic advantages of the technology, flexibility of operation as well as effectiveness in energy utilization. However, he never provided usable data or tools for proper engineering design. Nakajima [2] gave a more scientific approach to the problem through the introduction of a mixing diffusion model. Nakajima introduced a relation between the number of connected tanks and the temperature diffusion performance along the tank.

Matsudaira and Tanaka [3] simplified the water storage phenomenon by separating a piston flow zone from a mixing zone within the typical tank.
Moreover, they supplied analytical models of the problem, even based on the only case of response under a stepwise thermal input.
Nakahara [4] developed Japanese authors' research by monitoring actual multi-connected storage tanks behavior in combination with true HVAC systems thermal input. Because of both empirical and numerical calculation based approach, Nakahara's paper could be actually considered a fundamental reference for such a technology.
In order to introduce Nakahara experiences, a short introduction on TES for HVAC systems should be done.
Normally two circuit types are provided to interact with thermal storage for HVAC purposes (Figure 1) :

- Primary side: Generator circuit (i.e. chiller primary circuit)
- Secondary side: Air conditioning/Fan-coils circuits

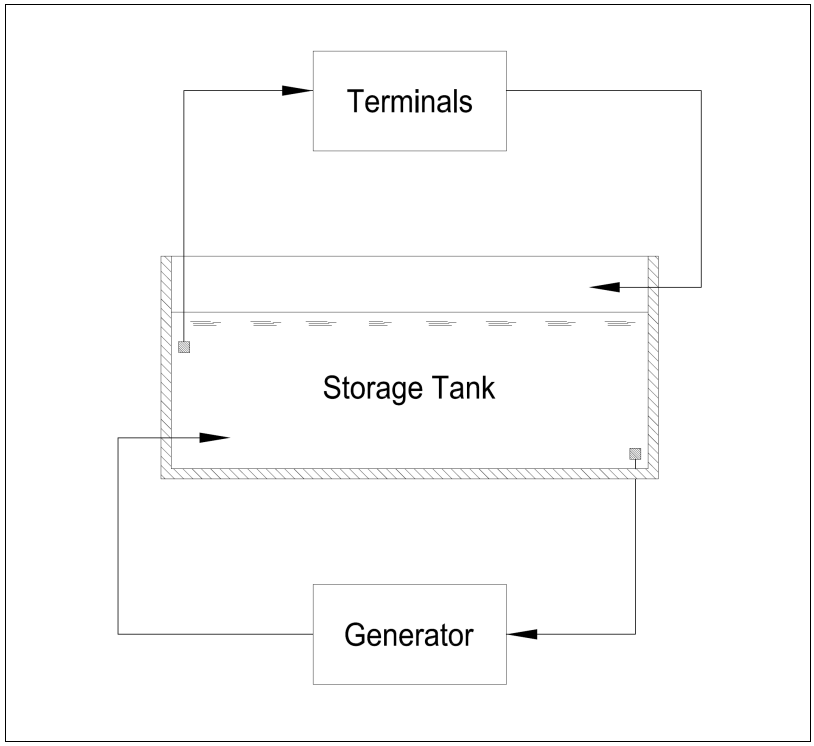

Figure 1 - Typical thermal storage system for HVAC services

Generator charges the thermal storage during low demand periods. On the other hand, as peak loads occur, it aids water storage to satisfy the secondary circuits demands.
Air conditioning and fan-coils circuits discharge storage capacity by energy utilization to keep thermo-hygrometric standards within buildings.
Thermal storage technologies allow generator schedules to be shifted with respect to heat load schemes as well as they permit generator capacity to be undersized compared to peak load demands.
It is notable to observe that thermal storage philosophy is suitable either for heating than cooling purposes, even if normally cooling services present more critical issues.

In accordance with those systems, Nakahara introduces a storage efficiency value which could not be evaluated out of an integrated system context between thermal storage and HVAC circuits.
He detected few significant parameters depending on which actual storage efficiency could vary.
These parameters describes the whole HVAC system specifications, including number of connected tanks, heat load schemes, generator or secondary circuits temperature responses, schedules of operation, HVAC systems regulating strategies and input/output connecting types between circuits and tank.
Finally, Nakahara worked out a numerical calculation algorithm through which proper design process could be followed in order to achieve desired performances.
Inlet temperature to generator should be controlled by a three-valve device at the inlet side in order to minimize water flow through the storage and conserve thermal exchange with the tank.
With respect to air conditioning or fan-coils side, inlet/outlet temperature difference should be kept as large as possible to promote piston flow and inhibit mixing effects (Figure 2).
Moreover, the typical thermal storage HVAC system behaviors are expected to depend on different boundary conditions.

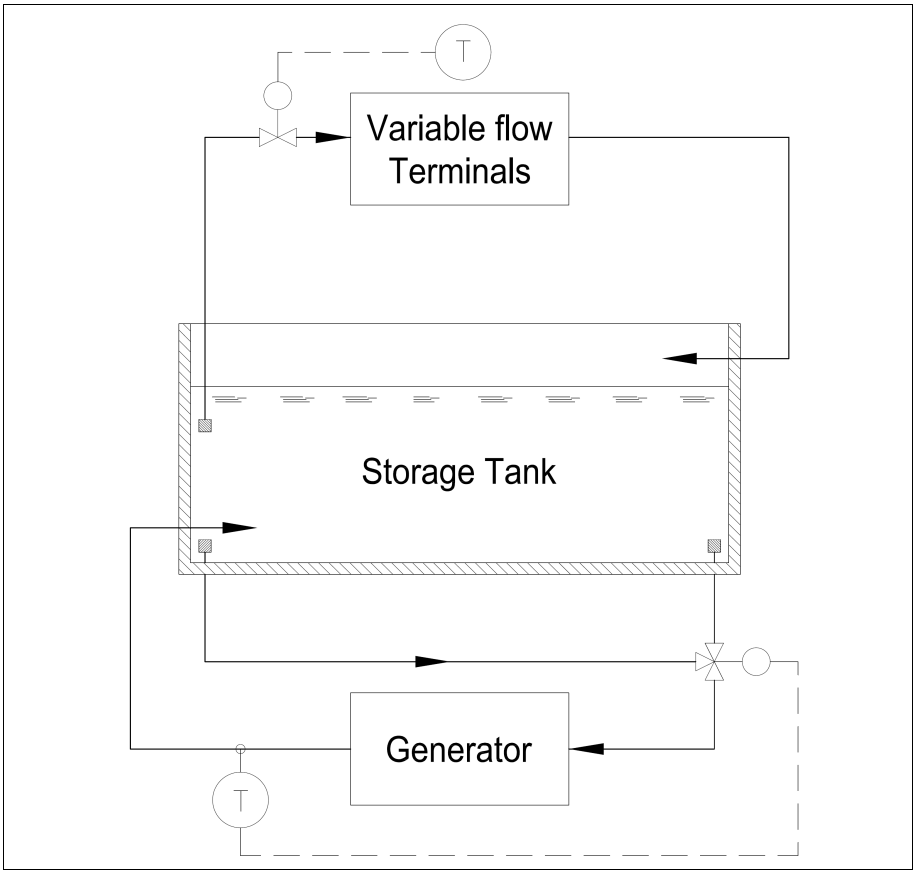

Figure 2 - – Nakahara regulation recommendations

Naki, Shucku and Sagara introduced dimensionless values, as volume ratios or heat capacity ratios, that uniquely identify the configuration of load energy required in relation with the

specific thermal storage capacity as well as generator capacity compared to maximum heat load.
As a result, operating heat load schemes and available generator capacity could directly address to a proper storage design to match desired performances.
Kitano, Iwata and Ishikawa [17] underline the importance of short-circuit flows within connected tanks. Short-circuits could affect storage efficiency because unused water mass is engendered.
A 2D analytical model ,based on mixing model for stratified tank, has been developed to predict thermal field vertical distribution within water storage tanks. Simulation results were compared to experimental data so that a literature reference is available for modeling validation.
Same way Kitano, Iwat, and Ichinose [17] stated that the best connecting holes arrangement is the alternate one, yielding that series of bottom to top connected and top to bottom connected tanks are advisable.

In the present thesis, a Matlab computational routine has been developed to simulate TES for HVAC and quantify heat exchanges between groundwater, the tank and the building. The Matlab code computes the main components size, evaluates heat-flows and electrical power consumptions, and finally define tank temperature profiles at a given day hour during the year.
The tank is here modeled as one-dimensional model through a range of mixing assumptions.
Simulations results point out the importance of avoiding mixing within the storage tank, and identify the optimal number of connected tanks into which a global storage tank may be split.
HVAC system behavior can be investigated for different building sizes and groundwater availabilities.
Significant dimensionless parameters relations have been chosen in order to obtain a more general representation of the problem. The results suggested some quick design criteria.
Even if exergy analysis id recommended by Dincer[7][9], only a few literature references are available for such an approach to the problem.
Thus, an exergy balance analysis has been carried out in order to underline HVAC system regulation influence as well as the significance of selecting proper thermal output terminals oriented to tank storage efficiency optimization.
Finally, a 2D CFD model has been developed within FLUENT to verify the reliability of Matlab assumptions with respect to buoyant flows effect on storage efficiency.
In the case of partitioned tanks, buoyant forces as well as geometrical aspect ratios could affect tank performance.
As a matter of fact, further investigation should be required to detect the proper range of reliability of complete mixing assumption within thermal storage tanks and define a quick one-dimensional model for stratification model.

1

Theoretical background

Mass flows in a fluid domain are carried out by a complexity of interacting driving forces, such as buoyancy, pressure fields, viscous shears. Several different appearances could occur within it, just like turbulent vortexes and fully mixing, stratification and piston flows. Nevertheless, the temperature field within a fluid domain is affected by such a complexity. Actually, it is needed to assume simplified models in order to significantly predict heat storage behaviours within a fluid.

Two opposed assumptions will be considered in the following researches:

- Complete mixing – the maximum level of turbulence and thermal conductivity are to be supposed, so that each fluid element has the same temperature at a given time

- Perfect piston flow – every single fluid element is to be considered as adiabatic and no vortex is expected to take place.

From the temperature field point of view, the complete mixing assumption let a fluid domain to be reduced to a zero dimensional body, being every single element behaviour equal to each other.

Under perfect piston flow hypothesis, no thermal exchange happens, so that thermal transport occurs as long as mass transport does. Moreover the mass transport occurs according to a first-in/first out logic, as tough a serial rigid displacement of masses took place, with no vortexes or short circuits events.

A few analytical models of thermal storage tanks will be explored in the next few paragraphs passing through an increasing level of complexity with the aim to detect

mathematical limits and necessity of numerical approach within water thermal storage systems investigation.

1.1. Simple tank response to a step input

A simple tank is referred to as a non partitioned one. Incompressible flows will be taken into account.

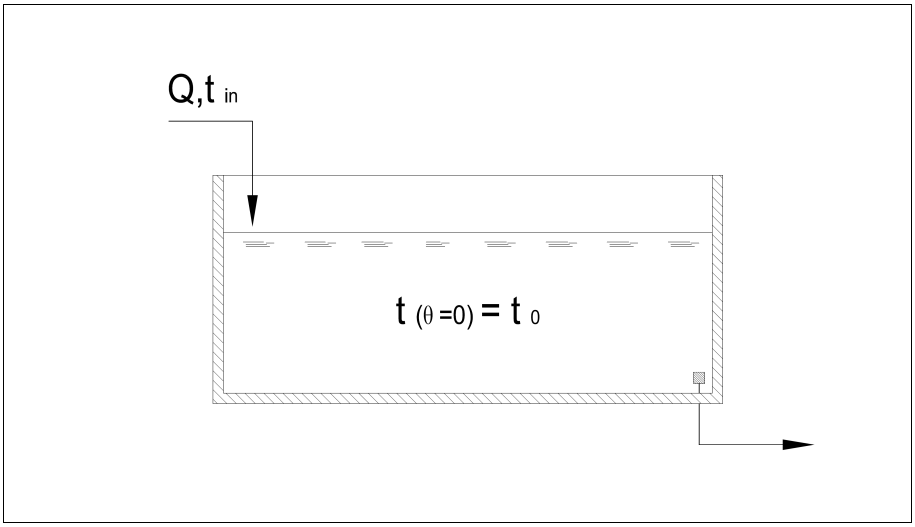

Figure 3 – Simple tank storage process

Under complete mixing assumption, being a simple tank at an initial temperature t_0, its temperature response to a constant flow rate Q at constant inlet temperature t_{in} will be described by the following first order expression:

$t(\theta) = t_0 + (t_{in} - t_0)\left(1 - e^{-\theta\frac{Q}{V}}\right)$	**Eq. 1**

Being the volume filling period defined as follows:

$\Theta = V / Q$	**Eq. 2**

Under perfect piston flow hypothesis, the inlet temperature t_{in} will be reached everywhere into the tank at the end of the volume filling period.
Since it is not possible to identify the thermal global state of the tank at a given moment through a temperature value, internal thermal energy will be used ad a state function.
Thus, the time depending expression of stored heat will be the following linear correlation:

$\Delta U(\theta) = \rho c Q \theta (t_{in} - t_0)$	**Eq. 3**

The piston flow charging process is much more efficient than the complete mixing one because at time $\theta = \Theta$ maximum storable energy ΔU_{MAX} is actually stored.

$\Delta U_{MAX} = \rho c V (t_{in} - t_0)$	**Eq. 4**

On the other hand, because of exponential law, complete mixing flows never permit that the maximum energy is actually stored.

For those reasons, the piston flow process is normally referred to as the ideal storage process and the complete mixing assumption could be associated to the worst storage process.

As a result, at every given time θ, for a real simple tank undertaking the quoted thermal input, it is possible to define a storage efficiency relating the actual energy stored compared to the maximum storable energy at time θ.

$\varepsilon(\theta) = \frac{\Delta U(\theta)}{\Delta U_{piston\_flow}(\theta)}$	**Eq. 5**

For a complete mixing tank, this efficiency assumes a regular value at the time $\theta = \Theta$.

$\varepsilon(\Theta) = \left(1 - \frac{1}{e}\right)$	**Eq. 6**

Eq. 1 could be reformulated in the most general way as a dimensionless variables expression:

$t' = e^{-\theta'}$	**Eq. 7**
$t' = \frac{t - t_{in}}{t_0 - t_{in}}$, $\theta' = \frac{Q}{V}\theta$	

Finally, in order to enhance storage efficiency, mixing diffusion should be avoided and piston flow effects promoted.

1.2. Simple tank response to a constant heat flux exchange

Under complete mixing assumption, a simple tank response to a constant heat flux exchange Φ is clearly described by the following linear expression:

$t(\theta) = t_0 + \frac{\Phi}{V \rho c}\theta$	**Eq. 8**

Constant heat exchange could be reached by constant inlet temperature t_{in}, constant available flow-rate Q and crossing flow-rate Q_{cross} controlled by a set-point t_{lim} of the outlet temperature, where $|t_{in}| > |t_{lim}| > |t_0|$.

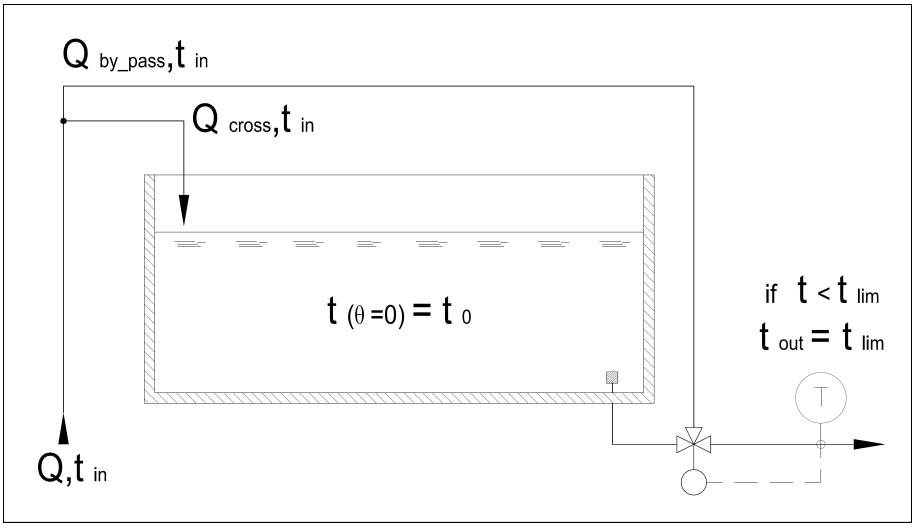

Figure 4 – Constant heat flux exchange layout

Simple tank exchanges constant heat flux Φ until t_{lim} is reached within the tank.
Whenever $|t| > |t_{lim}|$, by-pass flow rate occurs no longer and the simple tank behaves again as if it were subjected to a step thermal input.
The temperature ratio a is defined as follows:

$a = \frac{t_{\lim} - t_{in}}{t_0 - t_{in}}$	**Eq. 9**

Thus, the analytical law that a simple fully-mixed tank undergoes under constant flux control will be described by Eq. 10:

If $\left[t' > a\right]$ $t' = 1 - a\,\theta'$ Else $t' = a\,e^{-(\theta' - \theta'_{\lim})}$, where $\theta'_{\lim} / t'(\theta'_{\lim}) = a$	**Eq. 10**

The following figure shows constant heat flux controlled simple tanks under fully-mixing hypothesis at different temperature ratios a:

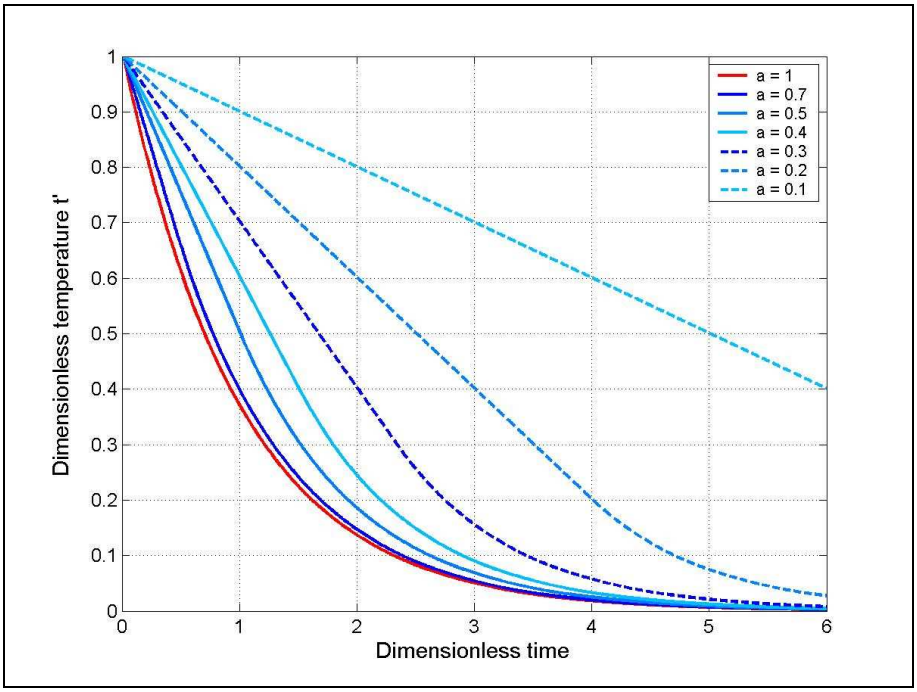

Figure 5 –Constant heat flux response at different temperature ratios a.

The more t_{lim} is close to t_{in}, the more the storage process is limited.
Anyway, as the tank temperature reaches the set-point temperature, the thermal storage is almost saturated, due to the exponential step response law.

Finally, it is important to observe that as long as constant exchange occurs, there is no notable difference, in terms of stored heat, between complete mixing tanks and piston flow tanks behaviours. On the other hand, during the tank step response storage efficiencies are remarkable far from each other.

1.3. Multiple tank response to a step input

Multiple series connected tank could be analytically investigated under complete mixing assumption and incompressible flows hypothesis.
For a given number n of identical sub-tanks, in the case of a constant volume flow rate Q, at a constant temperature $t_{in,}$ entering the tank, having an initial uniform temperature t_0, following first order system should be considered:

$\frac{d\,t_i'}{d\theta'} = -\left(t_i' - t_{i-1}'\right)$	**Eq. 11**
$t' = \frac{t - t_{in}}{t_0 - t_{in}}\ ,\ \theta' = \frac{Q\,n}{V}\theta$	

Index i addresses to the typical fully mixed sub-tank.

For the first sub-tank, $t_{i-1} = t_{in}$, so that $t'_{i-1} = 0$.

Eq. 12 shows the first order system closed solution for a typical i-th sub-tank:

$$t'_i = \sum_{j=0}^{i-1} \frac{\theta'^{\,j}}{j!} e^{-\theta'} \qquad \textbf{Eq. 12}$$

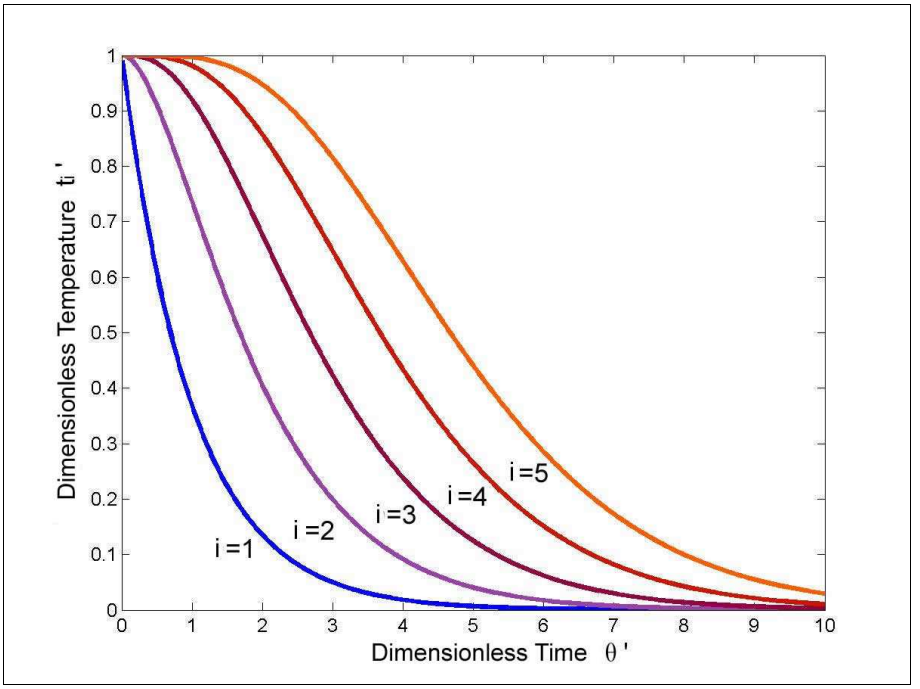

Figure 6 – Five sub-tanks multiple tank step response.

Note that simple tank dimensionless time is n times smaller than multiple tank one:

$$\theta'_{simple} = \frac{\theta'_{multiple}}{n} \qquad \textbf{Eq. 13}$$

This yields that multiple connected tank response is actually much more impulsive compared to simple tank response. Thus, tank partitioning could lead to storage efficiency improvement exactly as piston flow does.

1.4. Multiple tank response to constant heat flux exchange

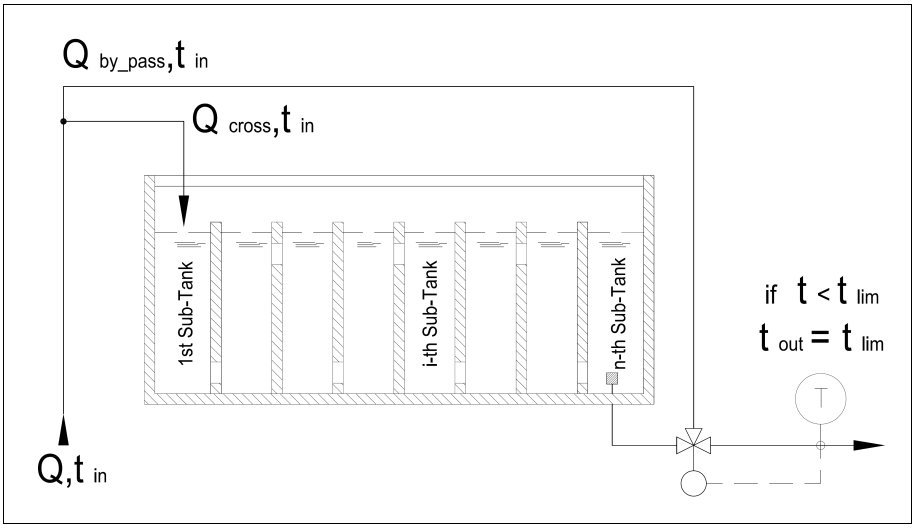

Figure 7 – Multiple connected tank subjected to constant heat flux exchange control.

Eq. 11 can be generally expressed as follows for a multiple series connected storage tank, built by n identical sub-tanks which is subjected to a constant heat flux control.

$\frac{d\,t_i'}{d\theta'} = -\frac{\left(t_i' - t_{i-1}'\right)}{t_n'}$	**Eq. 14**
$t_i' = \frac{t_i - t_{in}}{t_0 - t_{in}}$, $\theta' = \frac{Q\ n}{V} a\ \theta$	

First order system Eq. 14 is not linear, thus, numerical approach is recommended in order to solve such a problem.
A daily thermal groundwater storage system for office buildings HVAC purposes is going to be figured out in the next few paragraphs, where a constant heat flux control pattern will be needed.
First of all, the thermal storage will be set in a simple configuration and later in a multiple connected one.
Thermal storage behaviour under real building thermal load input as well as under constant heat flux exchange input could be subjected to first order non-linear laws, so that numerical calculations will be required.
Finally, thermal storage efficiency will play a crucial role to let it possible that in critical summer periods
daily stored heat could be fully discharged at night by groundwater cooling action.

2

Overview on groundwater thermal storage systems for HVAC

An office buildings complex by 6 to 7 stories, with glazed wall, by a 40.000 m^2 gross floor area is taken into account.
It is supposed to be situated in the north-east of Milan, it is expected to be occupied by about 3000 employees and it should be conditioned to grant standard thermo-hygrometric conditions for human comfort.
A water reservoir will be provided for fire-fighting purposes, thus there will be the opportunity to use it for thermal storage too. The architectural design team has assumed to prepare an available net volume by a maximum of 1200 m^3 at the first floor below-grade by providing a concrete rectangular tank 3m deep, 10m wide and 40m long. The tank volume and geometry comes from residual spaces left by the architectural below-grade car-parking and technical rooms layout, combined with structural foundation requirements.
Heating and cooling loads calculations have been carried out according to ASHRAE standard methods, showing that total maximum cooling power required during the critical summer day is supposed to be huge (Figure 8).
In the last few years, the first groundwater layers in Milan have been increasing their level, due to industrial processes dislocation. Nevertheless, industrial chemical pollution made these layers no longer potable, so they could be easily used for conditioning purposes. The underground water basin is at almost constant temperature all over the year and could be employed to dissipate or withdraw heat for buildings cooling and heating purposes through the reversible heat pumps technology. Within the present work, a reversible heat pump system is intended to be a system that produces cool or warm air for conditioning purposes depending on the comfort requirements. In fact, groundwater heat pumps assure remarkable operating energy savings and permit proper energy use for HVAC purposes.

However, for a given building work, local in force laws normally allow a maximum of 0.1 m^3/s of groundwater to be constantly pumped out in order to preserve underground basin environment.
The current office building is included within a large project, then the maximum groundwater flow-rate that is available for it amounts to 0.074 m^3/s .
Moreover, it is recommended by law to return the thermally exhausted groundwater in order to preserve the underground basin level. During the summer, the return flow must not be warmer than 20°, however there are no yet winter restrictions.
For a more intense groundwater withdrawal, or for any other derogation from law, it is required an exceptional environmental evaluations for the approval by local administration.

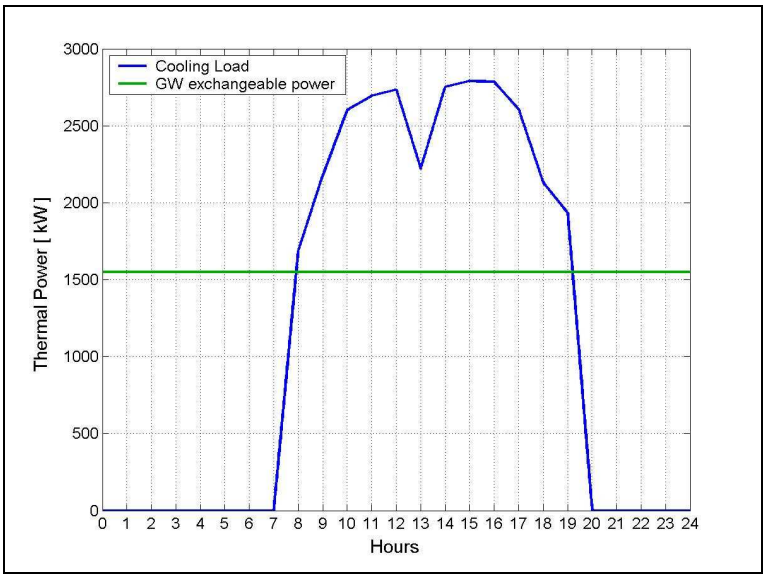

Figure 8 – Office buildings complex cooling load pattern with respect to groundwater limited cooling capacity during the critical summer day.

Geological surveys report a strict seasonal deviation of groundwater temperature from a minimum of 12°C to a maximum of 15°C.
As a matter of fact, the groundwater utilization offers a limited cooling exchangeable power in summer because of flow-rates bounds and due to the maximum value of discharge temperature by 20°C (Figure 8).
On the other hand the winter basin temperature could be not warm enough to assure the proper heat pumps operation during the coldest hours.
However, from an energy point, the cooling design conditions should be considered more critical than the winter ones. Indeed, during summer the thermal power rejected by the chillers overtakes the cooling load. Reversely, during winter, a weaker heat withdrawal is needed in comparison to heating load. Thus, a major amount of groundwater would be requested in summer than in winter.
In the critical summer day, even if the maximum rejected thermal power is largely bigger than the constant power that the groundwater can absorb, the total daily energy that can be discharged within it, it would be probably bigger, or at least equal, than the total daily energy which the conditioning chillers need to dissipate.
In that case, a thermal water storage philosophy can be performed to cope with law restrictions: the exceeding rejected heat could be stocked into a tank during the HVAC

system operation and it could be discharged into the underground water basin during the night in order to restore the initial temperature (Figure 9 and Figure 10).

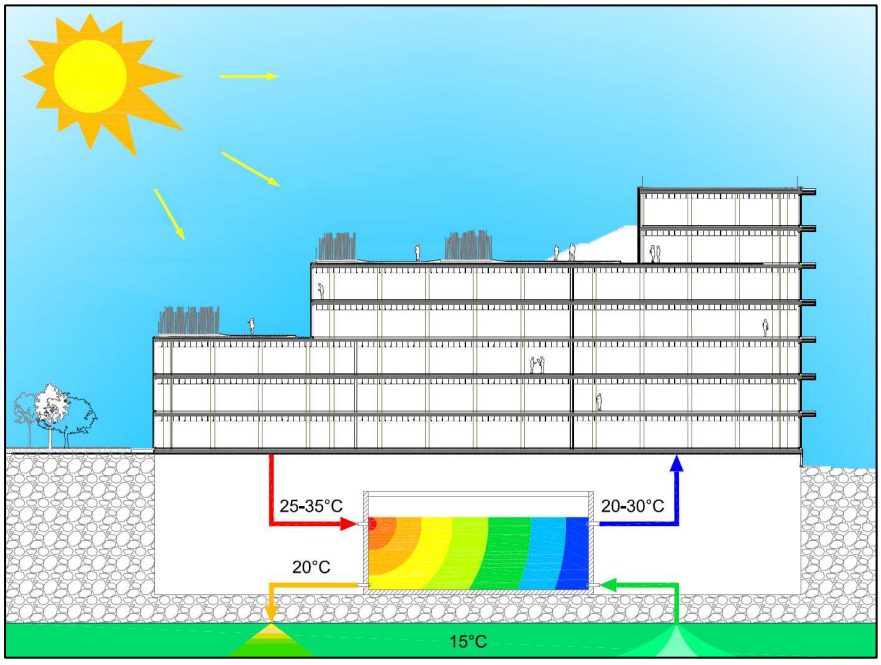

Figure 9 – Groundwater thermal storage strategy for an office buildings cooling: HVAC operating phase

Figure 10 – Groundwater thermal storage strategy for office buildings cooling: temperature restoration phase

A preliminary energy balance analysis has to be undertaken to determine whether thermal storage strategy could be suitable or not for the proposed office buildings complex.
Even if the cooling load scheme is given, in order to asses the expected heat to store within the tank, a prediction of the daily average COP of operating chillers is needed.
The actual heat rejection strictly depends on the interaction between thermal storage tank and the heat pumps operation: it is merely based on the available storage volume, the storage efficiency and the out of design behavior of the engines. As we will see later, the storage efficiency should be considered as the ability of the storage system to maximize the actual stored heat with respect to the theoretical one, by avoiding mixing phenomena or short-circuits within the tank, which would dampen the heat exchange between the tank and the external systems.
Therefore, a reliable thermal power rejection law should be output from a numerical simulation of the problem, as we are going to do.
Figure 11 gives a graphical view of the heat rejection assumed according to a reasonable average COP. It is overlaid to the constant groundwater cooling capacity (i.e. GW exchangeable power) so that the total heat that is expected to be stored could be compared to the total energy that the underground water basin can absorb during the night, with the aim to discharge the daily exceeding heat. If the nightly disposable heat overcomes or equals the expected stored heat, the storage philosophy could be successful.

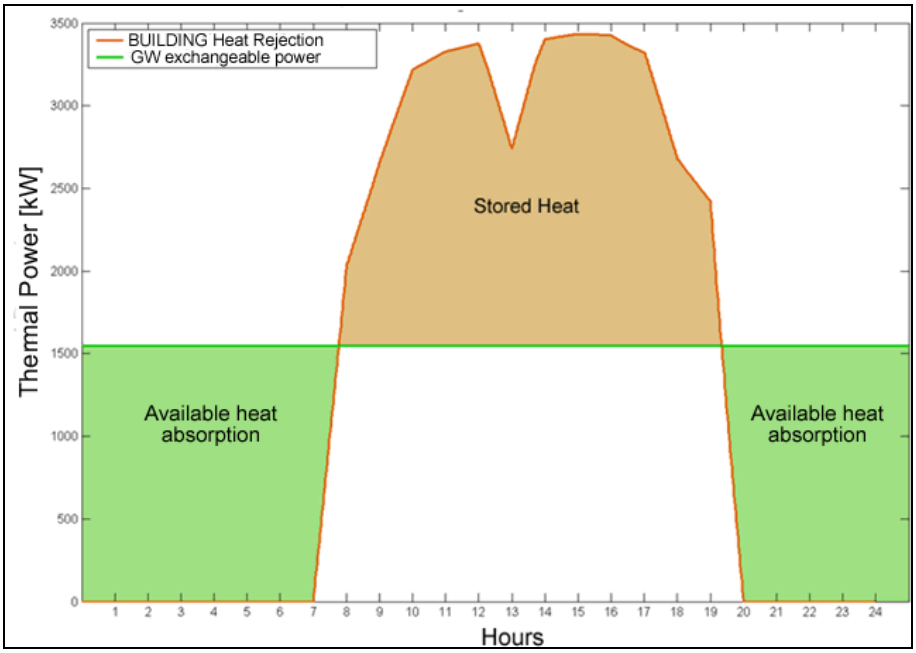

Figure 11 – Balance between heat to be stored and available energy absorption for thermal storage tank temperature restoration.

Even if such a preliminary energy balance is verified, there is no certainty about the actual daily thermal storage feasibility. As a matter of fact, the poor tank storage efficiency could affect the heat exchange between the tank and the HVAC system or underground basin, so that the energy balance predictions could be mismatched. Moreover the exact time-dependant COP response is a priori unknown. Finally, the energy balance tells us that thermal storage is theoretically possible if all components were perfect, otherwise a more detailed analysis should be recommended. That is the purpose of the present work.

Water cooled, variable refrigerant volume, direct expansion units (VRV®) have been chosen to be installed within the current offices in order to satisfy conditioning requirements. Those engines are built by water cooled external units and internal air units.

As it could be seen form Figure 12, modular external units are provided for every separated tenant's unit of the building. Then, refrigerant gas circuits are delivered from external units to reach internal air terminals, where the direct expansion occurs. A condenser water loop supplies water to all external units and delivers it to the heat rejection system.
The VRV®system consists in a sort of disjointed chiller whose compressor/condenser side is situated within the external units and the evaporator/expansion valve side is located into the internal units.
Partial loads are met through either a variable speed control of compressors operation than a local expansion valve regulation; that way, at partial load conditions, COP values could be even improved against the design conditions.
VRV® technology allows reversible operation so that heat pump service could be worked out as well as air cooling. Different connected internal units can perform heating or cooing independently at the same time, depending on the specific zone load request. Moreover, a three-tubes pattern permits a heat recovery within internal units, in a manner that compressors thermodynamic work is oriented to cope with the traded-off load only. However, such an advantage will be neglected in further simulation assumptions.
Each internal unit point of work is determined in accordance to each room exposures to the external environment. For example, a tenant's unit whose rooms are exposed northward and southward causes internal units expansion valves to be differently modulated to each other in order to meet the critical load. Then, as an example, in the critical summer day the external unit will operate in response to a combined average evaporation condition, coming form the global result of the internal evaporation valves different regulations. This combination effect yields that the whole system design efficiency could differ from the hypothetic nominal case in which all internal units were operating at the same evaporation temperature to meet the tenant's unit demands.
For that reason, external units COP is not only related to the loop water inlet temperature, that determines the condensation operation, it is not only related to the ambient set-point temperature, but it is also dependant to the combination to which internal units are subjected; where the combination means the level of operation variability of internal units due to the variability of geometrical miscellaneous exposures or of internal load gains to which they undergo.
Combination is quantified by an homonymous factor (i.e. combination factor) which approximately represents the ratio between the nominal performance and the actual one at a specific inlet temperature and internal set-point temperature. Given that winter set-point temperature amounts to 20°C and summer temperature to 26°C, external units performances will be modeled according to the technical data specified by manufacturer for assigned couples of combination factor and water inlet temperature to external units.
Due to a high level of tenant's unit exposures variability, further analysis will assume that at full load nominal performance will be improved by about 120% because of the specific combination to which internal units will be subjected. In other words the design combination factor will be assumed to be by 1.2.
However, since there is no direct relation between part load factor and combination factor and combination factor is not computable but engines performances are merely listed within the manufacturer datasheets depending on it, iterative calculations will be executed to identify proper combination factor to meet part load requirements. First, the combination factor will be placed equal to the part load factor, then the combination factor will be adjusted several times in order to meet part load cooling and heating requirements passing through the actual VRV® performances stated by the manufacturer.

VRV® external units admit a maximum inlet temperature of 45°C for condensation and only 10°C for evaporation. These thresholds will influence the HVAC thermal storage system so that winter critical conditions will need storage philosophy as well as the summer ones.
Even if no law restrictions exist about winter operation, given that the minimum supply temperature is by 10°C and in this condition ,according to VRV® technical data-sheets, the return temperature from the water loop would not be lower than 7/8°C, the groundwater winter temperature difference, from withdrawal to return, could not be bigger than 2/3°C at the maximum constant flow-rate by 0.074 m^3/s.
That way, even if not fixed by law, the maximum heat flux available from groundwater is limited in winter as well as in summer, so that thermal storage is finally recommended all over the year.
Anyway winter groundwater demand is much lower than the summer one, but the allowable temperature variation is much more higher in summer (from15°C to 40°C, as we are going to explain) than in winter (from 12°C to 10°C).
For that reason the tank volume should be verified for summer critical days as well as for winter critical days with the purpose that temperature will never fall below 10°C the tank.

In order to describe the rejection system to which the VRV®, please refer to Figure 12. The group of storage tank and groundwater withdrawal and discharge is conventionally called rejection system under the summer operation point of view, even if in winter it works as a withdrawal heat system.

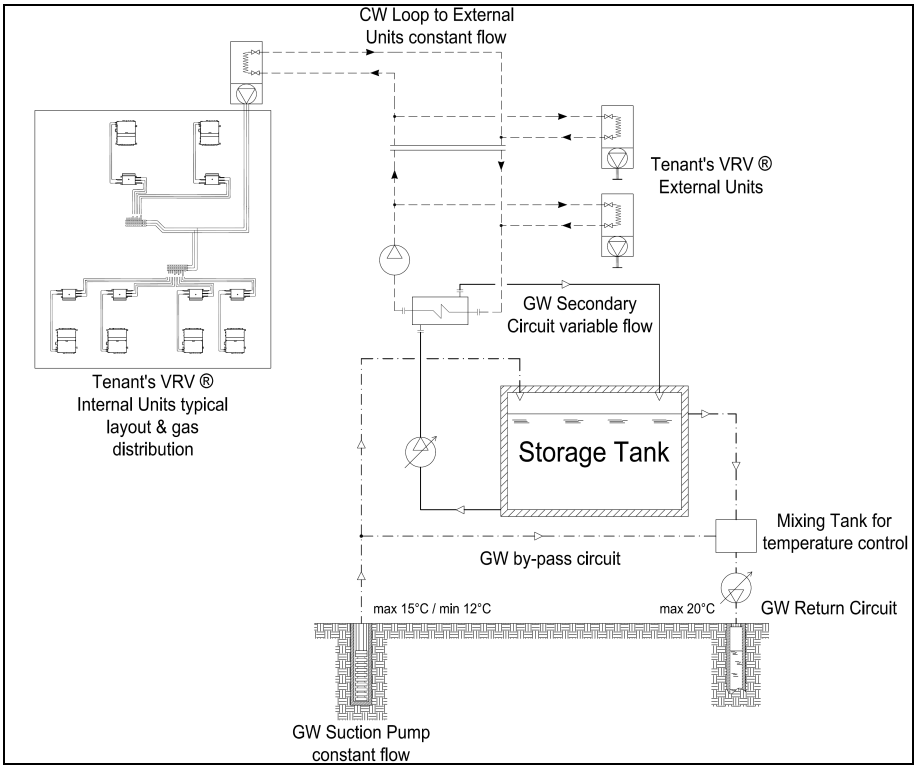

Figure 12 – Thermal storage system combined to VRV®.

According to Figure 12, suction pumps deliver groundwater to the storage tank. Thermal storage is realized by a self-balanced water tank at atmospheric pressure. Indeed, water level within the tank is automatically preserved by natural overflow of exceeding volume

thorough a weir (Figure 13). That way, tank works as thermal storage as well as pressure disjunction between groundwater suction and groundwater discharge.
Coming back to Figure 12, the expelled groundwater is gathered into a secondary tank where the return temperature to underground basin is strictly controlled. Thanks to a proper flow rate regulation through the by-pass circuit, the return temperature is inhibited to outrange law limits. A variable flow-rate secondary circuit pumps out the groundwater from one side of the tank and returns it back on the opposite side for the purpose to serve a plate heat exchanger. The heat exchanger is needed to chemically separate the groundwater from the condenser water pumped towards the external VRV® units. Moreover it to avoids external units loop to be drained out during shut-off period into the tank and it divides groundwater circuit variable flow from external units loop constant flow. Constant flow through external units is recommended by manufacturers because of evaporation concerns in winter and optimum operation.
According with Nakahara's advices [4], it could be initially predicted the tank storage behavior faced to the current heat rejection system.
The secondary circuit variable flow promotes the storage efficiency, however the groundwater by-pass flow increases the flow-rate crossing through the tank so that storage efficiency is damaged. Moreover, the heat exchanger station results in a condensation temperatures increase due to the temperature levels separation between the exchanging flows. It causes external units COP to get worse and raises the rejected energy to be stored. Winter operation is similarly affected.
Figure 13 represents the system regulation logic.

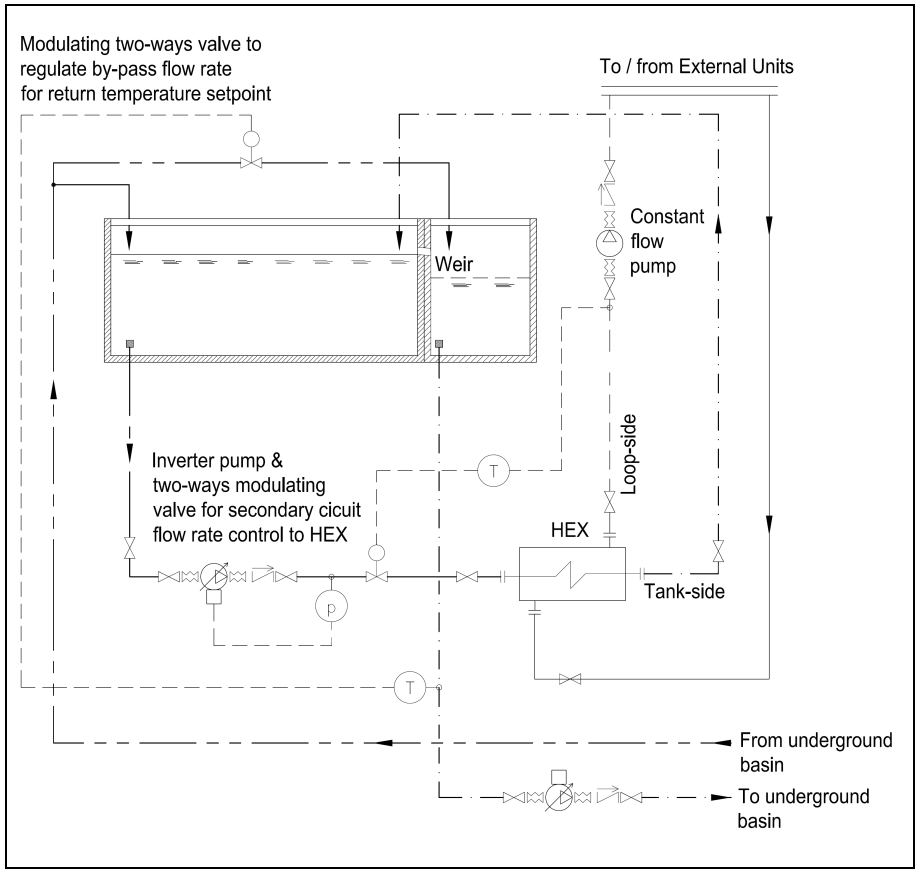

Figure 13 – System regulation strategy.

A set of withdrawal pumps ,represented in Figure 12, assures a constant groundwater flow-rate delivery to the tank.
A two-ways modulating valve controls the groundwater by-pass flow-rate in order to maintain the return temperature below the law threshold.
Variable flow groundwater pumps supply adequate flow rate to heat exchanger so that a proper temperature gap is maintained between the tank-side inlet and the loop-side outlet. Variable flow pumps are controlled to keep a constant outlet pressure and a modulating two-way valve is controlled by the set-point gap between the loop-side delivery temperature signal and the tank-side inlet one. That way stationary thermal balance is granted within the heat exchanger and the exact heat flux rejected or absorbed by external units is supplied through it. Given that the controlled gap value is by 5 °C, the maximum allowable temperature within the tank is amounts to 40°C.
Constant flow pumps deliver to external units their design flow rate.

Note that in the cooling operation the delivery temperature control is provided to keep the gap constant between tank-side inlet and loop-side outlet to permit a temperature raising shift either into the tank than into the loop.
However, in winter conditions, the supply temperature to external units should never be lower than 10°C because of VRV® operation concerns. Given that groundwater winter temperature could fall to 12°C, constant supply temperature control to external units is recommended in winter with respect to a constant gap control. Moreover, a back-up emergency boiler should be installed in series to external units loop in order to eventually raise the delivery temperature in supercritical cases.

Finally, following figures will supply a visual overview on typical summer operation phases of the system is presented in the aim to figure out further treatments.

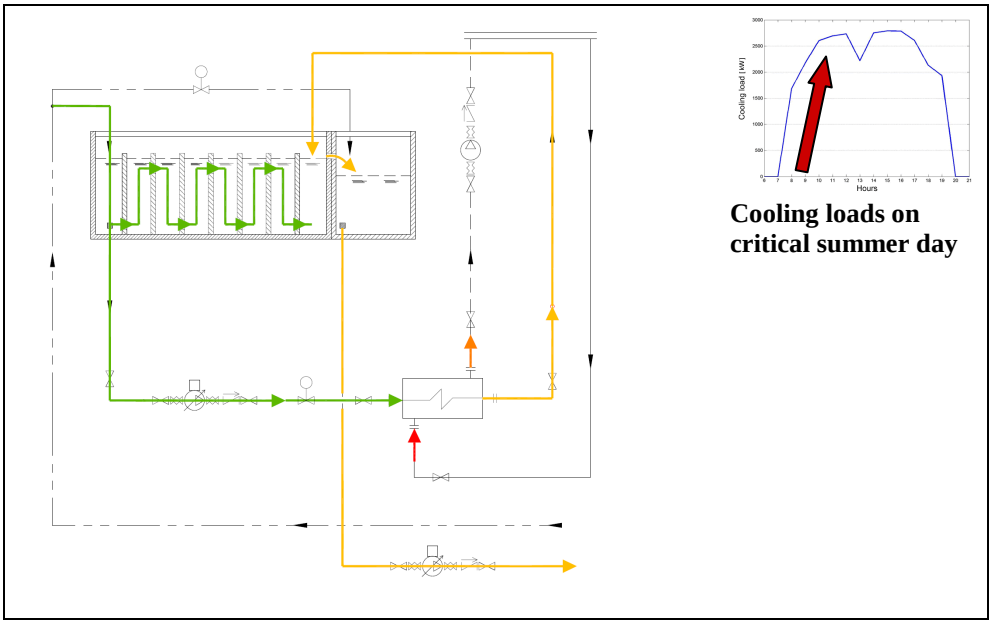

Figure 14 – Initial cooling load is fulfilled by GW capability.

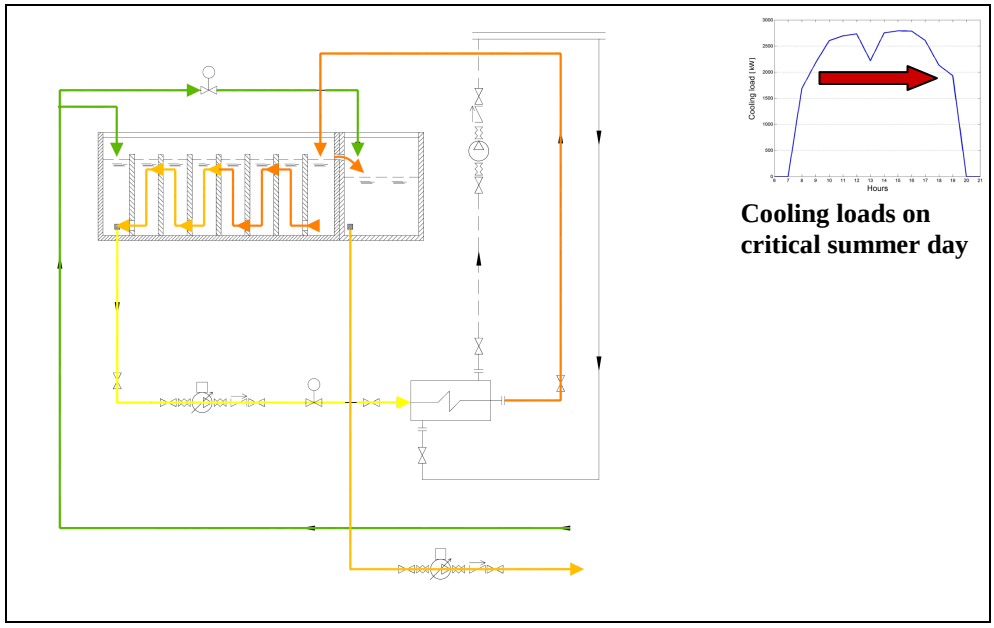

Figure 15 – Groundwater thermal storage normal duty.

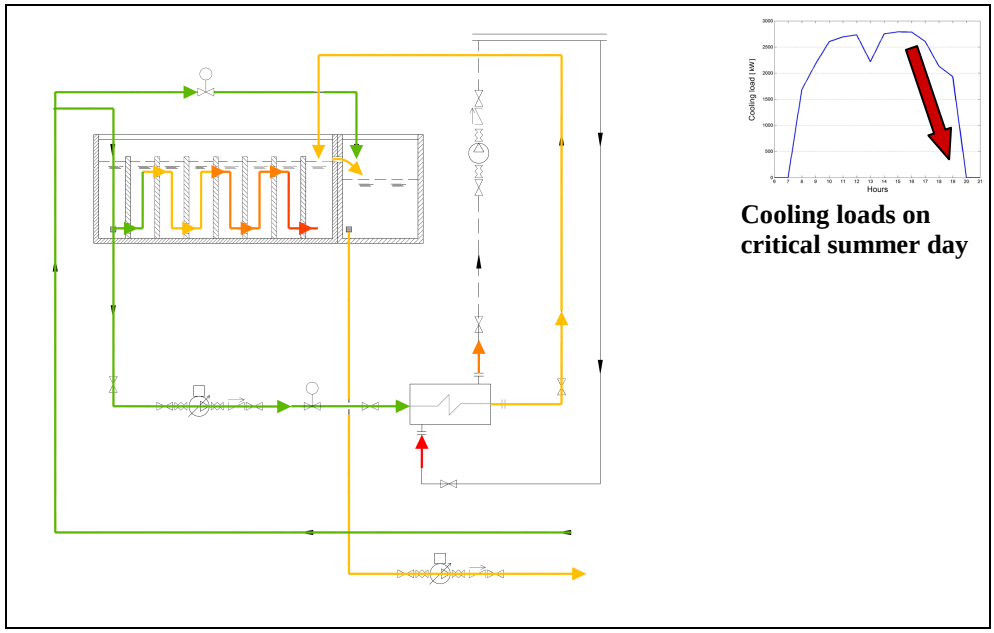

Figure 16 – Restoration on duty.

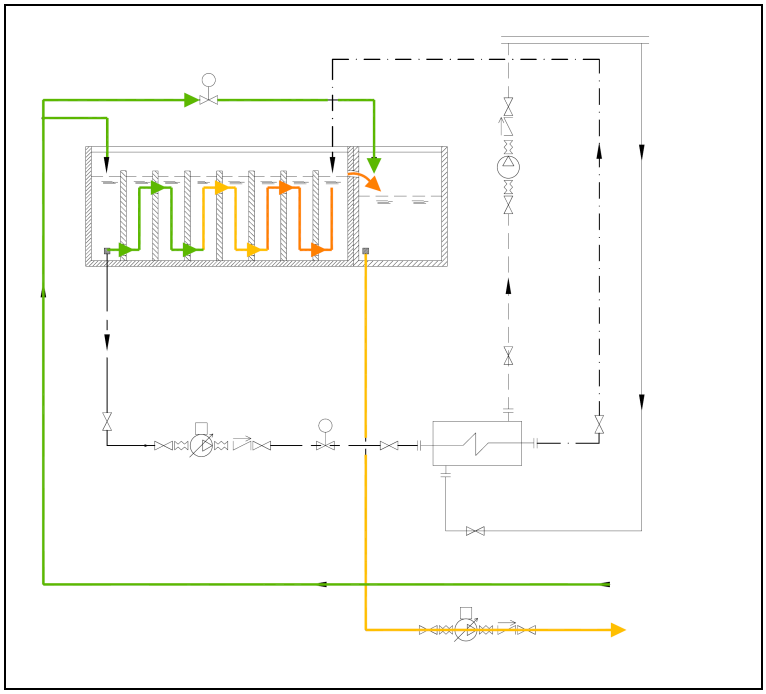

Figure 17 – Restoration, fully heat exchange.

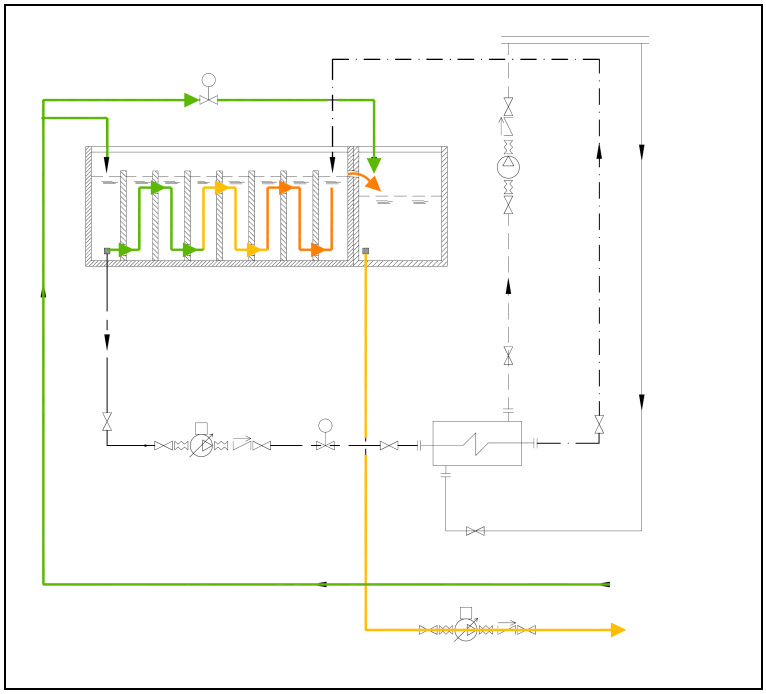

Figure 18 – Restoration, heat exchange saturated

3

Matlab Simulation

3.1. Purposes

A Matlab routine has been developed to model thermal storage strategy for VRV® technology in typical days all over the year.
Heating and cooling loads have been calculated from UNI 10349 and CNR seasonal climatic data for Milan in accordance to UNI 10339 standard indoor conditions as well as UNI 10339 occupancy data and sensible/latent persons emissions for design calculations.
Lighting and miscellaneous loads are taken from ASHRAE standards together with occupancy, lighting and equipments typical schedules.
Two typical days have been investigated for each month dividing sunny days by cloudy ones.
The simulation purposes were to estimate total electrical energy absorbed by VRV® compressors referred to an annual typical operation according to a simple tank system; however special attention has to be paid for critical summer and winter days in order to assess the strategy feasibility. Within each typical, the system operation simulation has been performed at every single minute in order to accurately take into account the tank transient responses.
An Optimization process, concerning the tank design and the regulating strategy, have been carried out in order to figure out proper integrated solutions.

3.2. Complete Mixing, Multi-connected series pattern and piston flow models

Three different assumptions have been made in order to compare water thermal storage efficiency in the critical days:

Complete mixing simple tank has been basically modeled through the following numerical method:

$$t(\theta_i) = t\ (\theta_{i-1}) + \frac{\left(\sum_k q_{in_k}\ t_{in_k} - \sum_z q_{out_z}\ t_{out_z} \right)}{V} \left(\theta_i - \theta_{i-1} \right) \qquad \textbf{Eq. 15}$$

Where index i is referred to as current simulation minute and indexes k and z address to the number of inlet and the number of outlet flow rates each. For the current case k=z=2, as shown in Figure 13.

Multi connected series pattern tanks are modelled the same way, unless the balance is to be made for each j-th sub-tank.

$$t_j(\theta_i) = t_j(\theta_{i-1}) + \frac{\left(\sum_{k_j} q_{in_{k_j}}\ t_{in_{k_j}} - \sum_{z_j} q_{out_{z_j}}\ t_{out_{z_j}} \right)}{V_j} \left(\theta_i - \theta_{i-1} \right) \qquad \textbf{Eq.16}$$

An exceptional method has been applied for the piston flow model.

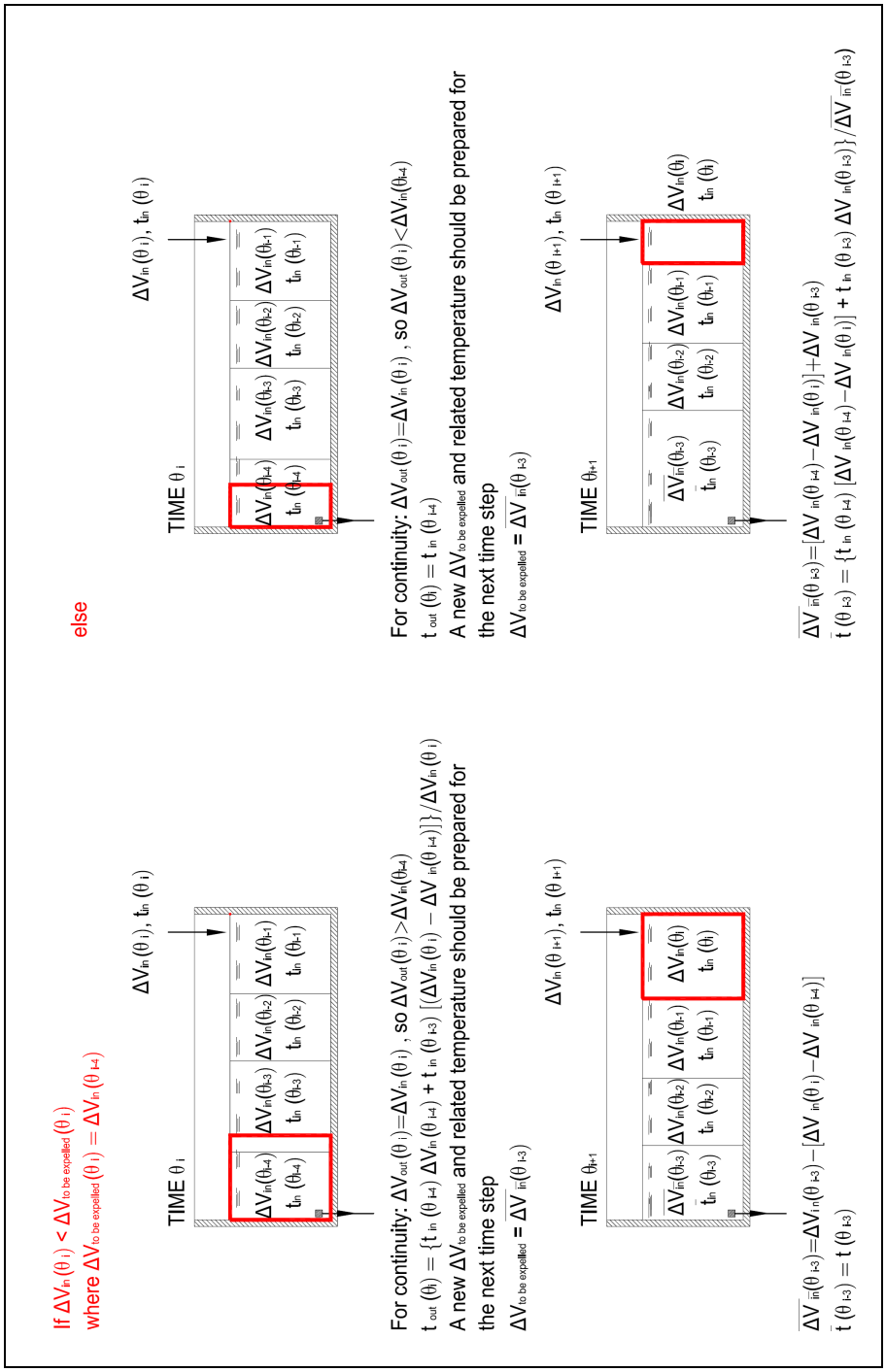

Figure 19 – Piston flow model assumptions.

Finite volumes enter tank at each given simulation time step as if they were train wagons. Time step has been assumed equal to a minute.
Volumes values could vary depending on current secondary system demand.
Each entering volume ΔV_{in} is registered into an historical array. After cumulative entering volume overcomes tank volume V, the first of the registered finite volumes will be partially or totally expelled out of the tank. Because of variable crossing flow rate through the tank, entering finite volume at a given time could be notably different from registered finite volume that is being expelled at the same moment. Actually, when it was registered, its value depended on entering flow rate at that time, that could significantly differ from current flow rate.
Volume merging or dividing operation is made on exiting registered finite volumes in order to match entering volumes to exiting ones for continuity. Moreover, registered finite volumes array, which actually encompass finite volumes distribution within the tank, must be updated at each time step in response to expelled and enclosed volumes, so that tank mass is always preserved.

As in Figure 19, proper outlet temperature calculation is also requested to model adequate heat exchange within the tank.

3.3. Initial Data

Daily mean temperatures and humidity have been found for both cloudy and sunny days from CNR sources.
Internal loads come from ASHRAE and solar heat gains depend on UNI 10349 data.
A Carrier simplified method has been carried out in order to achieve hourly distribution of heating and cooling loads.

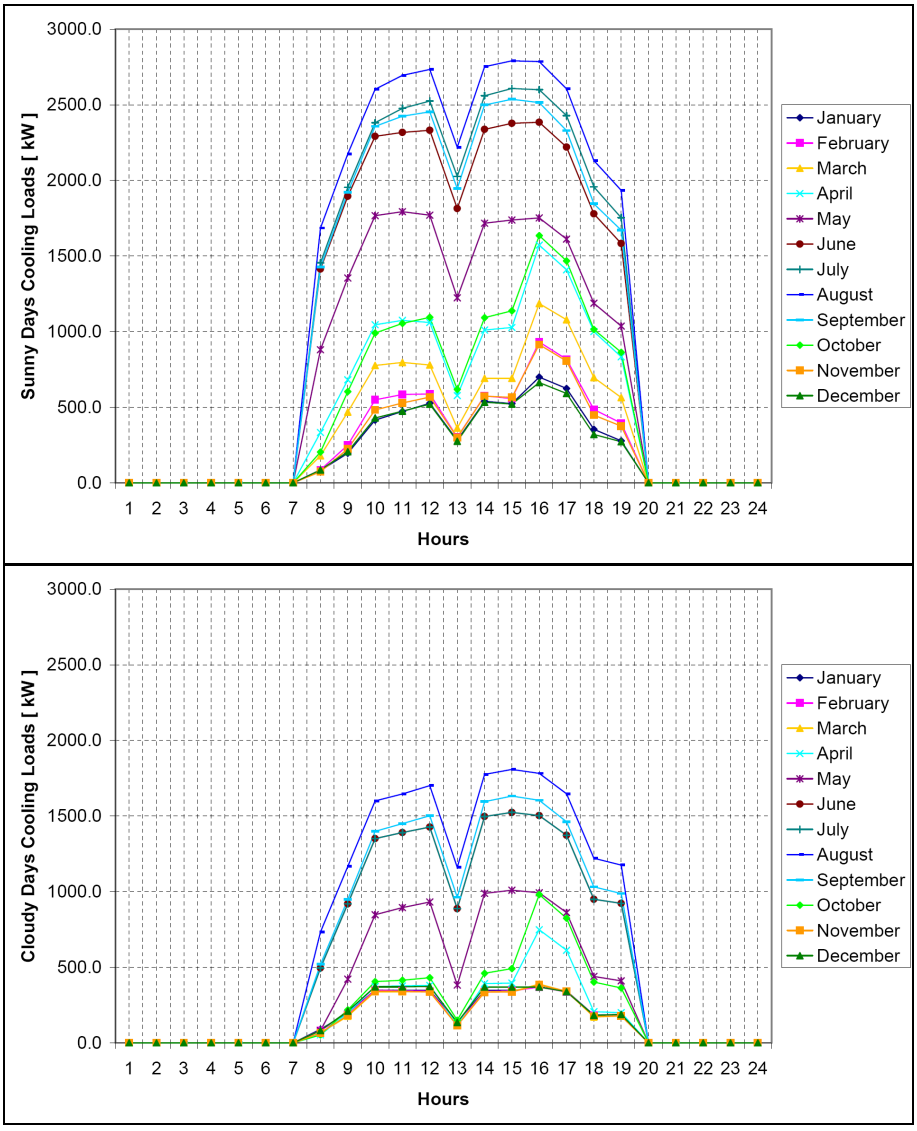

Figure 20 – Cooling loads.

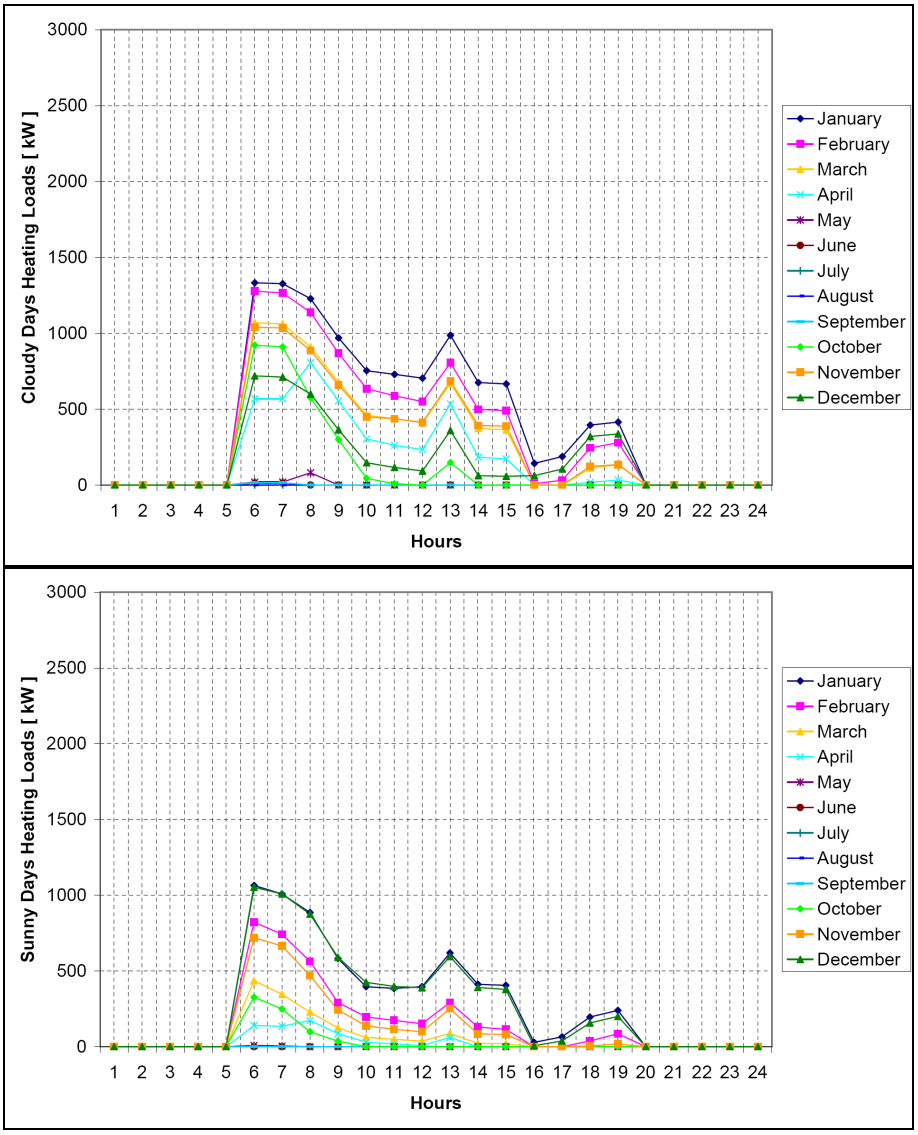

Figure 21 – Heating loads.

A linear interpolation has been applied to approximate loads for each minute all over the year.
As a result, 24 (two typical days per month) cooling and 24 heating load values are available into Excel datasheets as an input for Matlab simulation.
Same way, the technical data for part-load and fully load operation have been found within the manufacturer VRV® data sheet and have been transformed into Excel datasheets as an input for Matlab simulation.
Note that heating and cooling operation will be often required at the same moment. In the next analysis the heat recover that VRV® can undertake within each tenant refrigerant circuit will neglected, but the system will be modeled as though different groups of external units were working on cooling mode and heating mode independently so that heat recovery will be obtained through the condenser water loop circuit connecting all the external units.

The temperature engines working range must be underlined to be honestly introduced to following analysis:

- Maximum external units inlet water temperature: 45°C
- Minimum external units iinlet water temperature: 10°C

Note that such a range is pretty common throughout commercial chillers for HVAC services.

Even if several external units sizes are available on the market, only the smallest one has been considered into this work. Actually the bigger sizes are basically modular, parallel connected, combination of the basic one, so that they perform exactly as a sum of basic units does.
Heat exchangers out of design steady behaviours have been modelled through the following correlation that is especially valid for pleat heat exchangers:

$Nu_{d\_plat} = 0,374\ \mathrm{Pr}^{0,333}\ \mathrm{Re}_{d\_plat}^{0,668}$	**Eq. 17**

Where d_plat is the hydraulic diameter of a single plate exchanger channel.
Typical geometric parameters for plate heat exchangers have been found into literature in order to infer proper values for transmittance and exchange surface from the previous correlation.

3.4. Matlab Routine Structure

One main program calls several sub routines in order to simulate the system behaviour.

Main program is called DAY_SIMULATION.m. It requires the month number, a sunny/cloudy binary code and the tank whole volume, for simple complete mixing tanks and piston flow, or the sub-tanks volumes array for multi connected tanks.
First of all, DAY_SIMULATION.m imports Excel heating and cooling loads datasheet and records them into a matrix. An ON-OFF system schedule is inferred from loads Excel datasheet arrangement.
The most important sub routine is called FIND_VRV.m. It works as a quick tool to infer external units actual heat capacity and electrical power consumption depending on current part-load factor and loop water inlet temperature. Into FIND_VRV.m, an Excel datasheet containing engines technical data are imported and suitably manipulated, through proper linear interpolations, to give back required data at every possible condition to be enclosed in the manufacturer's declared test conditions.
The sub routine DESIGN_CALCULATION.m is called only one time at the beginning of the main routine, to implement the following operations:

- Sizing the number of external units to provide, by the comparison between critical summer and winter hourly loads requirements.
- Sizing plate heat exchanger surface through the NTU/ε method, by the comparison between critical winter and summer conditions, starting for each condition from the desired flow rates and temperatures values on both sides of the heat exchanger at remarkable conditions.

The main routine encloses a first `for` cycle to run along all minutes of the selected day. Whether the system is ON at the current minute, a sub routine called MIN_SIMULATION.m is executed. Actual external units performances are calculated, real plate exchanger efficiency and outlet tank-side temperature is evaluated as well as, the unsteady tank temperature profile is inferred. As thermal storage occurs, a secondary `for` cycle is recommended in order to correctly compute continuous adjustment of external units decreasing COPs along with the tank temperature arising. Within MIN_SIMULATION.m sub-routine, the actual time step of analyses falls from one minute to about three seconds.
Temperature signals delays due to pipes length are neglected.
HEAT_EXCHANGER.m is the routine that calculated real plate exchanger efficiency at each minute. It encloses a WHILE iterative cycle in order to implement the NTU/ε method along with the actual operating conditions, so that the required tank-side variable flow rate is calculated as well as the updated outlet temperature. The WHILE cycle is ended as the required heat flux to be exchanged is actually met by the heat exchanger performances.

Note that tank-side groundwater outlet temperature and the associated flow-rate represent such important values because they are directly connected to the storage tank behaviour and its storage efficiency.

Finally, a sub-routine called RESTORATION.m is executed as the system turns off . It evaluates the time that is needed by the tank to recover initial temperature during the system out of duty period.
Actually, RESTORATION.m output will outline whether daily storage strategy is suitable or not , depending on the fact that day period is overcome or not.

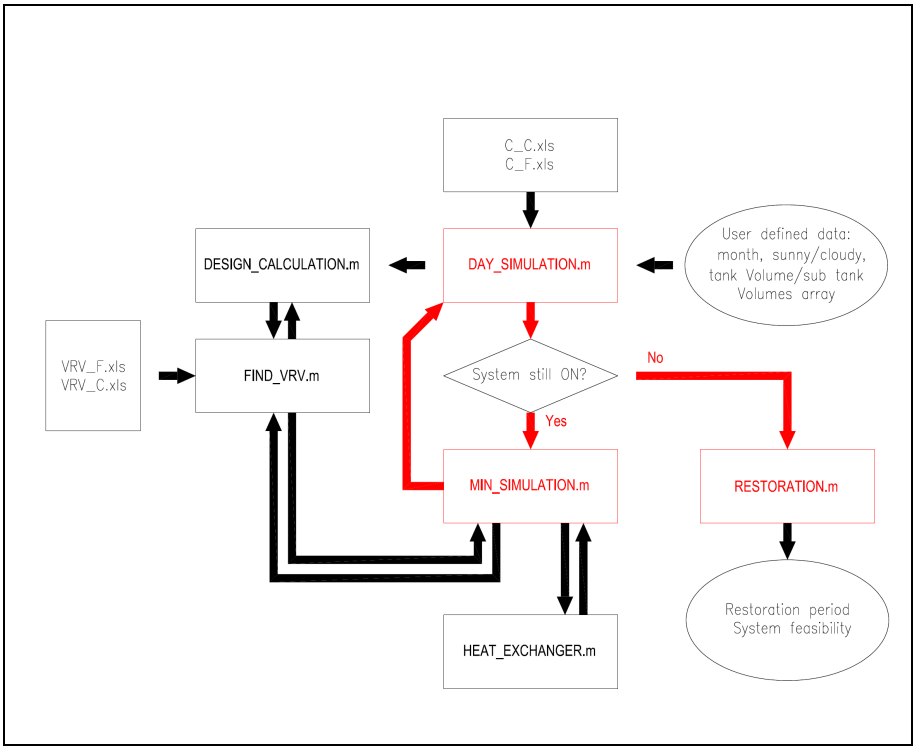

Figure 22 – Matlab program structure.

Matlab routines structure has been developed to permit that groundwater thermal storage systems can be run with no care about their equipment and tank actual sizes, so that thermal storage feasibility could be investigated through a variety of situations where storage efficiency could be also taken into account. Nevertheless, as it will be outlined in the next paragraph called “Validation”, the calculation program could be easily arranged to model every possible thermal storage systems that is not strictly related to groundwater use.

3.5. Results

The simulation results are going to be highlighted through a synthetic list of topics.
The available volume capacity V of the tank by 1200 m^3 is supposed to be used for thermal storage purposes.
It will be shown that tank partitioning is recommended either in the summer critical days than in the winter ones. Moreover, the compressors electric energy consumption difference between a simple tank and a multi connected tank pattern will be quantified throughout a typical year operation.

As a standard approach, the first tank will be conventionally expected to be the first sub-tank receiving the heat exchanger output. Opposite, the sub-tank that directly receives the groundwater flow rate will be considered the last tank.

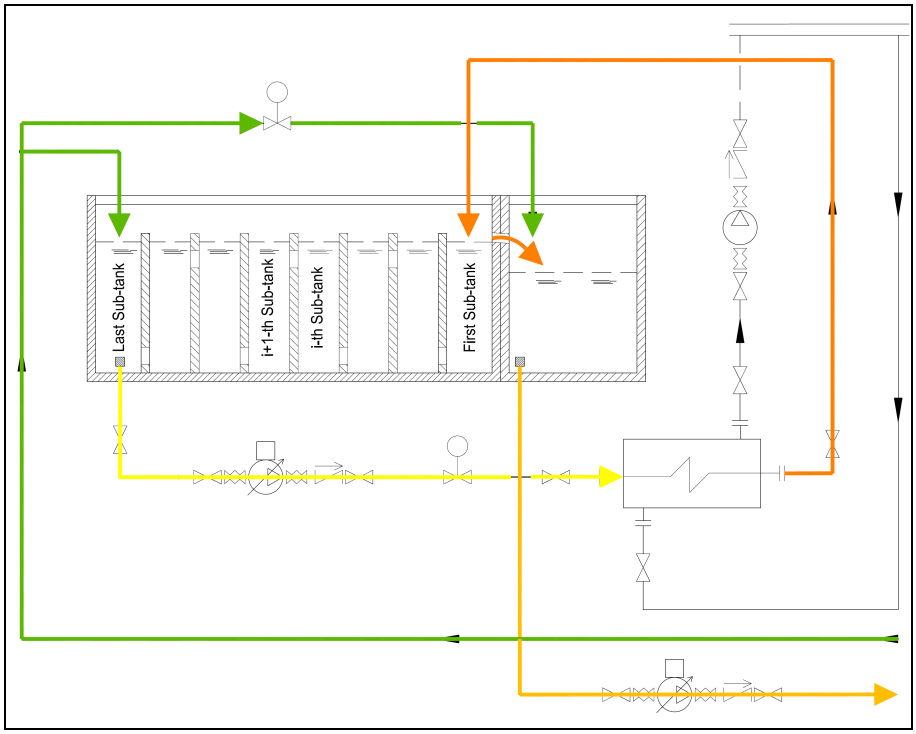

Figure 23 – Sub tanks conventional numerical order.

3.5.1. Simulation of the summer critical day

In order to infer the daily storage strategy feasibility for the current boundary conditions, the simulation will be undertaken at first in the summer day, where the expected stored heat is maximum.
In this case, it will be assumed that a complete restoration has occurred before the daily system switch on, so that the calculation will start from the desired groundwater uniform temperature within the tank by 15°C. Sub tanks temperature hourly profiles will be investigated until the restoration process will be completed and the needed time will be compared to the available one.
That way the simple tank pattern will be evaluated against the multi connected one in terms of storage savings and storage efficiency performances.
The following diagram figures out the system behaviour in the critical summer day (July sunny day) under simple tank and multi connected tank patterns.

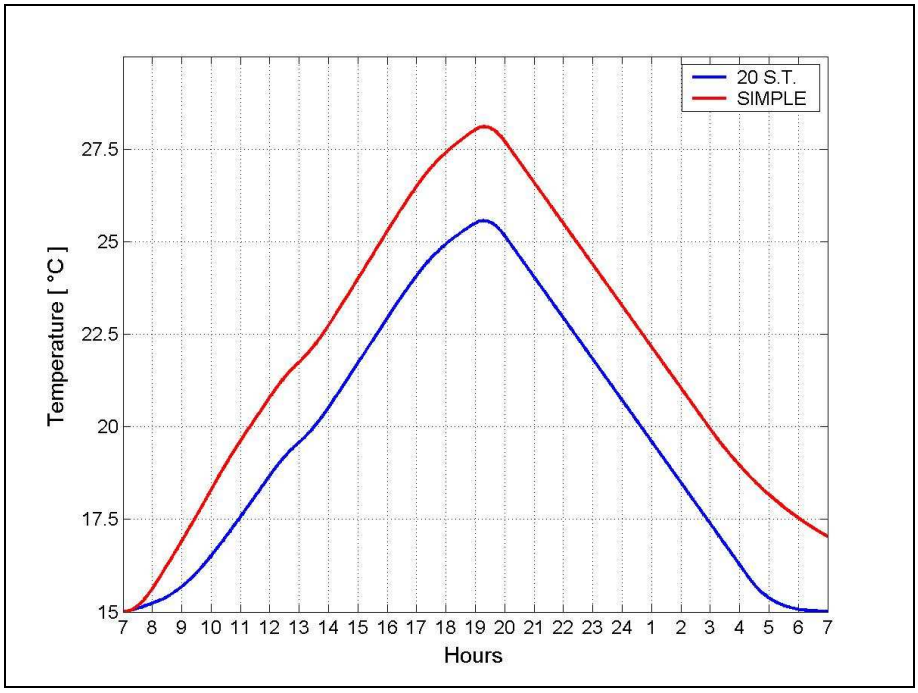

Figure 24 –Tank average temperature time dependant profile: comparison between simple tank performance towards 20 multi connected sub tanks, under complete mixing assumption.

Basically, the simple tank applied to the summer case leads to a poor restoration performance, the storage process needs more than 24 hours.
Even if energy the theoretical balance is verified, see Figure 11, the daily storage strategy does not work because of complete mixing assumption.
On the other hand, the tank partitioning allows the temperature short circuit process to be inhibited due to the mean allowable vortex diameter reduction.
Note that a proper number of sub-tanks into which main tank should be split is 20, at which restoration is almost perfect.
The operation and restoration phases are easy to be read on the sub-tanks temperature profiles as follows.

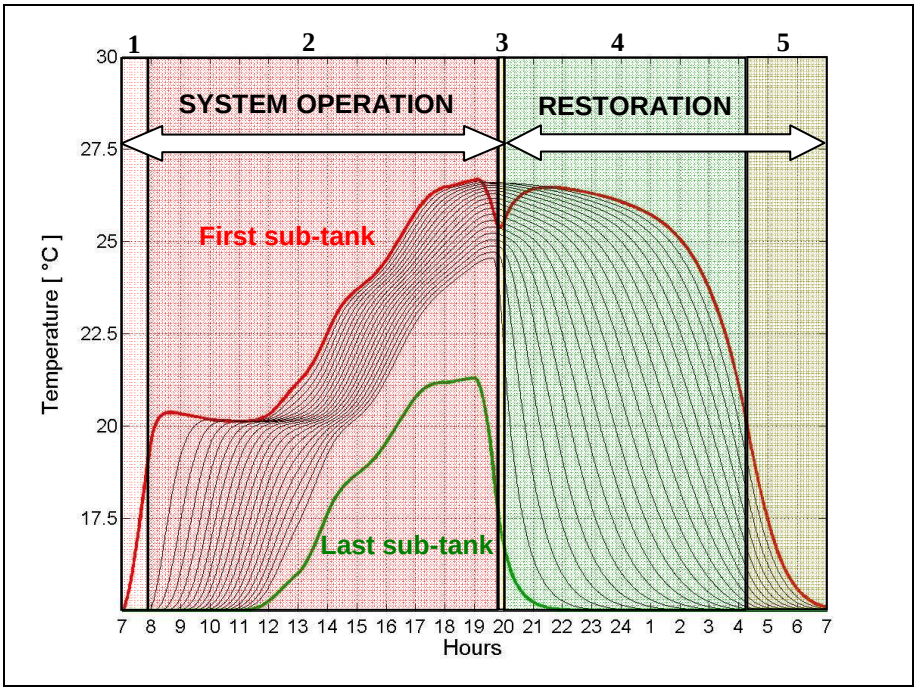

Figure 25 –Multi connected tank 20 sub-tanks temperature profiles and overlain storage cycle phases (see Figure 14to Figure 18):
1. Initial cooling load is fulfilled by GW capability (only first sub tank working)
2. Groundwater thermal storage normal duty
3. Restoration on duty (first tank temperature profile starts to grow before the system shut down, planned for 20 o'clock, that is due to a flow inversion within the tank)
4. Restoration, fully heat exchange
5. Restoration, heat exchange saturated (it begins as the last tank temperature is by 20°C)

The reasons why tank partitioning result in a better performance are listed below.

Tank partitioning results in more efficient ground water utilization.

During the first few hours of duty simple tank doesn't allow full groundwater thermal capability to be used, otherwise multi connected pattern minimize useless heat storage.

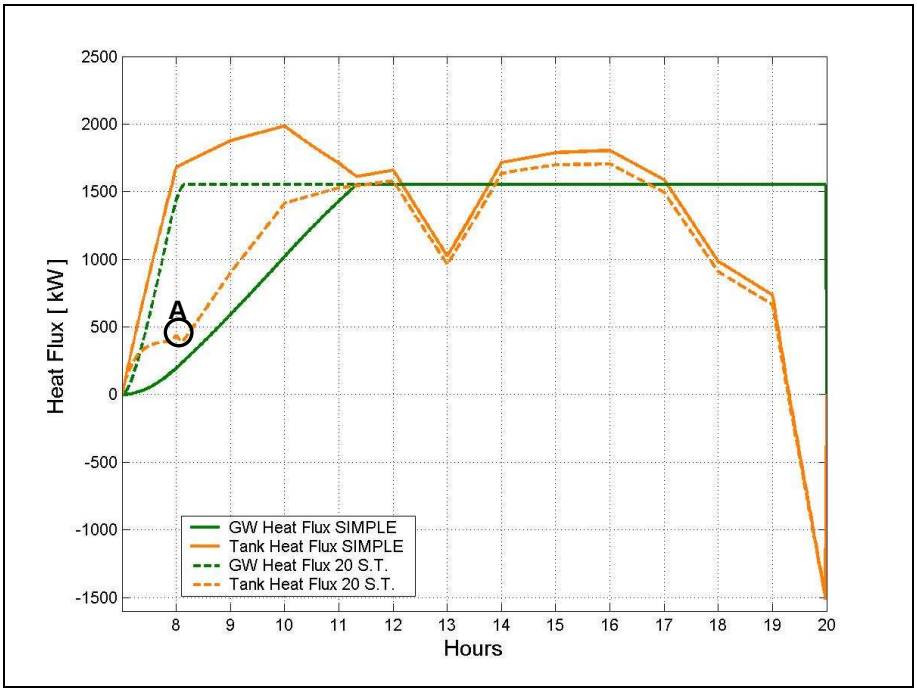

Figure 26 – Comparison between simple tank and 20 multi connected sub tanks about heat flux exchanged either by the tank than by ground water during the operation phase.

Note that, being the maximum heat flux that could be directly exchanged by groundwater is limited to around 1500 kW, the multi connected configuration allows the first tank to overheat fast so that the groundwater by-pass is activated and the fully direct groundwater use is earlier promoted. That way, useless heat storage within the tank is prevented all along the others sub-tanks.
As a result, the 20 multi connected configuration yields an initial smaller tank mean overheating so that external units can work at lightly better COPs. Heat rejection is than reduced in a manner that the heat storage cumulated over the operation phase within the tank is remarkably smaller.

In the case of 20 sub-tanks multi-connected tank, the detail A shows an abnormal peak along the tank heat flux curve. It occurs because the period during which the whole rejected heat is directly absorbed by the groundwater ends just slightly before that the first tank reaches 20°C, so that the by-pass valve is activated.
Remember that when the whole heat flux is dissipated towards the underground basin and no heat storage occur, except for the first tank, the available groundwater flow-rate overcomes the required flow-rate at the tank-side heat exchanger. As the available groundwater capacity is no longer able to fulfill the required heat, the flow direction inverses within the tank and the storage process begins. That implies the tank exchanged heat flux to increase.
However, since the tank-side heat exchanger flow-rate is regulated to cope with the heat rejection demand but the output temperature is not controlled, as the flow inversion occurs within the tank, the first tank temperature has not yet reached the limit temperature by 20°C, so that the maximum absorbable heat flux by the ground water has not be still obtained. As long as the first tank temperature rises towards 20°C the heat flux directly discharged by the groundwater increases as well.

Until the limit temperature by 20°C is not reached within the first tank, both tank exchanged heat flux and direct groundwater exchanged heat flux tend to increase, resulting in the abnormal behaviour outlined within the detail A

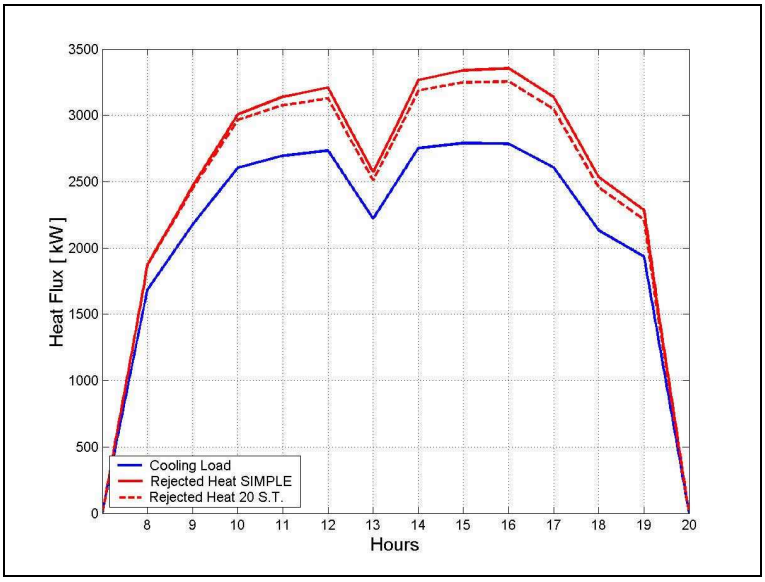

Figure 27 – Comparison between simple tank and 20 multi connected sub tanks about heat rejection rates under same cooling load conditions.

Given that the multi-connected tank and the simple tank rejected heat flux curves are olmost overlain, that implies that compressors electrical power saving does not appear so huge at the summer critical day, anyway a lower heat to store facilitate restoration to be quicker and daily storage philosophy to be successful.

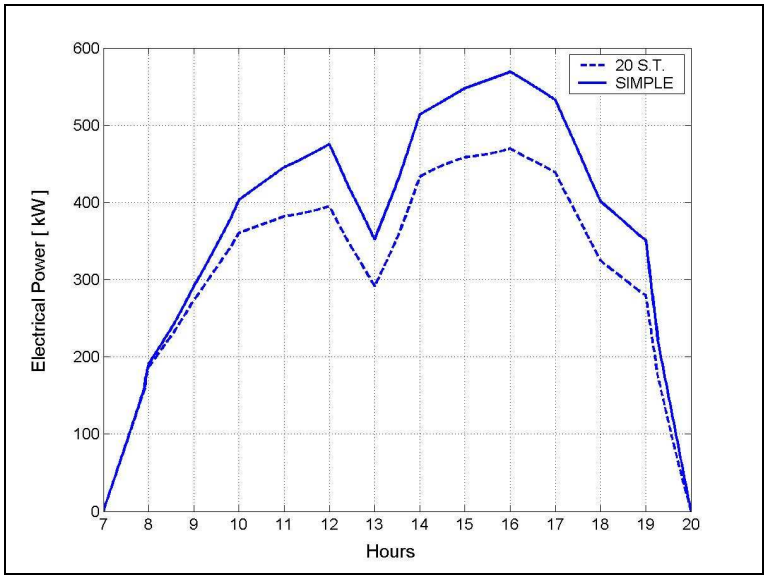

Figure 28 – Comparison between simple tank and 20 multi connected sub tanks about electrical power consumption under same cooling load conditions.

Although, the all year long simulation will figure out in a more outstanding manner as the tank partitioning strategy could result in a significant energy saving.

The following figure shows the comparison between multi-connected pattern and simple tank in terms of important flow-rates profiles.

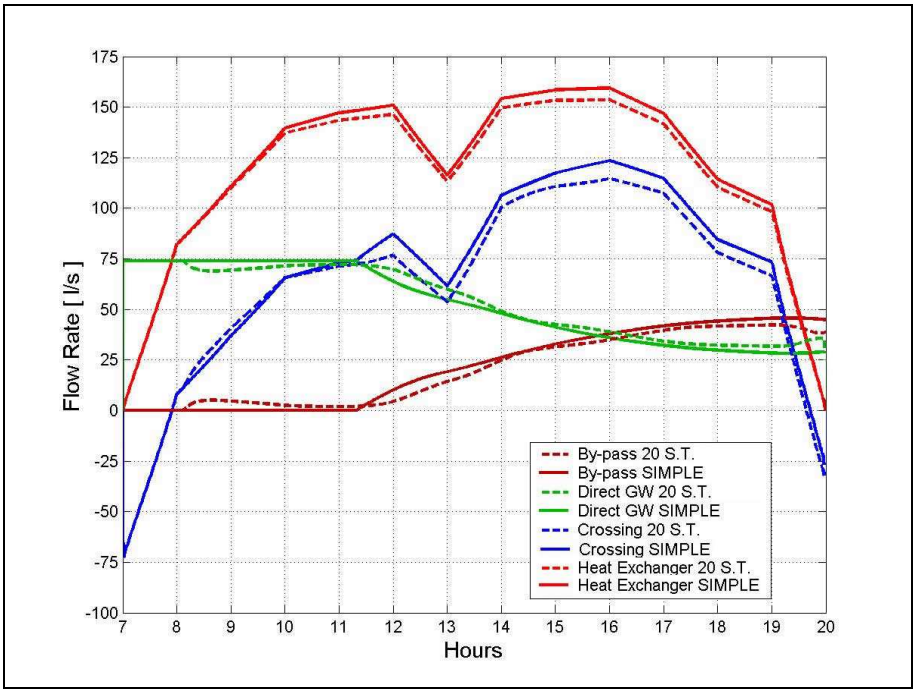

Figure 29 – Comparison between simple tank and 20 multi connected sub tanks about flow rate through heat exchanger, crossing flow rate through the tank, by pass flow rate and GW flow rate directly entering the tank.

Multi connected pattern shows an initial slightly bad performance about ground water flow rate directly entering the tank and crossing flow rate through the tank. That is why first sub-tank is quickly overheated, see Figure 25, and a little groundwater by-pass is needed, because the temperature difference through heat exchanger slightly overtakes the value by 5 degrees and return maximum temperature by 20°C is violated.
However, the first tank overheating is a benefit because it allows groundwater thermal capability to be fully used during initial hours and useless thermal storage to be avoided.

Moreover tank partitioning results in a more efficient restoration phase due to storage efficiency improvement.

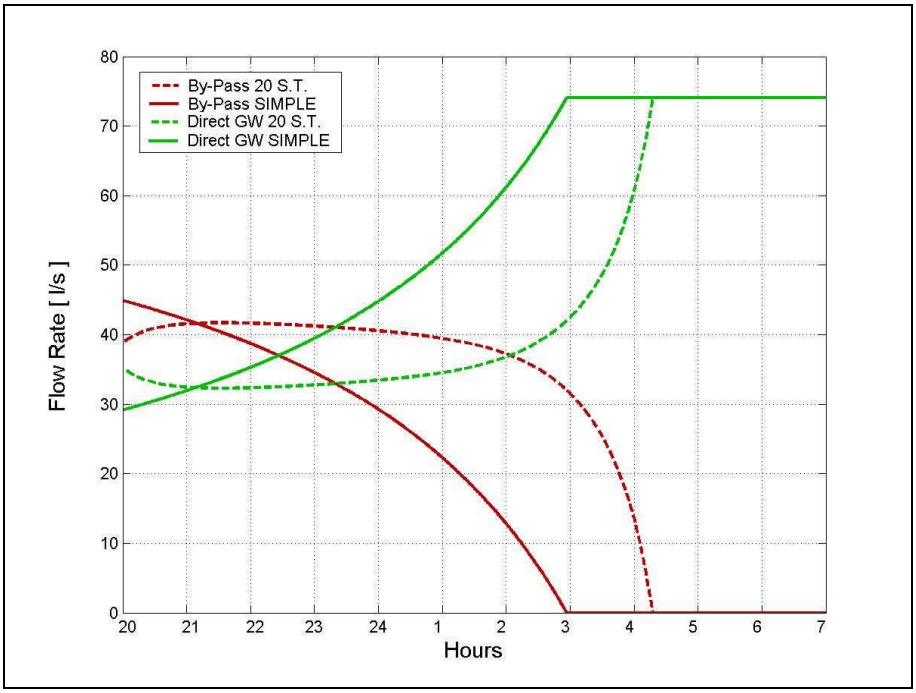

Figure 30 – Comparison between simple tank and 20 multi connected sub tanks about restoration phase.

Tank partitioning causes mixing diffusion reduction and a fully heat exchange period extension so that daily thermal storage strategy is feasible.

3.5.2. Simulation of the winter critical day

Simple tank applied to winter case leads to external units shut off temperature to be reached, unless severe pumping consumption is paid in order to keep minimum heat exchanger approaches.
Multi connected pattern separates cold heat exchanger output from the system supply temperature and allows an higher heat exchanger approaches to be preserved.
As a result, whenever groundwater reached minimum temperature of 12°C, it could lead to a danger with a simple tank configuration because external units supply temperature could overtake the minimum threshold of 10°C and pumps maximum flow rate would be achieved, in a manner that engines could be forced to a sudden safety block.
A back-up boiler in series to water loop should be necessary in such a case.

Multi-connected configuration avoids such an emergency and permits a better pumps operation.
The current system is then subjected first to a simple tank and than to a 10 sub tanks multi connected under the critical winter day boundary conditions (cloudy January), in order to emphasize performance differences.

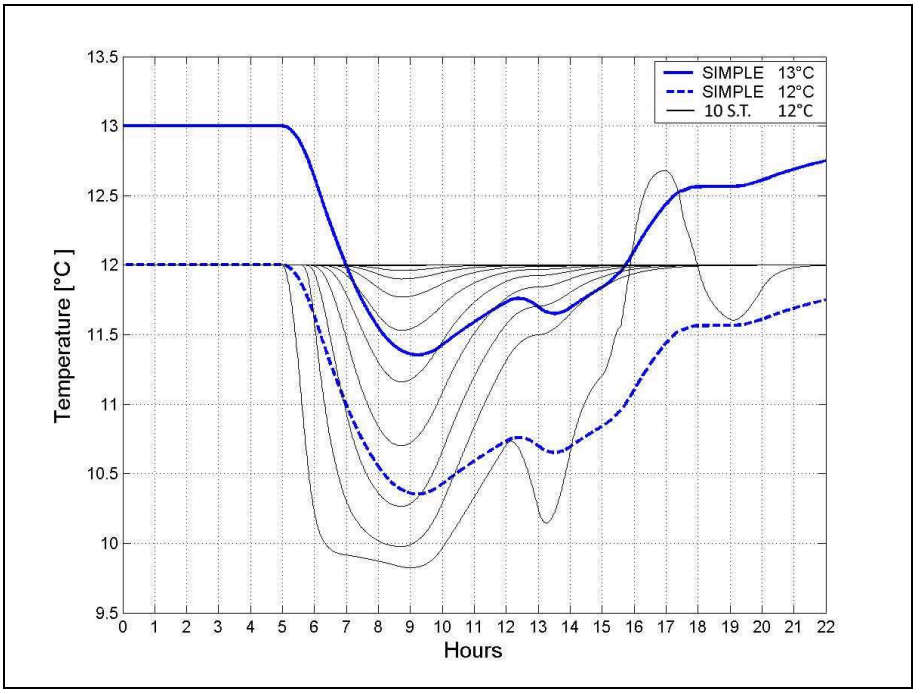

Figure 31 – Comparison between simple tank and 10 multi connected sub tanks in the winter critical day.

As we can observe, simple tank assures proper operation if winter groundwater temperature were above 12°C, vice versa minimum temperature of 10.5 °C is expected to be supplied to heat exchanger. Remember that variable flow rate pumps address to a constant temperature of 10°C during the winter so that a very severe approach of a half degree would be required to be maintained. That will lead maximum variable pumps flow rate to be reached and external units minimum temperature set-point to be eventually lost.
Note that after the first few hours, the first tank behaviour deviates from the adjacent sub tanks temperature profiles. It happens because on duty restoration occurs. Then, the first tank remains the only one subjected to heat exchanger output signals.

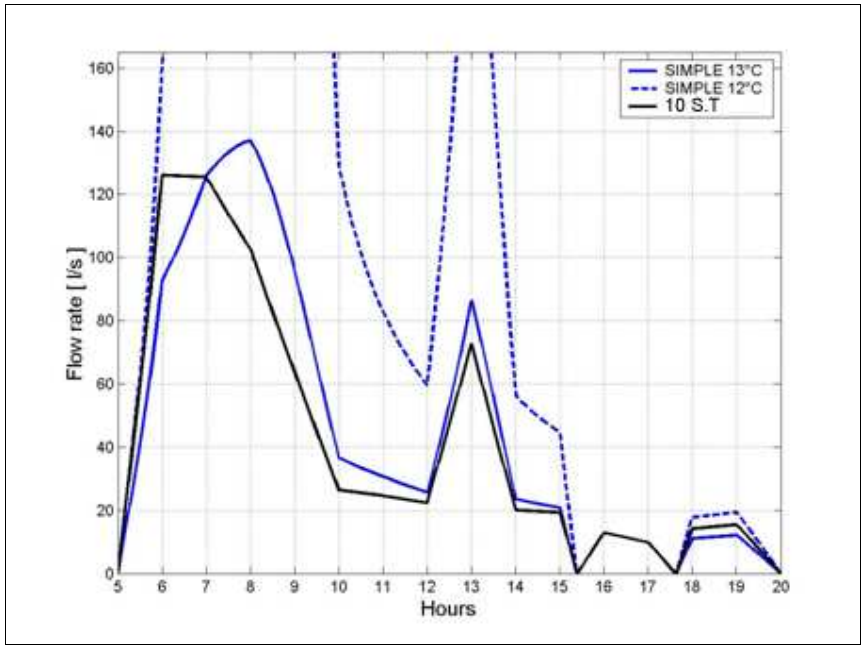

Figure 32 – Comparison between simple tank and 10 multi connected sub tanks about flow rates through heat exchanger.

Under the value of 13°C groundwater temperature, simple tank is not recommended.
Even if groundwater temperature were 12°C, the multi connected tank pattern allows supply temperature to heat exchanger to be constant and pumps flow rate to be adequate.

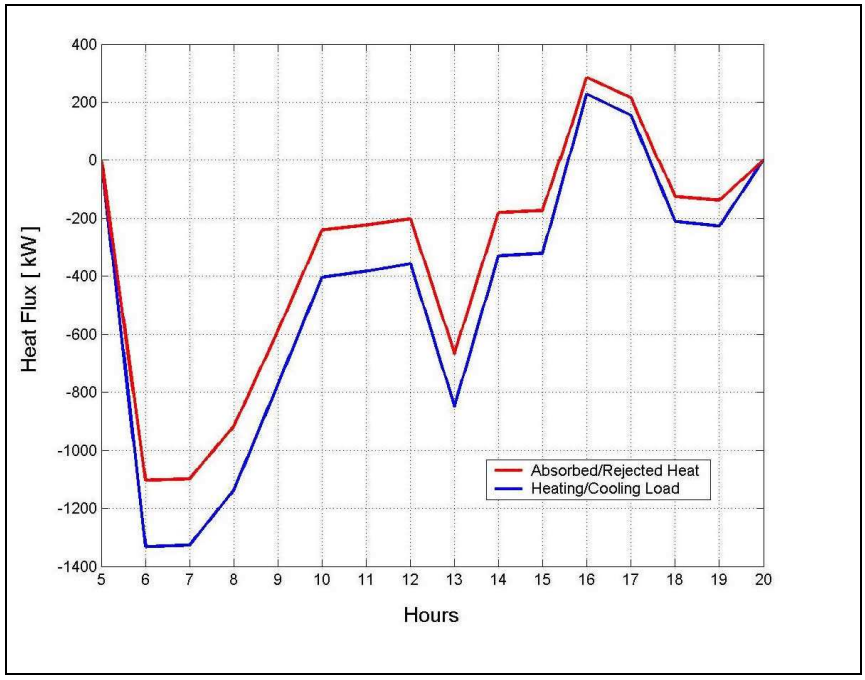

Figure 33 – Absorbed/Rejected heat fluxes against heating/cooling loads.

Even at the winter critical day, offices glazed curtains as well as lighting gains yield to a cooling load period during the evening.
Absorbed/rejected heat flux curve represented in Figure 33 is valid either for multi-connected tank case than the simple tank because external units operate under 50% combination factor all over the day. Thus intermittent working is assumed and the same resulting COPs is considered in both situations.

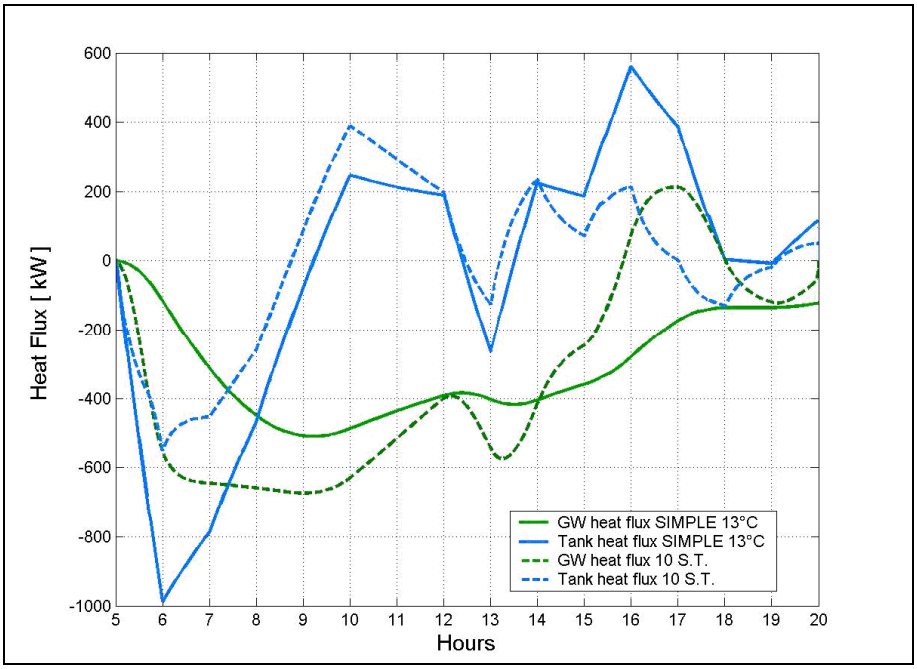

Figure 34 – Comparison between simple tank and 10 multi connected sub tanks about heat fluxes exchanged either by the tank than by groundwater during the system operation.

As we could notice for the summer case, tank partitioning allows best groundwater utilisation so that tank overheating or overcooling is minimized.
Moreover, as heat flux arithmetical signs are opposed, restoration on duty occurs.

3.6. Convergence between piston flow and multi connected tanks

Separating the tank volume into sub-volumes, so that they are physically independent and mutually adiabatic, it makes the temperature forcing signal coming from the building to be delayed at the last tank. Maximum vortex diameter is limited and short-circuits avoided.
Partitioning benefit could be easily understood by imaging what will happen whether perfect piston flow occurred.
Referring to summer case as an example, during operation period, water supply by 15°C to heat exchanger is maximized, so that its duration matches with tank filling period. That way external units COP is maximum during initial few hours. Moreover this implies that

rejection heat is limited too, as a consequence groundwater flow rate through heat exchanger is also the lowest. Therefore initial piston flow tank filling period is also the longest possible. Nevertheless, as heat exchanger inlet temperature is maintained at 15°C, a proper heat exchanger approach control around 5°C, along with a correct heat exchanger surface design, naturally lead to a temperature returning to the tank that equals or slightly overcomes 20°C. That way maximum groundwater thermal utilisation is always granted and tank duty suitably is minimized.

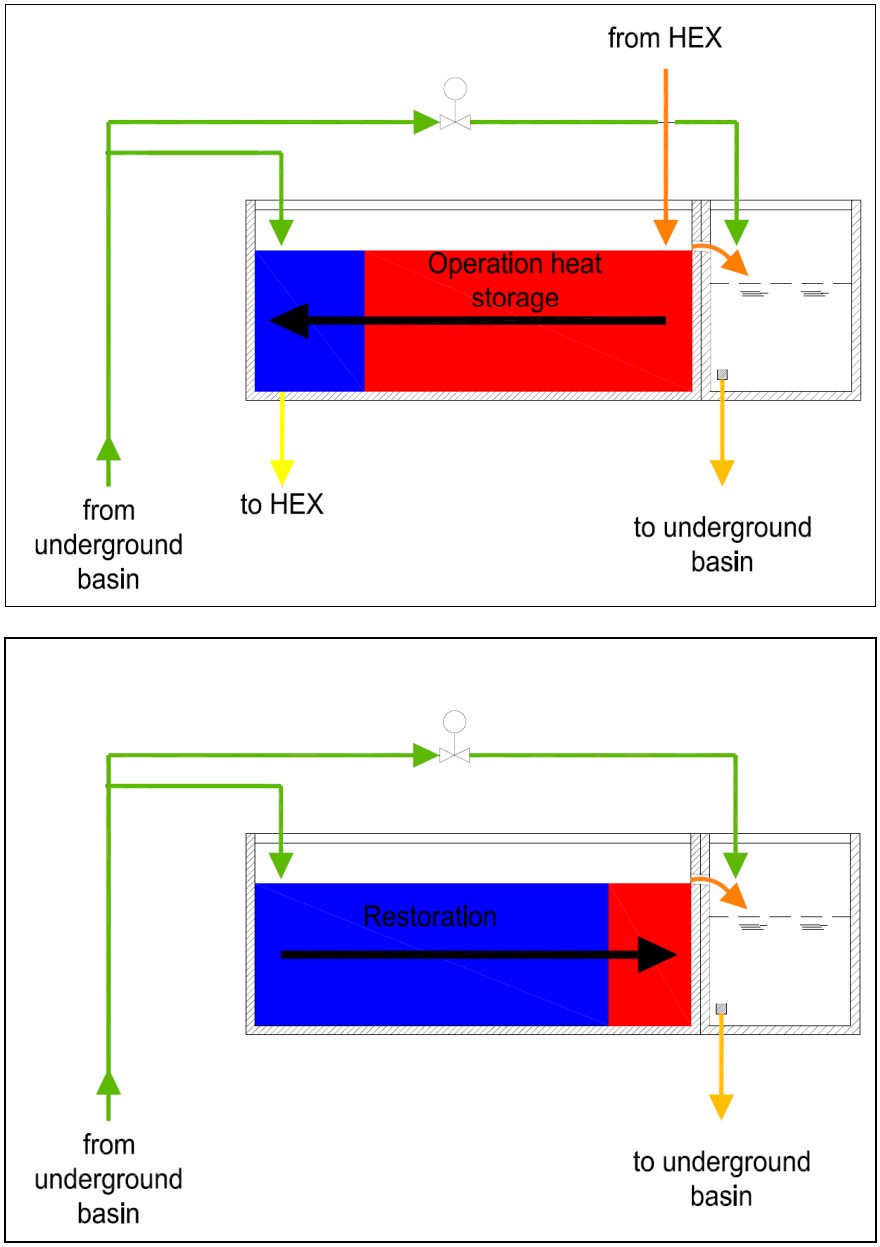

Figure 35 – Piston flow effects on storage efficiency.

Restoration is optimized as well under piston flow assumption. Restoration period perfectly overlaps with fresh groundwater tank filling period. However, remember that during the

system shut off period, fresh groundwater flow rate directly entering the tank depends on water temperature at weir. As it were bigger than 20°C, the bypass flow rate would be suitably modulated to control return temperature to the underground basin. That makes the actual filling period different form the constant available groundwater flow filling period of the tank global volume.
Anyway, it should be said that piston flow permits the smallest tank overheating during system operation. As a consequence, no matter what will be the temperature hourly curve at weir during restoration, under piston flow assumption, restoration period will be the shortest possible, for a given tank subjected to a given heating or cooling pattern. Furthermore, starting from a given temperature distribution within the tank, after system operation, and assumed that average temperature within that distribution overcomes return temperature limit by 20°C, piston flow will absolutely assure the maximum period of constant heat exchange between groundwater and the tank.

Therefore, if on one hand it is definitely pointed out that piston flow should be recommended, on the other hand, it seems that tank partitioning could lead to piston flow performances.
In order to demonstrate this trend, a Matlab routine has been developed to evaluate piston flow incidence on the given system. Moreover, convergence has been investigated between multi connected tank performance at rising number of sub tanks and piston flow.

Following figures denote convergence at increasing number of sub tanks of hourly temperature profiles during system operation period.

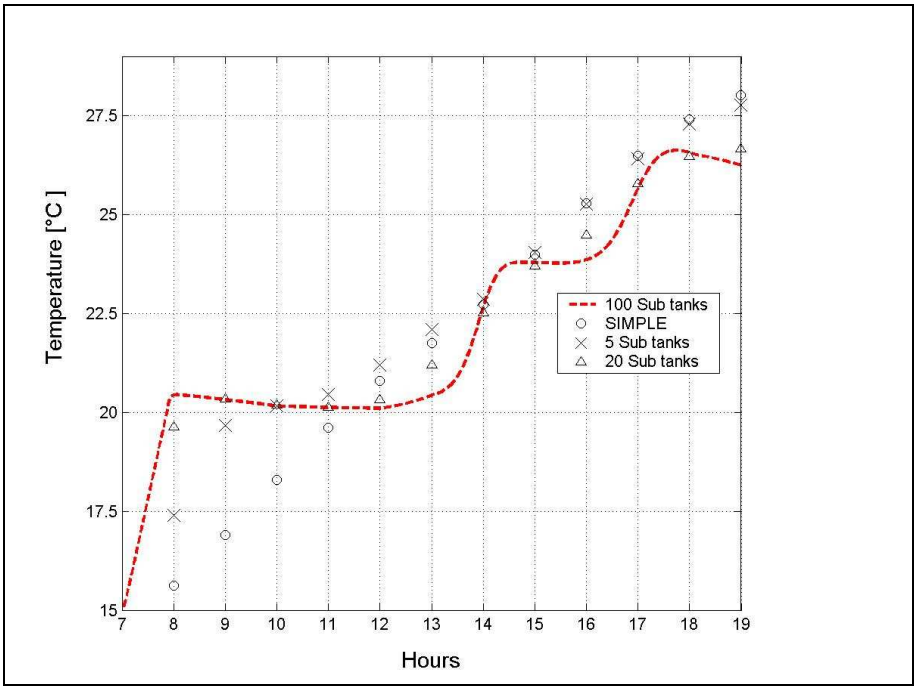

Figure 36 – Convergence of the first sub tank temperature profile.

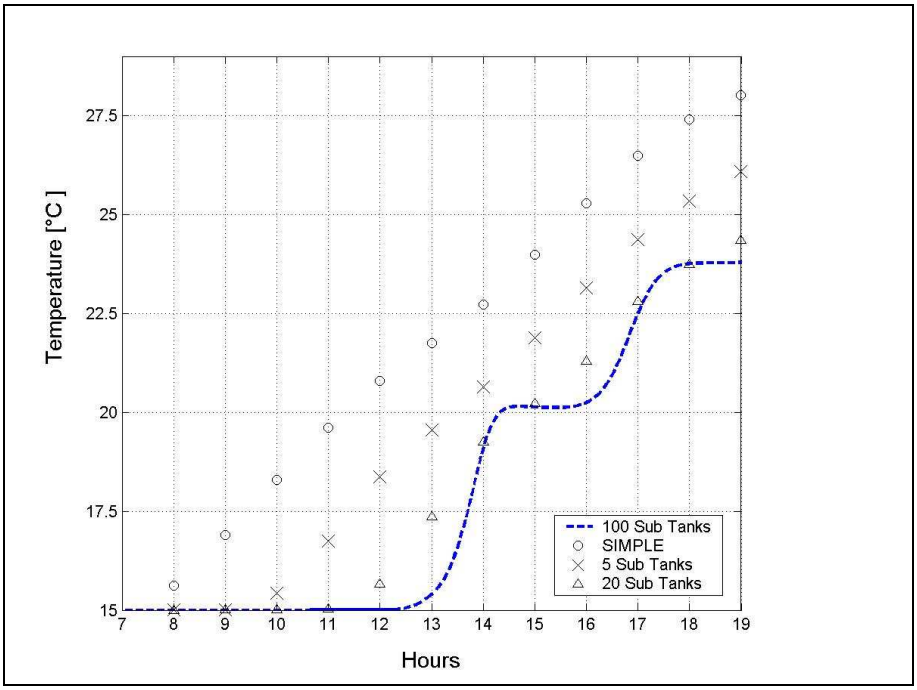

Figure 37 – Convergence of the second last sub tank temperature profile.

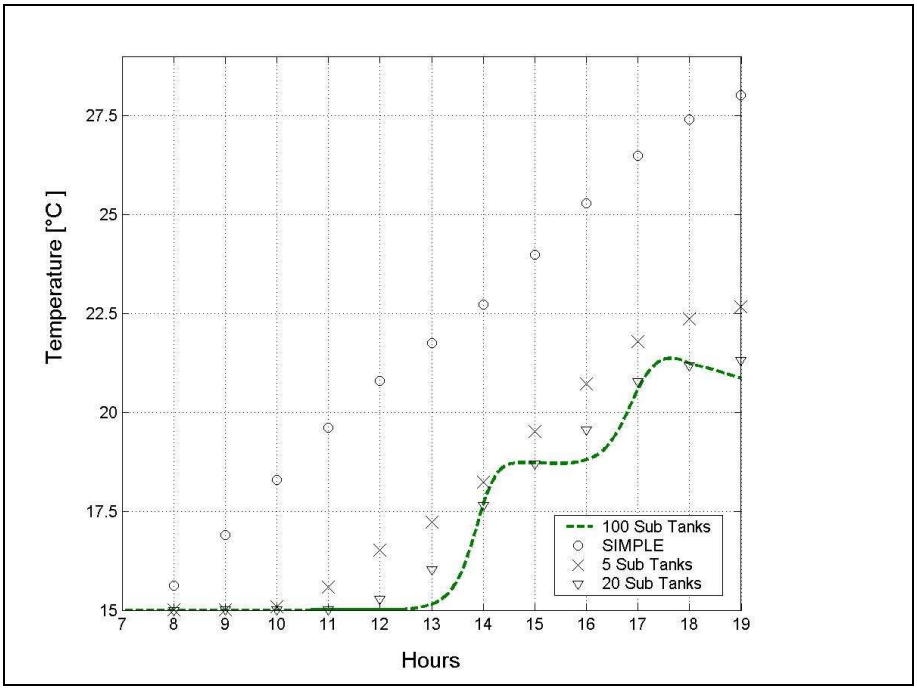

Figure 38 – Convergence of the last sub tank temperature profile.

Next figure shows the correspondence, in terms of flows concerning the tank operation, that has been detected between a theoretical piston flow tank and a multi-connected tank groundwater thermal storage systems.

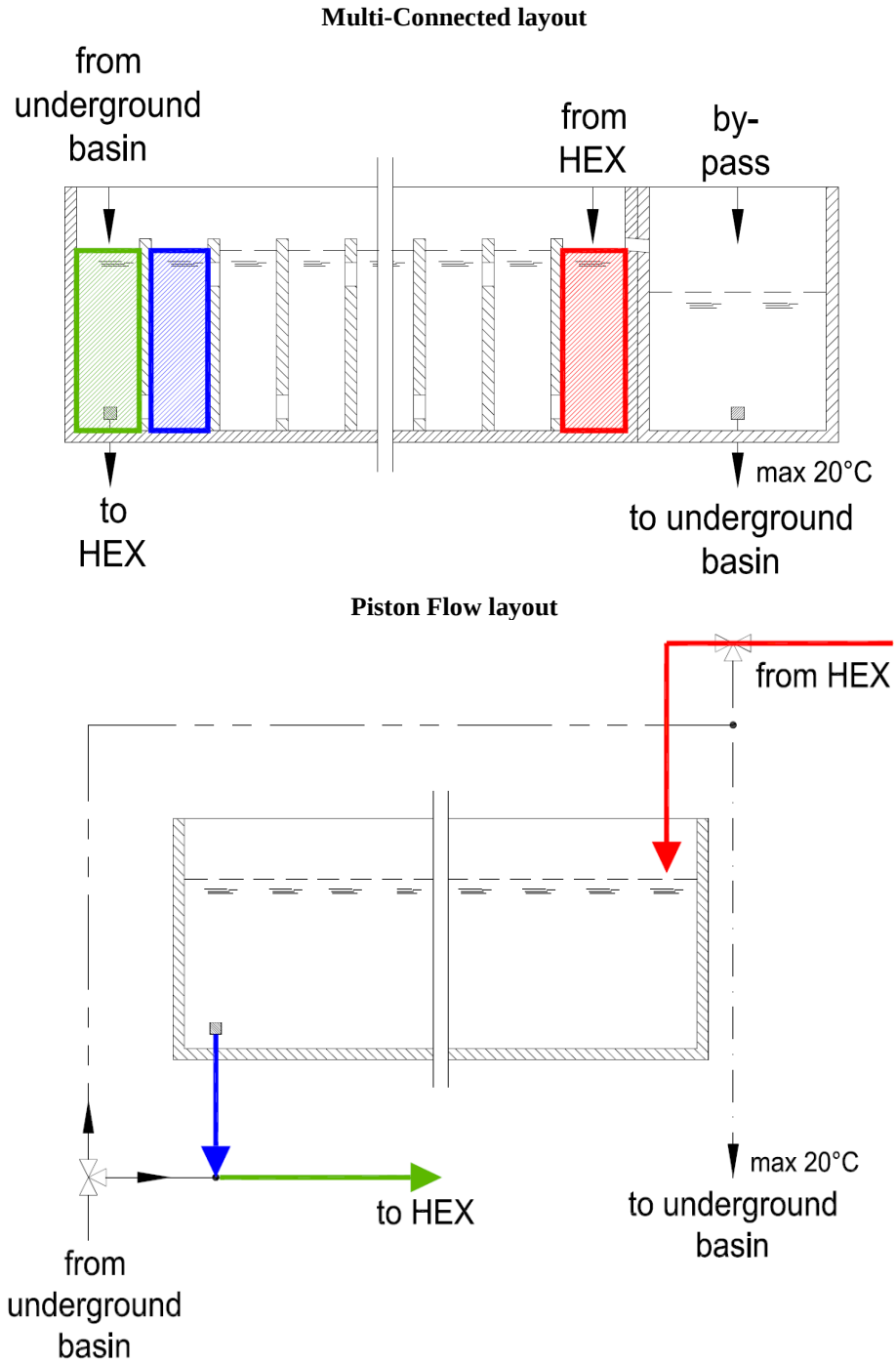

Figure 39 – Flows chromatic correspondence between a piston flow tank system and a multi-connected tank one.

Especially, a chromatic key has been taken in place in order to identify, within the following figure, the temperature signals associated to the each flow.

In Figure 40, during the operation period, temperature profiles for an hypothetic 100 sub tanks multi-connected tank (dashed lines) are perfectly fitted by piston flow representative temperature curves (solid lines).

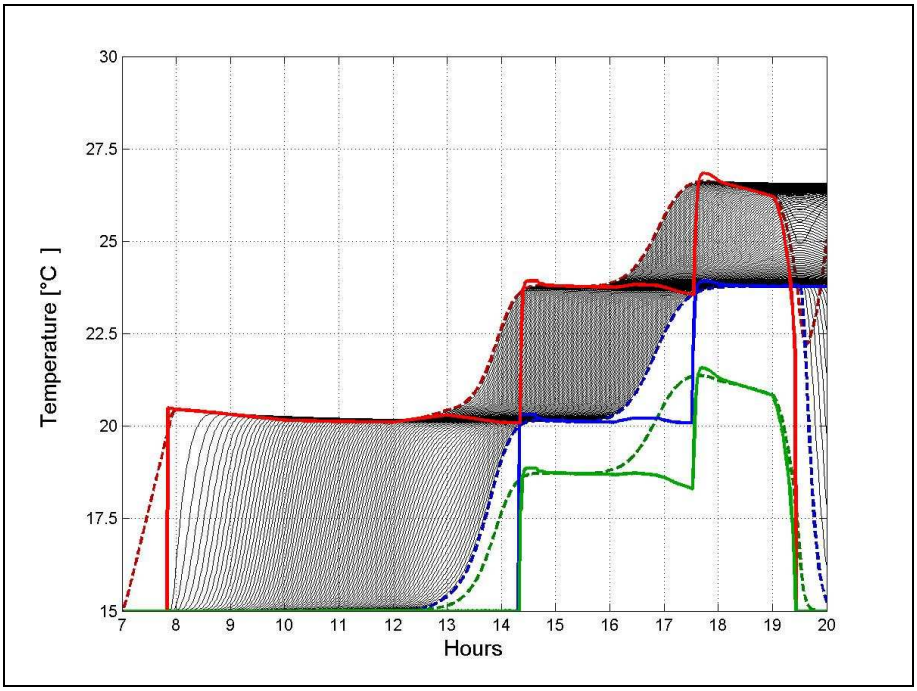

Figure 40 – Convergence between multi connected (dashed lines) and piston flow models: temperatures profiles (solid line) – operation phase.

First tank, second last tank and last tank multi connected temperature profiles clearly tends towards piston flow law.

Groundwater flow rate directly entering the tank and by-pass flow rate converge as well to corresponding piston flow signals as follows.

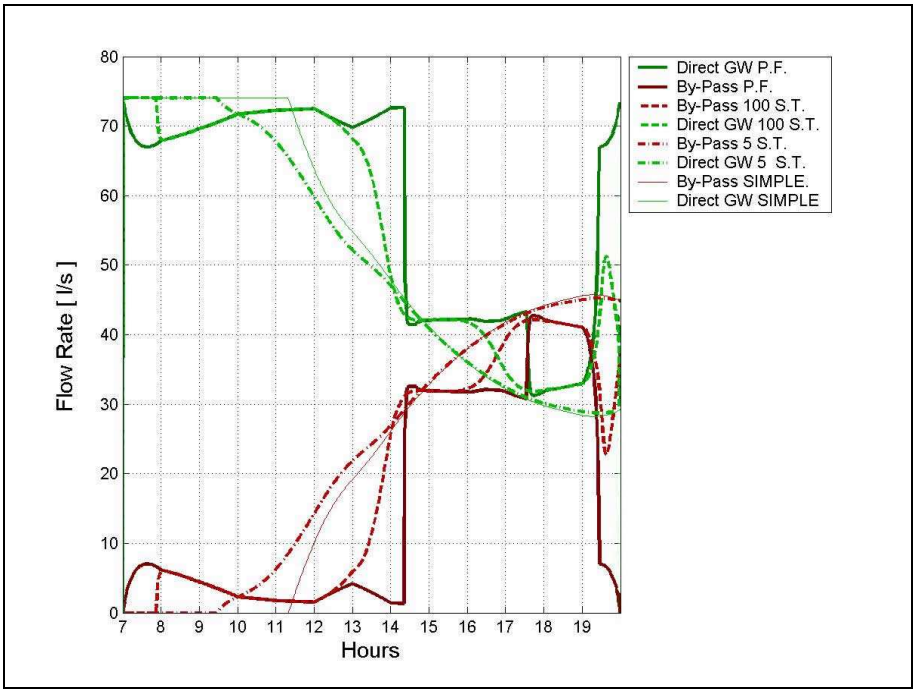

Figure 41 – Convergence between multi connected and piston flow models: flow rates profiles - operation phase.

Restoration period and electrical energy consumption have been evaluated at increasing number of sub-tanks and at different global tank volumes V under multi-connected fully mixed tank hypothesis, in order to investigate tank partitioning implications and the critical number of tanks over which piston flow could be allowably assumed.
Restoration period has been evaluated as the period after system shut off that is necessary to reach the starting temperature by 15°C, with a 5% tolerance range with respect the exact temperature value. The criterion is applied to the first tank in the case of multi-connected pattern.
Daily average COP has been investigated has the ratio between total heat removed form the building during the critical summer day on total daily compressors electrical consumption.

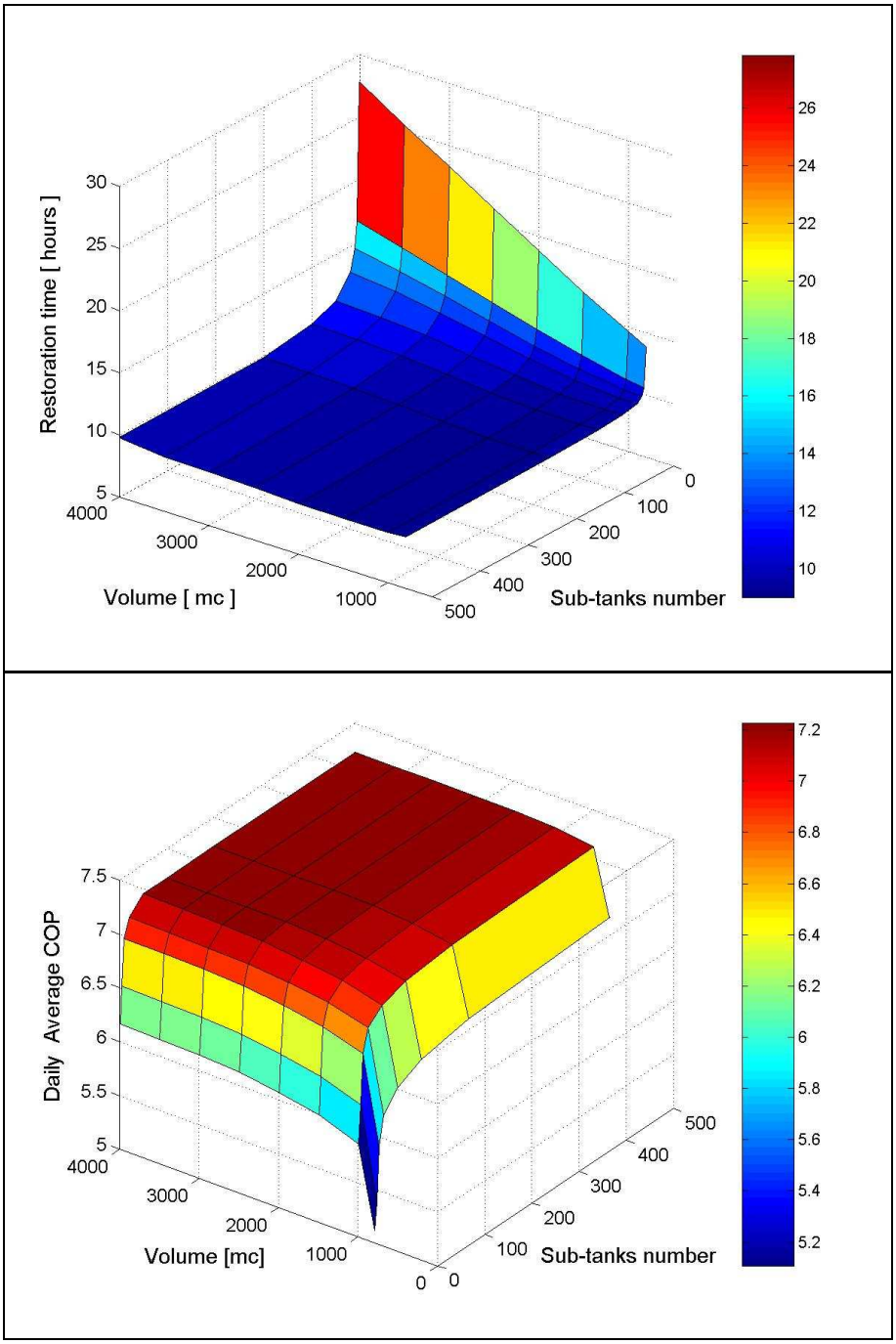

Figure 42 –Restoration period and average COP surfaces related to global volume V and sub-tanks number.

Surfaces contour analysis could led to a more significant investigation.

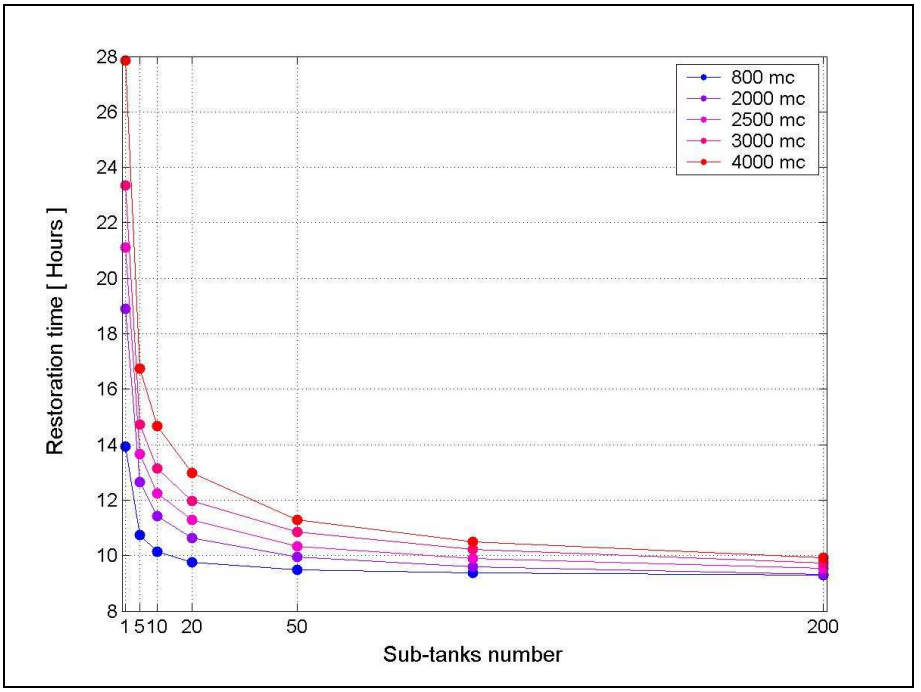

Figure 43 – Convergence between multi connected and piston flow models: restoration period

Restoration period drastically decreases as number of sub tanks overtakes 10 to 15 tanks.

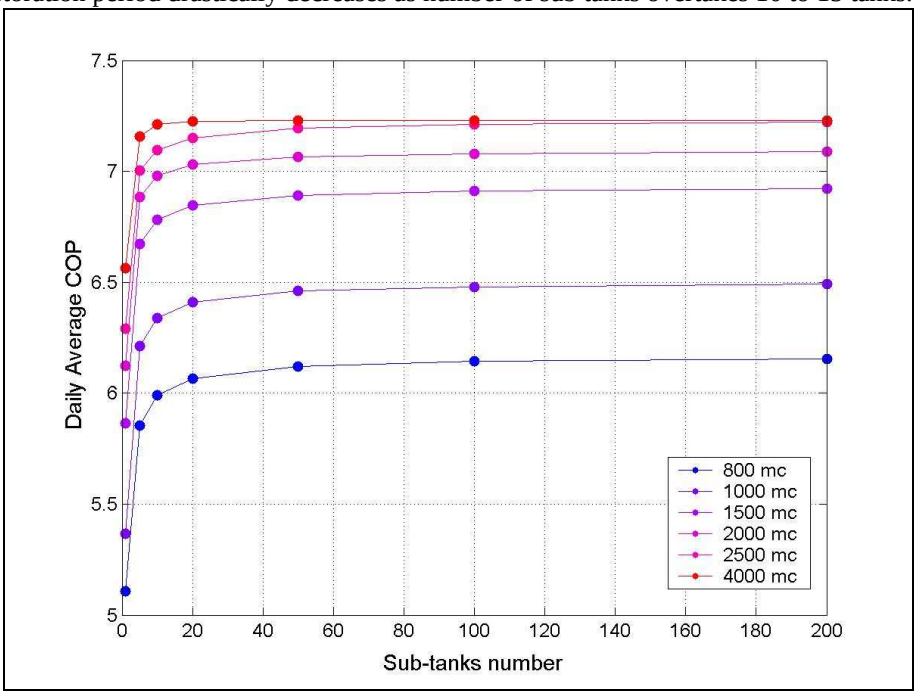

Figure 44 – Convergence between multi connected and piston flow models: daily average COP

On the other hand a quite important electrical energy saving is expected to be obtained in response to tank volume partitioning.

Finally, mixing temperature transportation results in a big issue with respect to daily storage feasibility and it has an influence as well on external units COPs.

For instance, restoration periods and COPs distributions along with tank volume increasing are interesting to be analyzed.

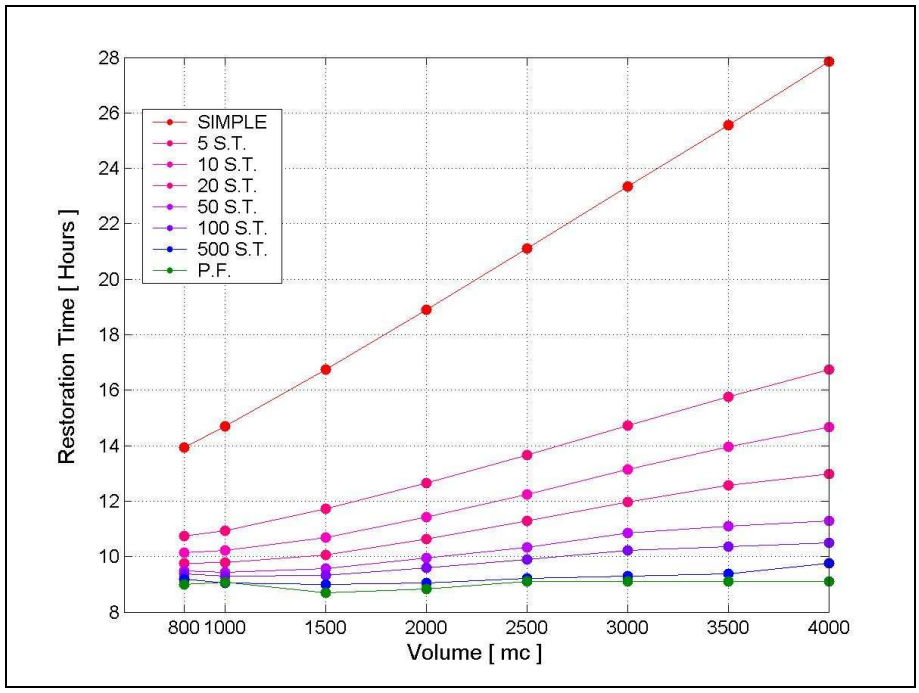

Figure 45 – Convergence between multi connected and piston flow models: restoration times at increasing number of sub-tanks with respect to piston flow, along with increasing volumes .

Simple tank restoration time law tends to be linear, in accordance to the following analytical expression that is valid for constant initial temperature t_0.

$$\theta_{res} = \frac{V}{Q_{GW}} \left[\frac{(t_0 - t_{in})}{(t_{\lim} - t_{in})} - \ln\left(\frac{(t_{5\%} - t_{in})}{(t_{\lim} - t_{in})} \right) \right] \qquad \textbf{Eq. 18}$$

Note that under piston flow hypothesis, there is a threshold tank volume over which restoration time doesn't increase any longer. Actually there is a volume at which tank is not filled more than once which will be identified as the threshold restoration period volume .
If heat exchanger temperature difference were controlled to exactly 5°C, that threshold volume would correspond to minimum groundwater volume necessary to make current building conditioning without thermal storage aid.

3.7. Thermal storage feasibility

In the previous paragraphs, it has been outlined that the current system performances are limited on one side by VRV® allowable operation temperatures and on the other side by the maximum available period for daily tank restoration. Depending on the climatic boundary conditions, to the underground water availability and to the tank global volume V, those thresholds could be reached or not during the critical summer and winter days.
Given that the summer critical day yields a bigger amount of heat to be stocked within the tank with respect to the winter case, the summer critical day case will be treated first in order to produce a quick design tool useful to infer the system storage strategy feasibility field.

As a matter of fact, external units maximum permitted inlet temperature t_i during cooling operation is by 45°C and the maximum restoration period matches with the period of non-occupancy of the building, by about 10h.
Similarly to Naki, Shucku and Sagara, a few dimensionless coefficients could be taken in place that uniquely identify boundary conditions which the current system is subjected to.

- R_V is called volume ratio and represents the ratio between the actual tank global volume V on total ground water available volume all day long: it measures the piston flow restoration capacity.
- R_C is called load ratio and represents the ratio between the maximum cooling load and the constant GW cooling capacity: it measures how much the storage philosophy is suitable.

Nevertheless, R_V / R_C points to tank predictable overheating .
For each couple (Rv,Rc), for a given cooling load curve shape (for the current system refer to Figure 8) and for the outlined system regulation method and number of sub-tanks, the compliance of the system response to the restoration time and inlet temperature thresholds could be tested in order to define the system feasibility field.
In the paper [19] it was pointed out that such a graphical representation could be very useful in order to preview the underground water thermal storage strategy success, starting from the current couple (Rv,Rc) and taking into account storage efficiency losses.

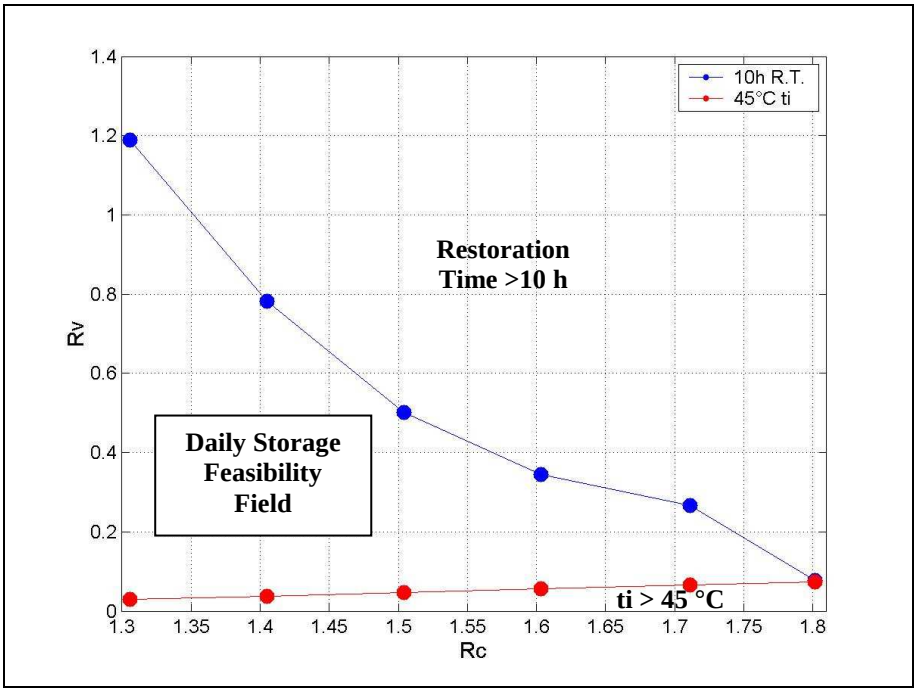

Figure 46 – Feasibility field for an office building GW thermal storage system conditioned by VRV® - (2% tolerance restoration time)

Figure 46 is valid for a 20 sub tanks multi connected tank applied to cooling load patterns shaped has in Figure 8and comes from several Matlab simulations run under the system control logics described in previous paragraphs.

Remembering that high inlet temperatures yield poor external units energy efficiency, moving throughout the (Rv,Rc), there is an inverse relation between restoration period improvement and VRV® coefficients of performance.

Considered that winter threshold by 10°C of input temperature to external units is much nearer to the underground water temperature than the summer temperature threshold, a winter feasibility test should be suitably undertaken after the summer condition will be verified, in order to completely infer system feasibility. However, given the low intensity of energy demand in winter, the bound condition connected to winter critical delivery temperature by 10°C will provide a negligible limitation on feasibility filed of Figure 46Figure 46 – Feasibility field for an office building GW thermal storage system conditioned by VRV® - (2% tolerance restoration time), as the summer temperature bound already does.

3.8. All year long simulation

The summer critical day analysis has shown that electrical energy could be reduced by choosing a multi-connected pattern with respect to simple tank system. Although such a result cannot be meaningful stand-alone, but it could gain an economic importance by an annual saving estimation.

An all year long simulation has been undertaken in order to quantify the electrical energy saving which could be earned by tank partitioning. The available global tank volume has been preserved constant along with the two simulations: V= 1200 m^3.
The analysis assumptions are listed in the following table in terms of sunny/cloudy days distribution within each month and groundwater temperature.

Month	Percentage of cloudy days	Percentage of sunny days	Total working days	Groundwater temperature[°C]
1	88%	12%	21	13
2	76%	24%	20	13
3	43%	57%	21	13
4	44%	56%	21	15
5	45%	55%	21	15
6	38%	62%	20	15
7	28%	72%	22	15
8	26%	74%	16	15
9	34%	66%	21	15
10	62%	38%	21	13
11	83%	17%	21	13
12	91%	9%	15	13

Table 1 – Annual simulation assumptions .

Please refer to Figure 20 and Figure 21 for cooling loads and heating loads.
Total number of modelled days matches with total working days for a typical year.
Holidays, summer annual leave days and every Saturday will be considered as shut-off periods for the system.
The simulation has been made under simple tank system hypothesis as well as under 20 sub-tanks multi-connected tank pattern in order to infer compressors electrical energy saving due to tank partitioning.
Since the storage cycle is closed under the critical summer day, the 20 sub-tanks multi-connected tank complies with daily storage strategy under the current annual loads conditions.
Thus, energy consumption could be calculated as the sum of cloudy days and sunny days individual contribution all along the working year. Actually the sunny and cloudy energy contribution has been split within the monthly balance with respect to the related duration percentage reported within the table.
Although, in the case of simple tank, on typical days of May, June, July, August and September, the daily storage fails so that a weekly simulation is needed in order to correctly infer the electricity consumption.

So, following typical weeks have been assumed taking into account the duration percentages of cloudy days with respect to sunny days for each current month. These assumptions have been chosen with the aim to promote the weekly restoration of the tank so that the final consumption estimations will be careful and eventually better than reality.

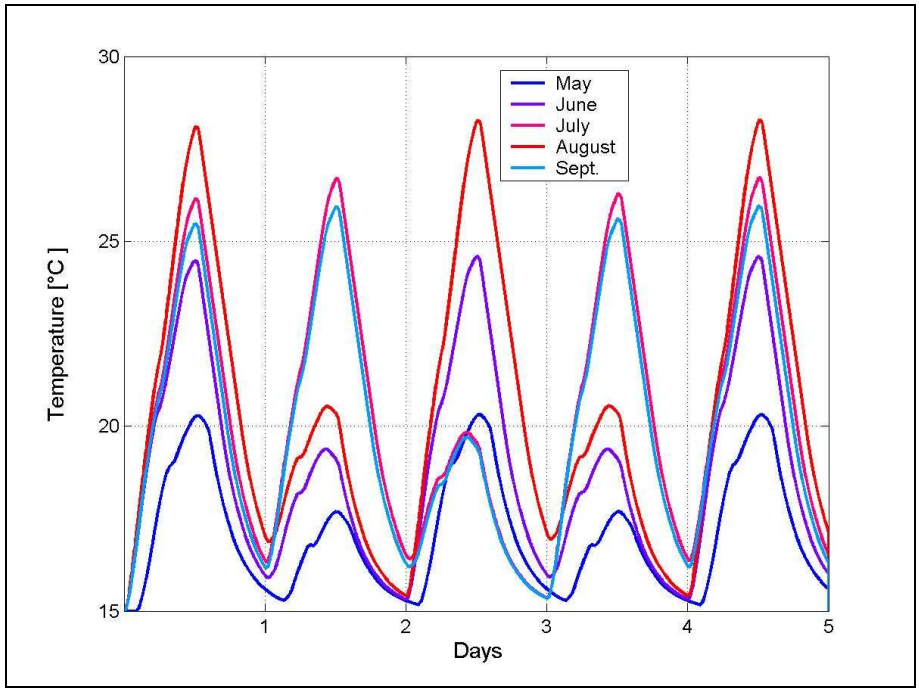

Figure 47 – Typical weeks temperature profiles for simple tank systems summer months .

The electrical energy consumption inferred from each typical monthly week has been calibrated with respect to actual working days within the current month in order to imply the monthly significant consumption.
Finally the following comparison has been obtained:

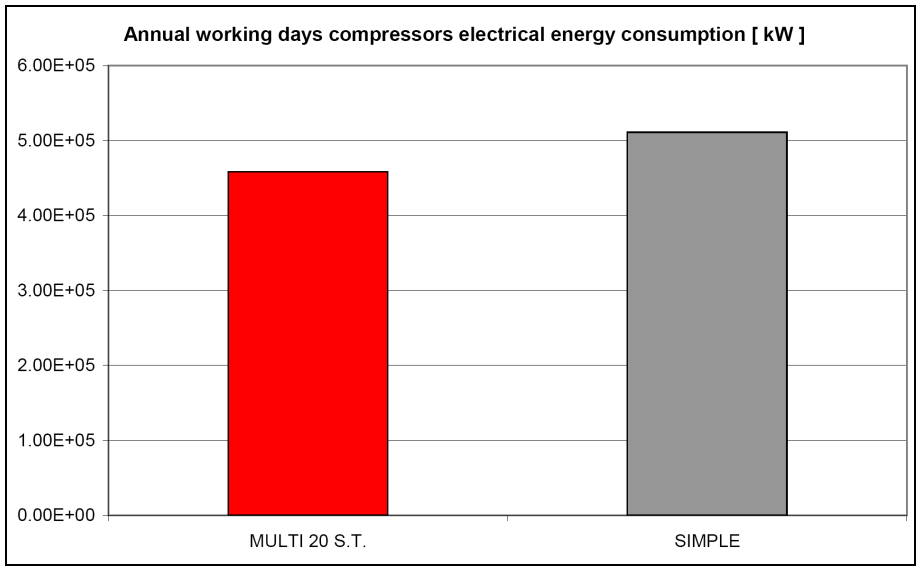

Figure 48 – Comparison between a 20 sub-tanks multi-connected system and a simple tank system: annual electrical energy consumption.

A calculation saving by 10,34% could be earned by tank partitioning.

Moreover, tank partitioning also leads to strong tank-side variable flow circuit flow-rates reduction that yield outstanding pumping power savings.

3.9. Model Validation

The prepared Matlab model could be adapted to any water thermal storage system. As matter of fact it has been applied to a case study that neither lays on VRV technology than refers to underground water withdrawal.
Nakahara [4] carried out several experiments on water storage tanks connected to chilled water generators and HVAC terminals. Many different load schemes have been analyzed in accordance to a few schedules of generator and terminals operation. An empirical correlation has been inferred by experiments in order to preview storage efficiency, depending on specific patterns of the system features. As well, Nakahara proved the convergence of a complete mixing numerical model towards empirical results.
One of Nakahara case study has been chosen in order to verify the Matlab model consistency.

A 280 m^3 multi-connected tank is partitioned into 10 sub-tanks. It is subjected to a flat schedule chiller operation and serves two different HVAC circuits.
The first is a variable flow-rate system that is controlled in the same manner as groundwater secondary circuit we talked about in previous paragraphs.
The second one is a constant flow circuit (e.g. direct expansion terminals, as VRV external units).
In order to achieve a good storage efficiency, a delivery temperature control is provided for both generators and constant flow terminals, through a three-ways valve engine.

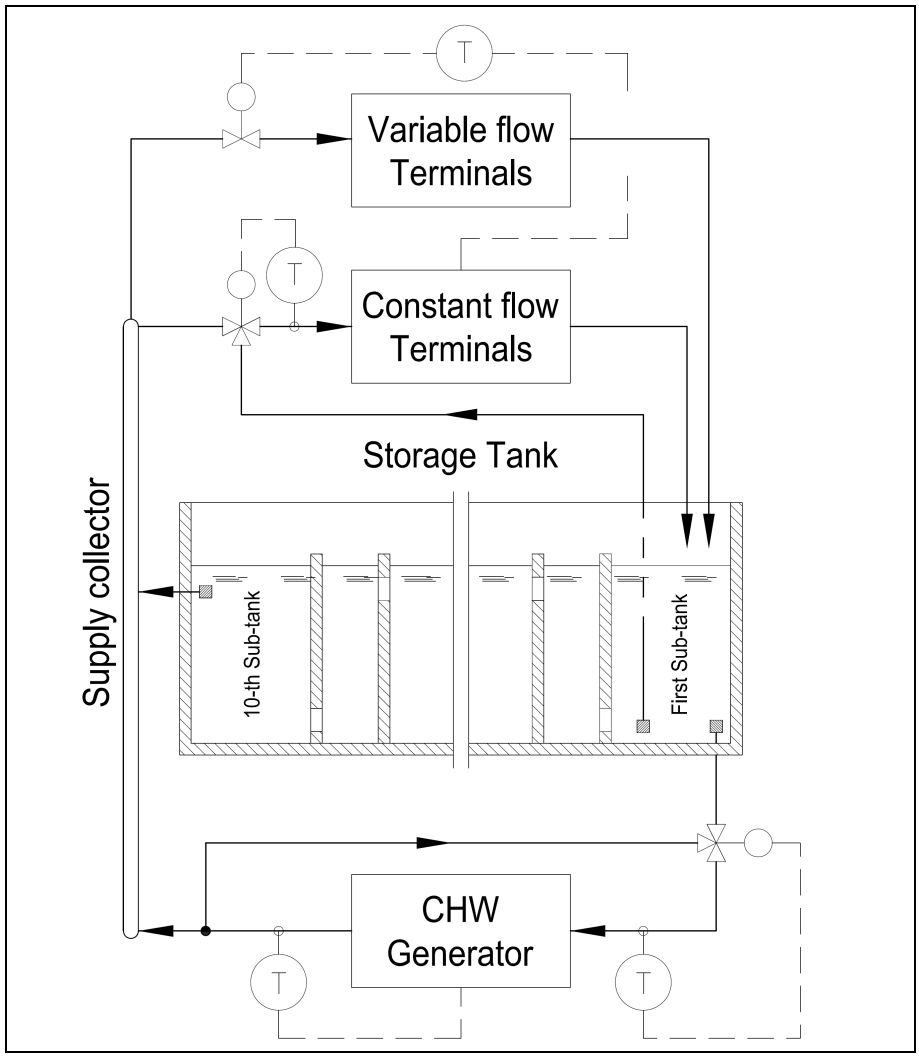

Figure 49 – Validation system.

Unlike the groundwater case study, the current system presents HVAC water delivery from a collector. This collector connects the tank outlet to the HVAC supply circuits as well to the generator output pipe.

Nakahara introduced a storage efficiency factor as the ratio between the actual heat stored during the operation period and a theoretical tank heat capacity.
That capacity is evaluated in accordance to a weighted average value of temperature difference Δt_0 to which the tank is expected to be subjected by HVAC systems work.

$\varepsilon = \frac{H_{stored}}{V \rho c \Delta t_0}$	**Eq. 19**

The theoretical storage capacity should be interpreted as the maximum heat that could be stocked within the tank after one filling period under Δt_0 temperature difference signal.

The current system significant parameters are the following:

- Chiller schedule duration 24h (at about 93% part load)
- Chiller design cooling capacity: 560 kW
- Chiller controlled inlet temperature: 9°C
- Chiller controlled outlet temperature: 5°C (equals the basic storage temperature)
- HVAC systems weighted average temperature difference on cooling loads (Δt_0): 12°C
- Daily cooling energy to deliver: 46057 MJ
- Heat to be stored: 21538 MJ

Starting from those input conditions, Nakahara calculated the collector hourly temperature profile and the last tank temperature curves along the typical daily behavior. Moreover, Nakahara provided a number of tanks on temperature diagram, in which spatial temperature distribution within sub tanks is outlined for each operation hour.
Then, the Matalb model has been adapted to the previous basis in order to provide the same graphical output as the ones supplied by Nakahara.
The following figures highlight a tolerable match between the Matlab simulation and the Nakahara results.

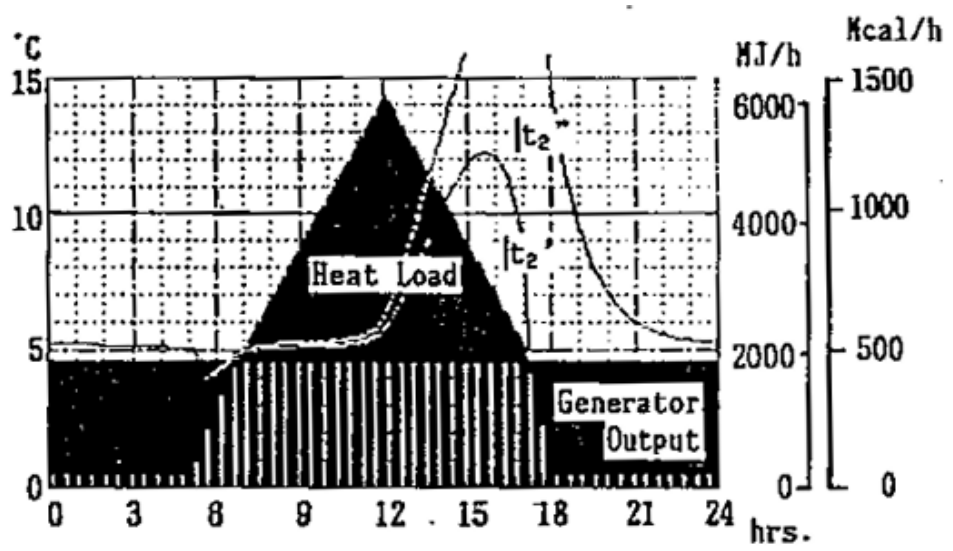

Figure 50 – Validation exercise: cooling loads, generator capacity and schedule, significant temperature profiles –Nakahara results

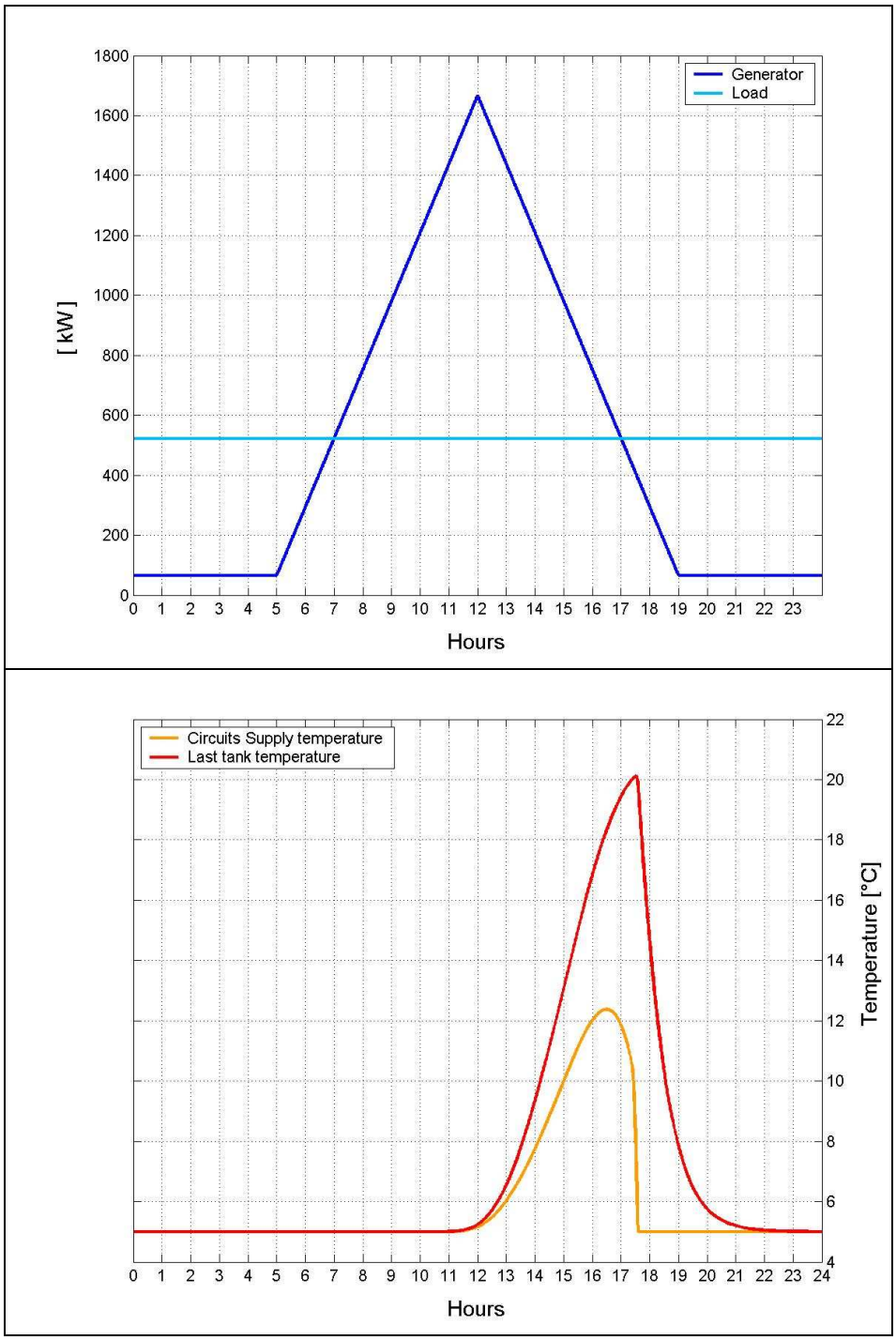

Figure 51 – Validation exercise: cooling loads, generator capacity and schedule, significant temperature profiles –Matlab results

Little deviations are due to the actual terminal types and sizes, as well as to uncertainty on operation parameters or controls, that are unknown factors in the author's paper.

Agreeable assumptions were made to better cope with Nakahara evidences.
Hourly temperature profiles have been evaluated by Matlab for each sub-tank.

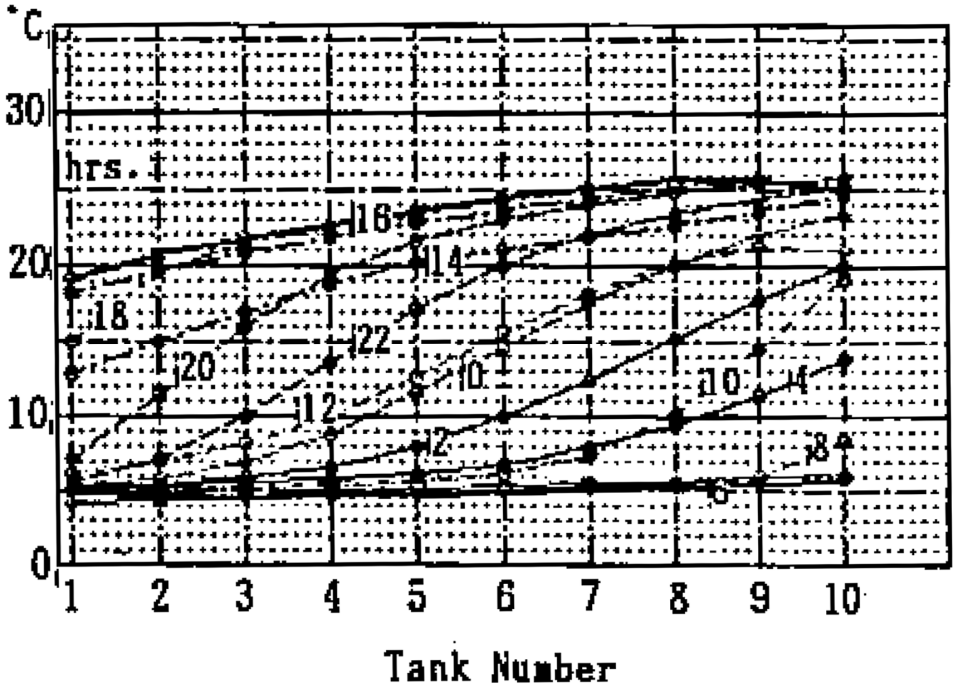

Figure 52 – Validation exercise: spatial temperature profiles at significant operation hours: Nakahara results.

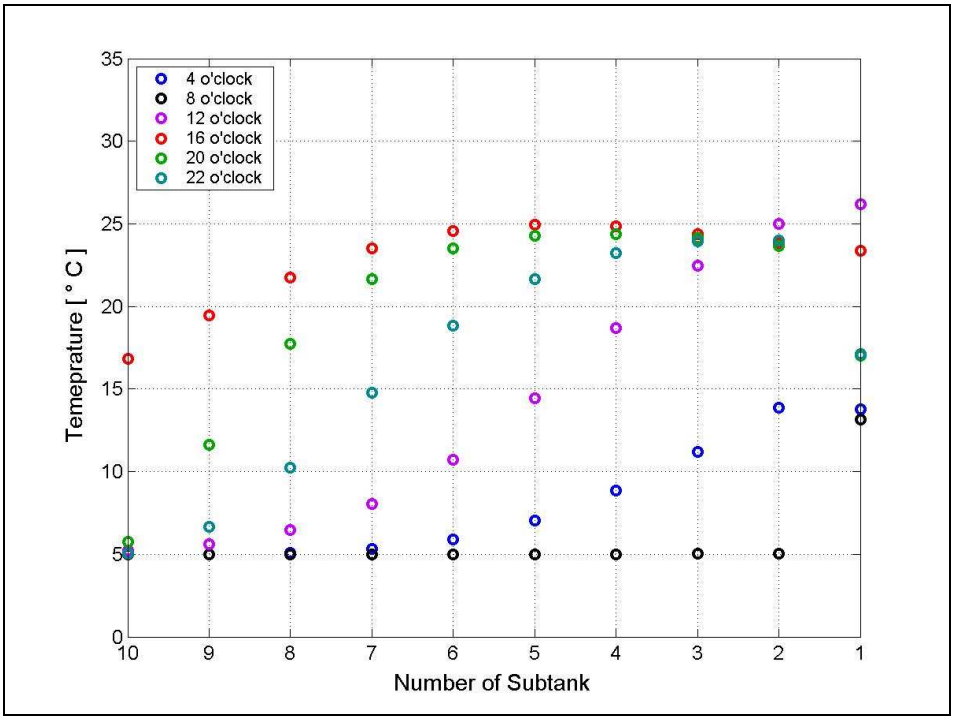

Figure 53 – Validation exercise: spatial temperature profiles match at significant operation hours Matlab results

The previous and following diagrams report the stationary solution after three day of iteration.

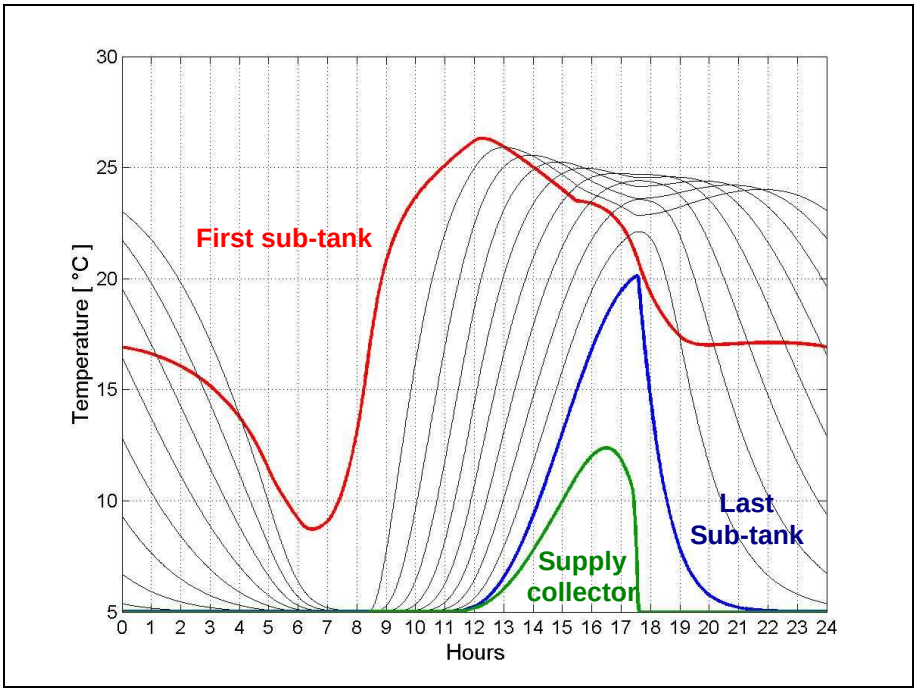

Figure 54 – Validation exercise: sub tank hourly temperature profiles and collector supply temperature to HVAC.

The storage efficiency has been enhanced by tank partitioning so that only the first tank is actually subjected to terminals heat discharge during the hours when heat storage is not needed, thus useless heat storage is avoided. Moreover the delivery temperature freshness is properly preserved all day long in order to allow terminal optimum performances.
Finally a significant a comparison is presented between Nakahara estimated and calculated storage efficiencies with respect to Matlab value.

Nakahara	Matlab
Empirically estimated $\boldsymbol{\varepsilon} = 1.414$ Calculated $\varepsilon = 1.532$	$\varepsilon = 1.479$

Matlab result is acceptably close to author estimations.
Note that storage efficiency overcomes unity only because the water tank is filled more than once during the day.

4

Exergy Analysis

The groundwater system for the office building in Milan has been examined through an unsteady energy model. Tank volume partitioning suitability has been exposed under complete mixing hypothesis.
The next chapter will face the current problem under the point of view of exergy in order to detect design criteria for improvements.
The summer critical case will be chosen for that treatment.

Given that exergy analysis detects thermodynamic useful work wastes throughout an energy system, it will be carried out in order to let us figure out how and where the current system could be modified to improve COP without affecting restoration time.

Three significant exergy destruction positions could be pointed out on current system functional diagram (please refer to Figure 12):

- Heat exchanger
- Tank
- Mixing node for return to underground basin temperature control

4.1. Heat exchanger exergy model

The heat exchanger operation is needed in order to dissipate building rejection heat.
A constant approach is preserved between GW inlet temperature and loop water outlet temperature in order to properly manage the heat exchange. An optimum value by 5°C has been applied with the aim of best compromise between GW flow rate reduction and external units delivery temperature control at low values. Although, a heat exchange between two

sides at different temperature levels is an irreversible event, that under adiabatic hypothesis between heat exchanger and surrounding environment, implies an entropy generation rate as well as an exergy destruction rate which can be evaluated as follows:

$$\dot{E}_{HEX} = \left[T_a \dot{S}_{irr}\right]_{HEX} = C_{loop}\left[\left(T_{in} - T_{out}\right) - T_a \ln\left(T_{in}/T_{out}\right)\right]_{loop} + \\ - C_{tank}\left[\left(T_{out} - T_{in}\right) - T_a \ln\left(T_{out}/T_{in}\right)\right]_{tank} \qquad \textbf{Eq.20}$$

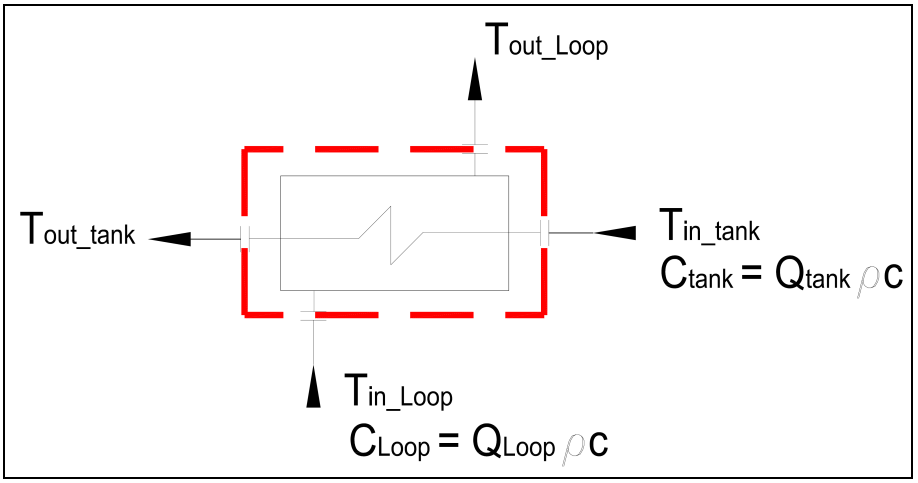

Figure 55 Exergy balance: heat exchanger.

4.2. Tank exergy model

Exergy destruction also occurs into the tank, during storage and restoration phases.
Actually, the complete mixing model implies heat exchange between the flows entering each sub-tank and the water masses stocked within them occurs at different temperature levels so that irreversibilities happen.
Then, for the i-th sub tank, the following exergy balance could be assumed:

$$\dot{E}_{i_{S.T.}} = T_a \dot{S}_{irr,i} = C_{cross}\left[\left(T_{i-1} - T_i\right) - T_a \ln\left(T_{i-1}/T_i\right)\right] + \\ + \sum_j C_j \left[\left(T_j - T_i\right) - T_a \ln\left(T_j/T_i\right)\right] - \frac{dE_i}{d\theta} \qquad \textbf{Eq. 21}$$

$$\frac{dE_i}{d\theta} = \frac{dU_i}{d\theta} - T_a \frac{dS_i}{d\theta} \qquad \textbf{Eq. 22}$$

Where index j refers to eventual inflows or outflows from or to the outside system (e.g. the last and the first tank).
Note that the piston flow model states that water masses are stored at the same temperature they enter the tank. Therefore piston flow model could actually be assumed as ideal because no useful work is lost along with it.

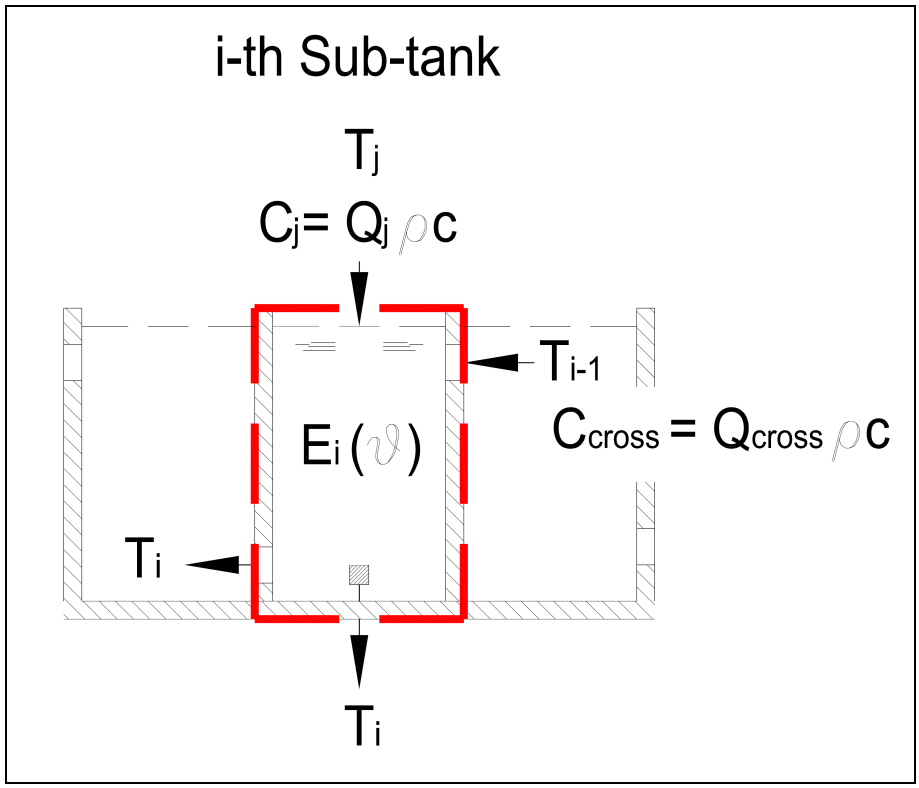

Figure 56 Exergy balance: i-th sub-tank.

4.3. Exergy model of return temperature control mixing node

Complete mixing assumption is also adopted to estimate the proper GW bypass flow rate to assure the return to underground basin threshold temperature by 20°C. As a result, it is eligible as a significant exergy destruction node. Being the current node perfectly adiabatic towards the external environment, the related exergy balance is expressed as follows:

$$\dot{E}_{M.N.} = \left[T_a \, \dot{S}_{irr} \right]_{M.N.} = C_{bp} \left[\left(T_{bypass} - T_{lim} \right) - T_a \ln \left(T_{bp} / T_{lim} \right) \right] + \\ + C_{GW_d} \left[\left(T_{ft} - T_{lim} \right) - T_a \ln \left(T_{ft} / T_{lim} \right) \right]$$

Eq. 23

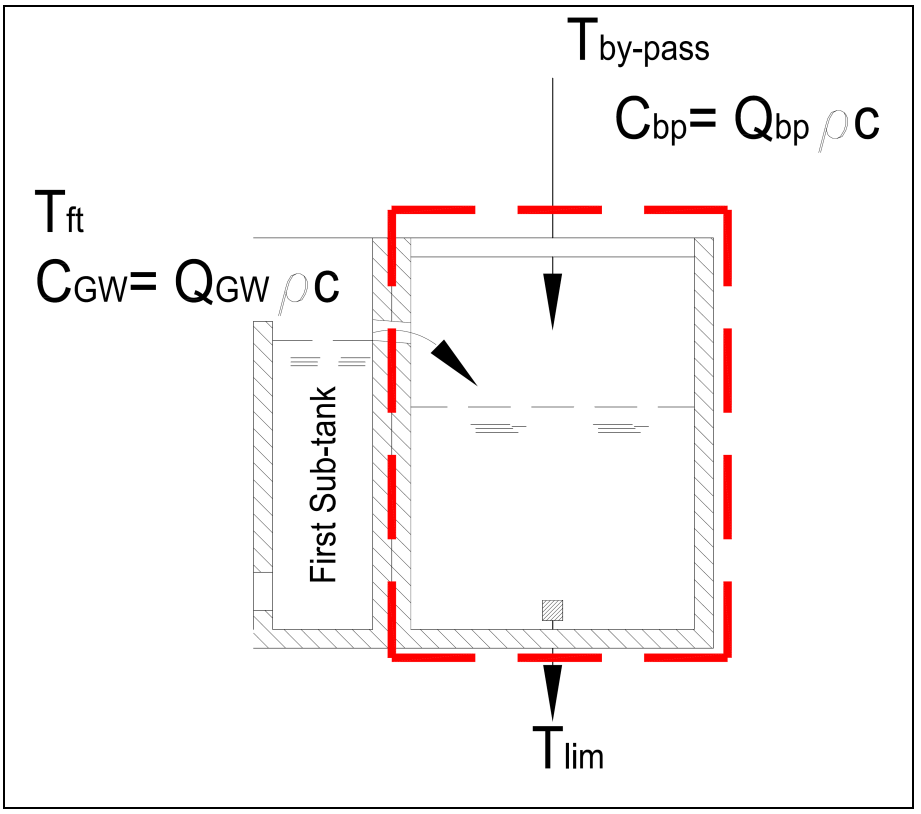

Figure 57 Exergy balance: return temperature mixing node.

4.4. Exergy analysis results

First of all, the exergy analysis will be developed for each significant position in order to estimate local exergy destruction rates. Simple tank results will be overlaid to 20 sub tanks multi connected tank evidences to highlight partitioning effect on storage performance and ground water direct utilization. Heat exchanger will assume predominance in exergy destruction so that different heat exchanger sizes will be tried and a new system management will be compared to the current one in terms of exergy performance.

The following figures describe the exergy destruction rate behavior for the quoted positions within the current system during the summer critical day.

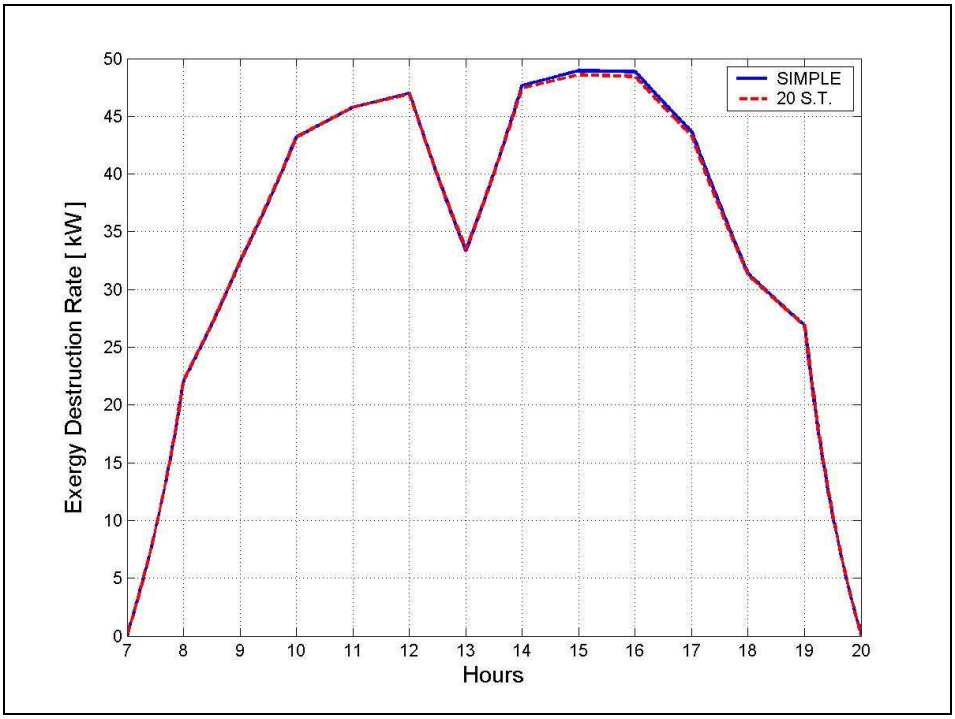

Figure 58 – Exergy destruction rate within heat exchanger: comparison between simple tank and multi-connected tank under complete mixing assumption

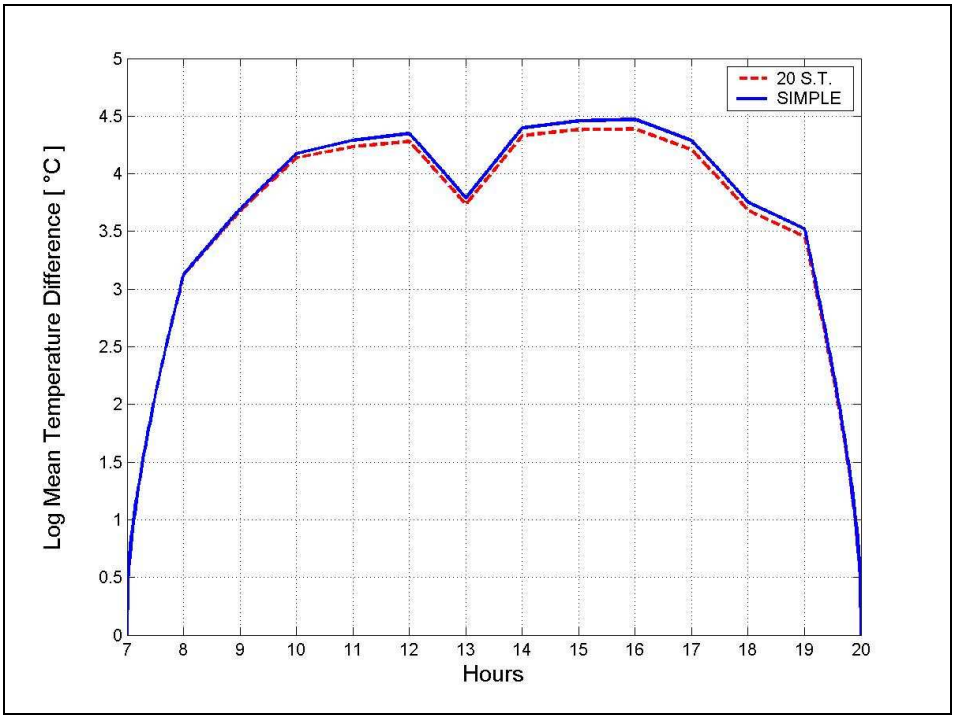

Figure 59 – Logarithmic mean temperature difference: comparison between simple tank and multi-connected tank under complete mixing assumption

Tank partitioning does not imply any significant result on heat exchanger performance.
The following figure will describe the exergy destruction distribution within each sub-tank in the case of the 20 sub-tanks multi-connected tank subjected to the critical summer day conditions.

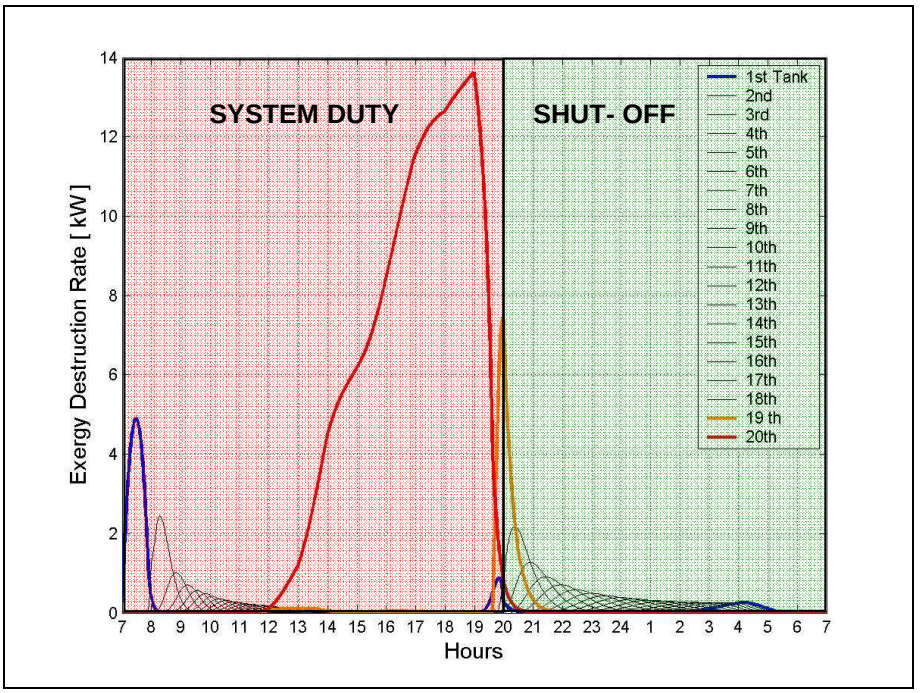

Figure 60 –20 sub tanks multi-connected tank: exergy destruction rate split for each sub tank.

Fist of all, it is important to separate the two main phases of operation and restoration into which exergy destruction could be read under two different points of view.
Under operation, the exergy destruction leads directly to a compressors electrical energy saving.
Under restoration, that mainly happens during shut-off period, exergy destruction is desired unless it overcomes the minimum required for temperature reset.
Generally, sensible exergy destruction rate occurs as fresh groundwater meets overheated volumes. That happen in the first hour (from 7 to 8 o'clock) when the outlet heat exchanger water enter into the first sub-tank, but it also takes place at the second last tank in the very moment when the flow crossing through the tank reverses its sense (20 o'clock), due to restoration on system duty phenomenon. Therefore, the most important exergy destruction within the tank is caused all over system operation period by the continuous fresh groundwater mixing with overheating water into the last tank.
Note that the other tanks are slightly concerned by exergy destruction which means that volume partitioning allows exergy destruction to be localized only at the border edges.
The following figure highlights the difference between the simple tank behavior and the multi-connected performance under complete mixing hypothesis.

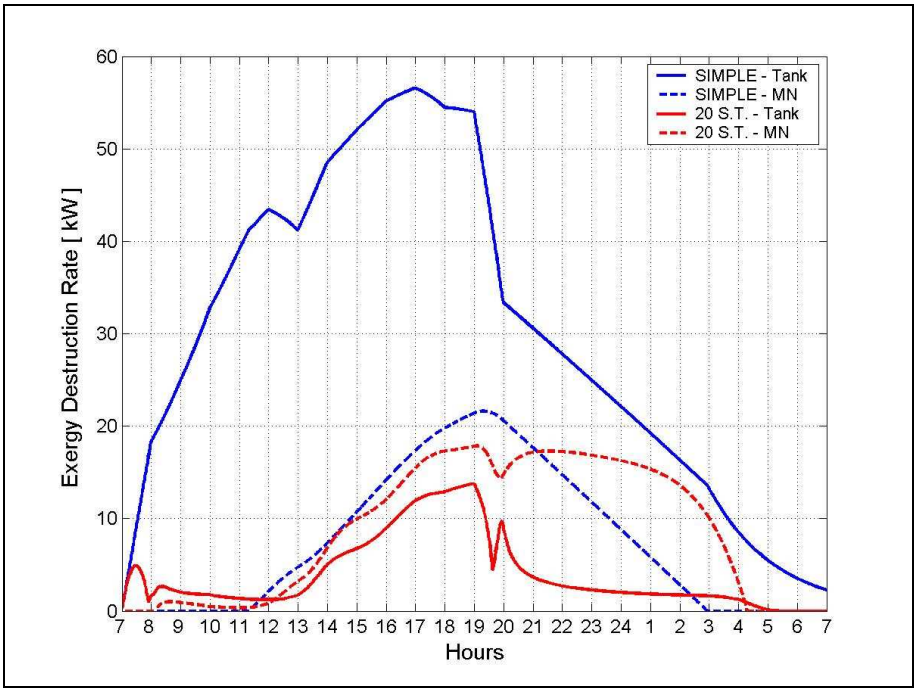

Figure 61 – Total exergy destruction rate within the tank and at the mixing node for return temperature control: comparison between simple tank and multi-connected tank under complete mixing assumption

As we could expect, the volume partitioning has a huge relevance on the system performance: it implies a remarkable improvement on storage efficiency.
During operation, the exergy destruction saving results in an electricity saving of external units compressors consumptions.
Exergy destruction rate during system operation period is lower for multi-connected solution as a consequence of tank lower overheating.
During the shut-off period it is remarkable that the restoration process occur in a more efficient way whether tank partitioning is adopted.
As a matter of fact, under piston flow hypothesis no exergy destruction would take place within the tank during restoration but the whole destruction would occur at the mixing node for return temperature.
Note that in the case of simple tank, the exergy destruction is much relevant within the tank which implies a poor refresh process of internal water masses, due to a sort of wastage of the heat that was previously stored.
On the other hand under multi-connected tank hypothesis almost no exergy destruction occurs within the tank but the destruction rate at the mixing node notably overtakes the simple tank performance in terms of intensity and durability.
In spite of that, the restoration phase total exergy destruction is anyway minimized by tank partitioning, which results in a more ordered and efficient water temperature reset process.

Total exergy destruction for 20 sub tanks multi connected tank is shown in Figure 62 and each singular position contribution is suitably overlaid.

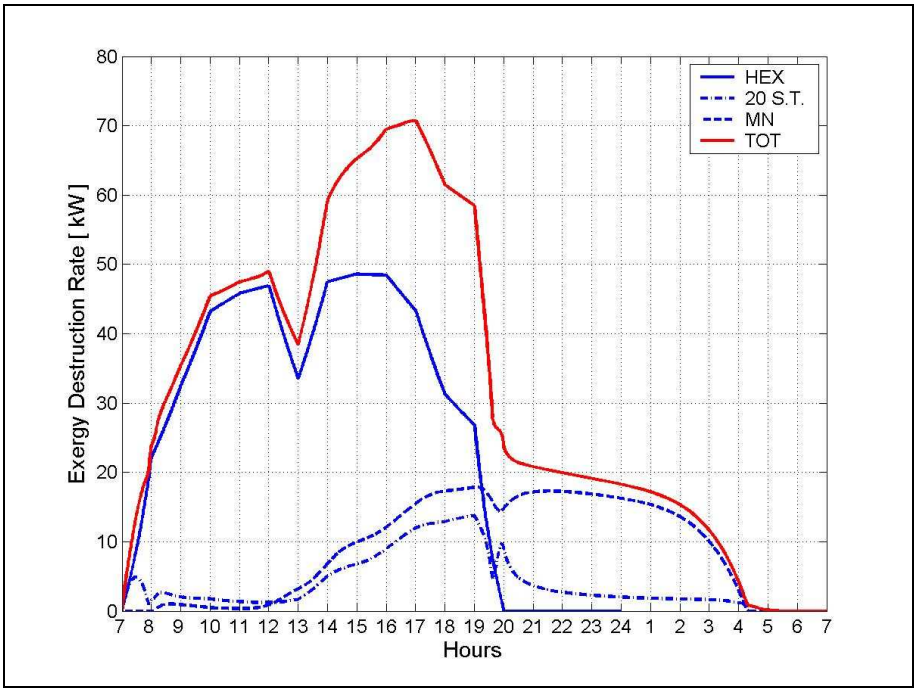

Figure 62 – Total system exergy destruction rate and its singular contributions.

The most important contribution to exergy destruction is definitely related to heat exchanger performance.
Volume partitioning optimizes tank storage efficiency, however exergy analysis gives evidence about possible further improvement on heat exchanger management.

Therefore, heat exchanger design size will be modified in order to figure out the exchange surface impact.
Heat exchanger design criterion comes from a standard comparison between the summer and the winter needed surface to assure proper heat exchange under critical condition with the design temperature approaches.
Exergy analysis could give a more integrated point of view and would point to proper size oriented to the whole system optimization.
Improvements by 30% and 90% with respect to the design exchange surface have been examined as well as a reduced surface by 15%.

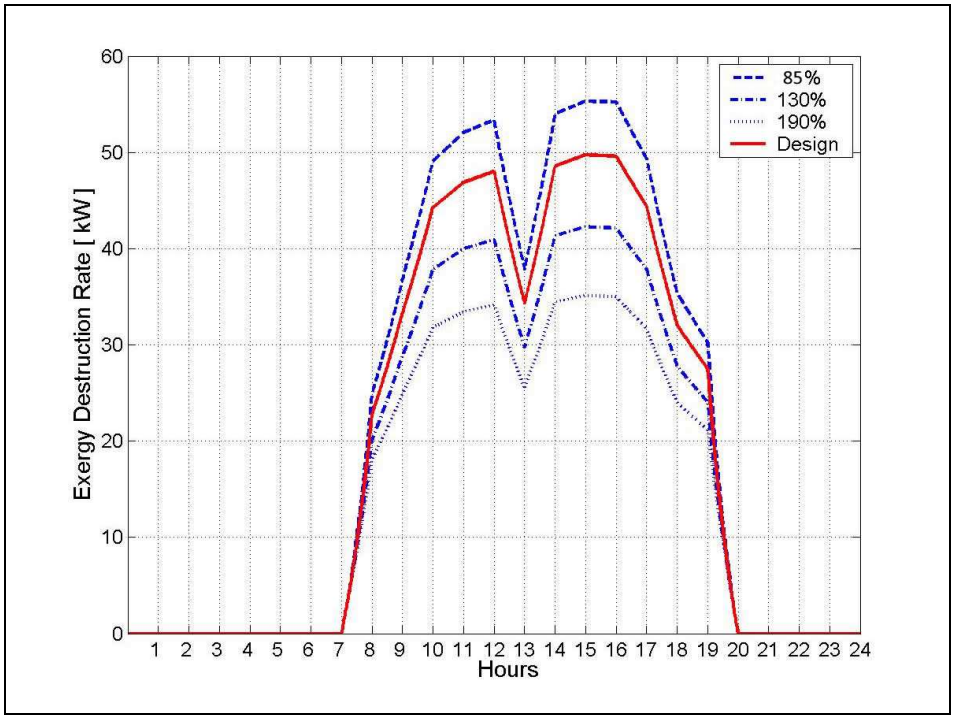

Figure 63 – Heat exchanger exergy destruction at different exchange surfaces.

As we could expect, a better performance is assured by more extended surfaces.

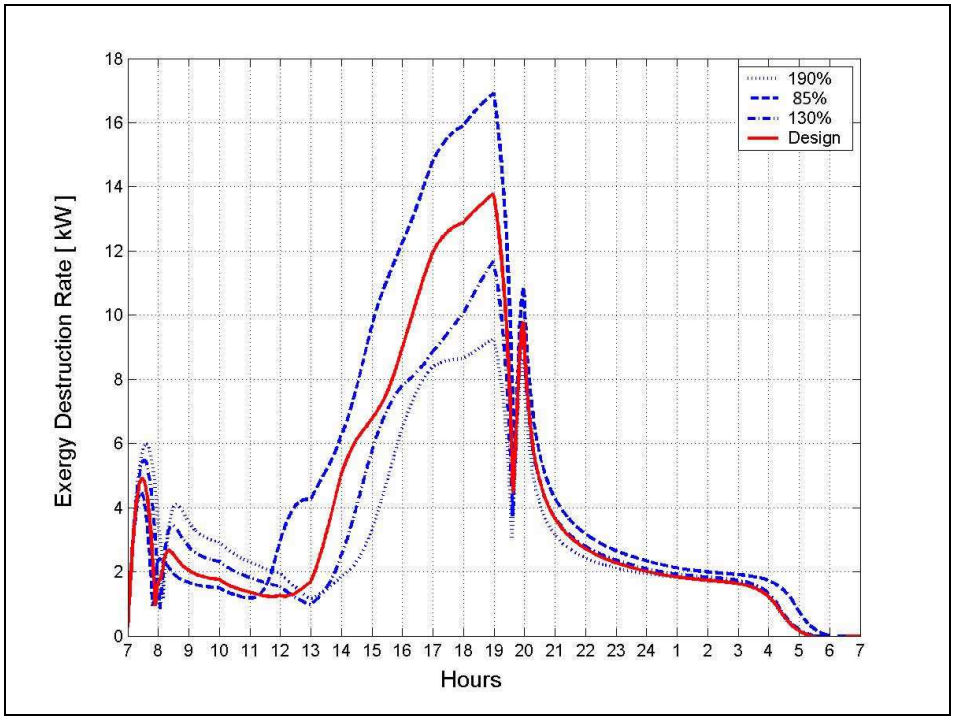

Figure 64 – Multi connected tank exergy destruction at different exchange surfaces.

A larger heat exchange surface implies on one side a larger temperature difference through the heat exchanger as well as at tank edges and on the other side it causes smaller flow rates. Then, the storage efficiency will be surely increased. In the restoration period, a remarkable exergy destruction shift could be noted only for surface reduction, as could be noted in previous and in the following figures.

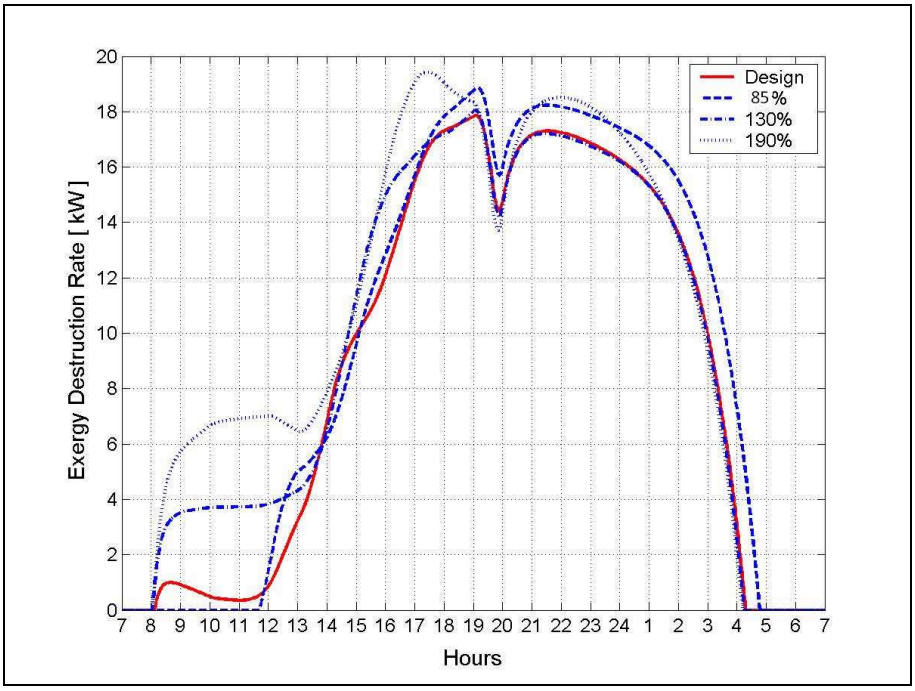

Figure 65 – Return temperature mixing node exergy destruction at different exchange surfaces.

Growing the heat exchange surface, the first tank overheats much more due to the temperature difference increase. Thus, at the return temperature mixing node, the right compromise in terms of exergy destruction is actually assured by the design surface.
The advantages we got using larger surfaces about heat exchange exergy efficiency are slightly balanced by mixing node poor behavior. On the other hand, the first tank overheating allows a better groundwater direct utilization during the initial few hours so that the tank proper performance is pursued.
Finally, the heat exchanging performance is quite remarkable in a manner that an average COP improvement throughout the operation period could be gained by about 3% with respect to the design value when the exchanging surface is 90% bigger than the design one.
During restoration, due to high level of separation of exergy contents between first sub-tanks and last sub-tanks, in the case of 90% bigger surface, an initial higher exergy destruction is followed by a slightly weaker destruction rate.
As we could expect, given that the heat exchanger does not work during shut off period, the restoration time does not earn any relevant advantage by heat exchange surface improvement.

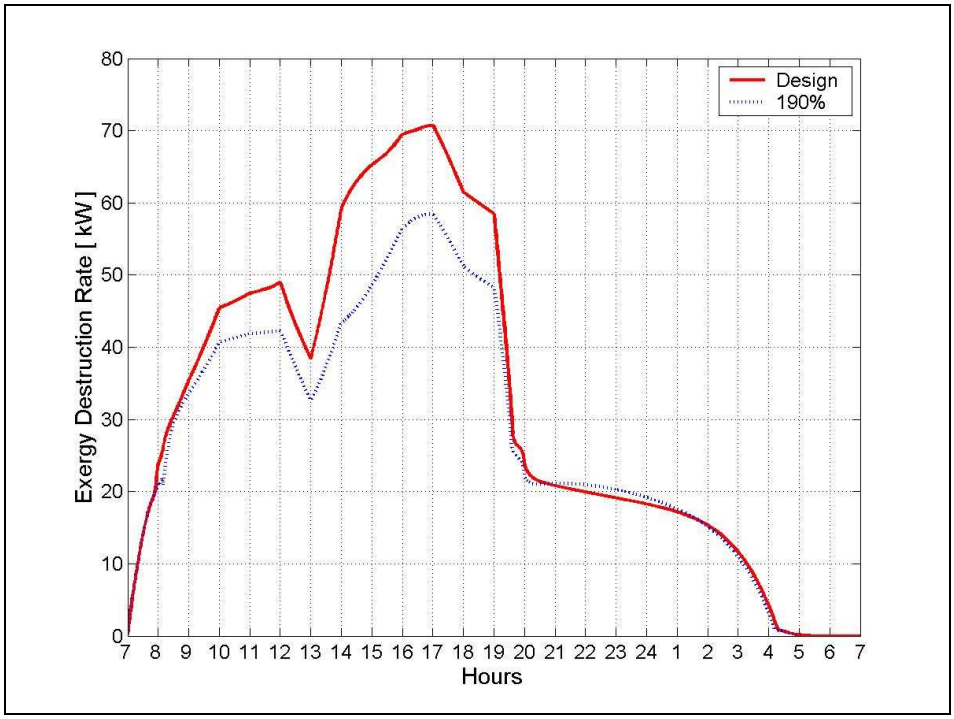

Figure 66 – Total exergy destruction rate comparison between the design heat exchanger surface and the improved by 90% one.

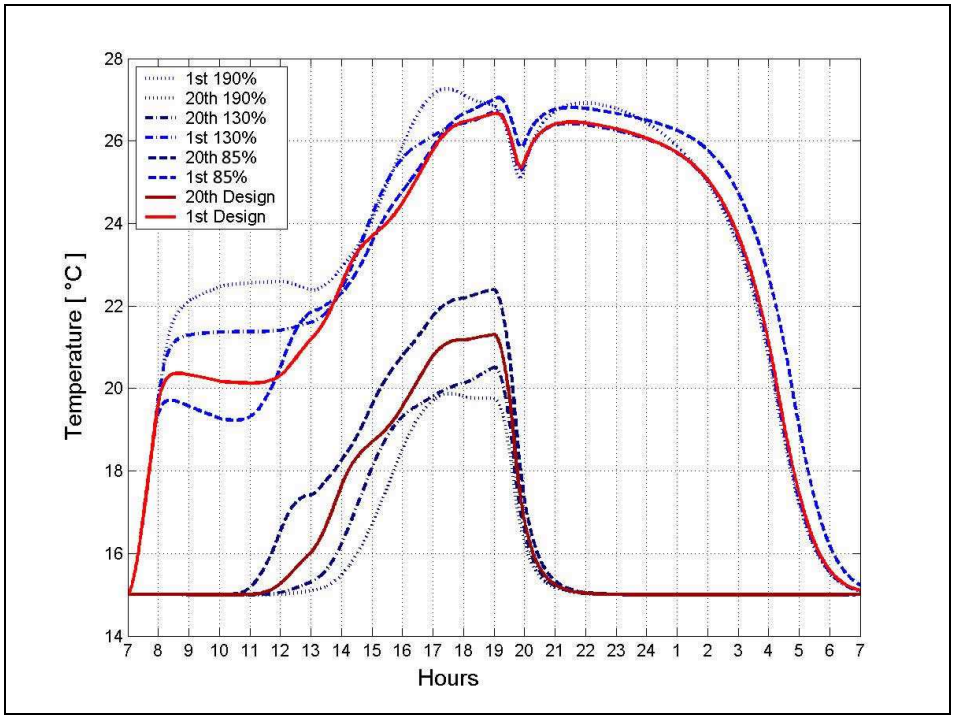

Figure 67 – First tank and last tank temperature profiles at different exchange surfaces.

Surface improvement results in a reduction of the flow-rate crossing the tank along with a growth of the mean temperature difference between the first and last tank. That implies a more efficient operation of external units.

In the following paragraph it will be tried the attempt to get the whole advantages by heat exchanger surface improvement with the aim to avoid the initial exergy destruction at the return temperature mixing node.
Then, the heat exchanger surface increasing will be accompanied by a proper control management of the whole system in order to reduce the described inefficiencies.

For that reason, the current system regulation has been modified in order to be better adapted to a parallel double heat exchanger configuration. The new system will be called "double system" and the current one will be named "baseline system".

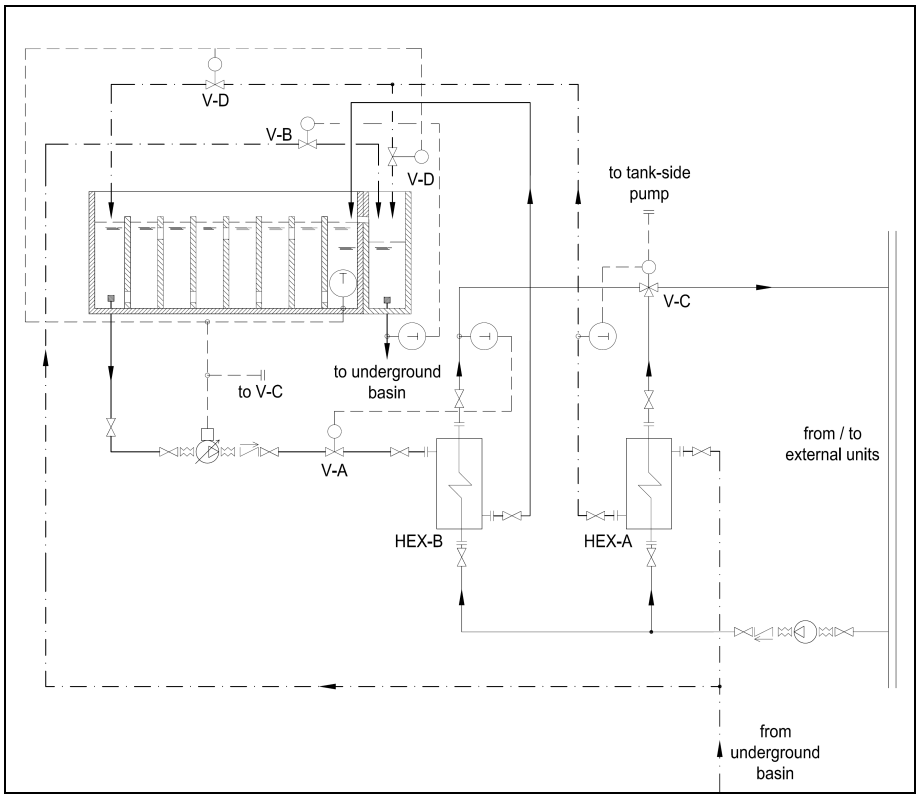

Figure 68 – Double parallel connected heat exchanger diagram.

Control valves V-A and V-B work the same way we explained for baseline system.
The three ways valve V-C starts fully open to allow the whole external units flow rate to pass through the heat exchanger HEX-A. At the beginning, HEX-A is the only heat exchanger to be activated that discharges groundwater into the mixing tank by-passing the storage tank.
The V-D valve serving the return to underground basin mixing tank starts fully open and HEX-A spontaneously exchanges heat between loop-side constant flow and constant available groundwater flow-rate. Until the groundwater discharge temperature does not match with the activation temperature of the valve V-C, no active control dynamics occur.

As groundwater outlet reaches the limit return temperature by 20°C, valve V-C permits HEX-B heat exchanger to be activated. Note that HEX-A discharges directly out of the tank so that no exergy destruction will occur for return to underground basin temperature during the beginning of the operation period.
Second heat exchanger will be designed in order to enlarge the temperature difference and consistently reduce the flow rate passing through the tank. Actually the aim is to get advantage from an efficient heat exchange at HEX-B.
Moreover mixing phenomena are avoided at the last sub-tank but they are merely shifted loop side at valve V-C position.
V-D automatic system will be activated at system shut off in order to execute restoration washing back the tank in the reverse sense with respect to operation. In fact, this was the same restoration strategy that was chosen for baseline system because it allows optimum heat removal.
Note that, HEX-A+HEX-B surface is doubled with respect to baseline system and almost equally distributed between two exchangers. For that reason the baseline pattern to which the double system will be compared is the one that provides a heat exchange surface improvement by 190% with respect to the design value.

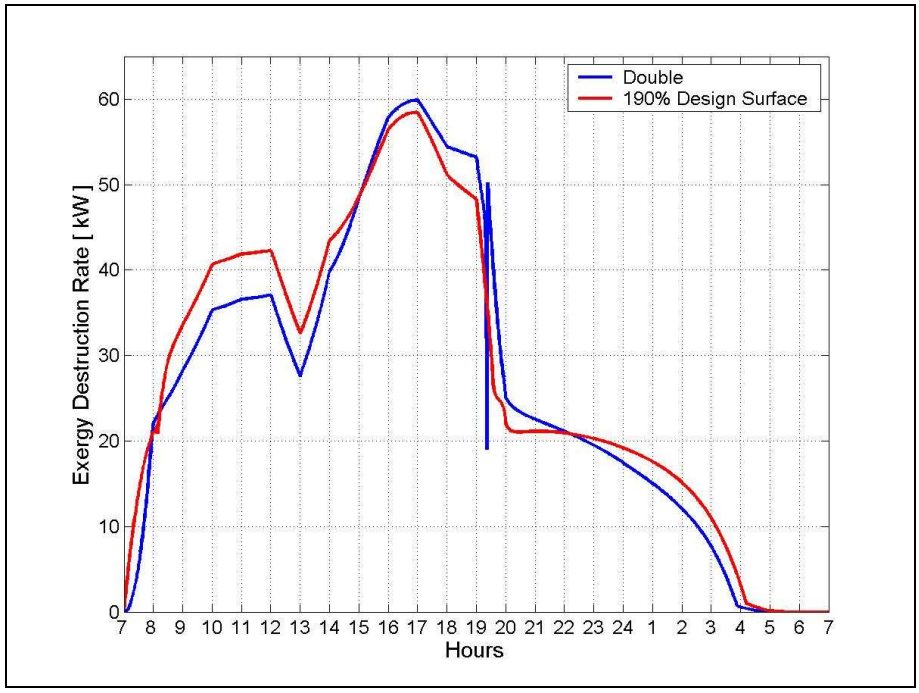

Figure 69 – Double system total exergy destruction compared to baseline system total exergy destruction rate referred to a heat exchange surface improved by 90%.

An expected initial exergy destruction saving is actually balanced by final poor behavior during operation phase.
An exergy analysis of the system at the main positions would make easier to understand the global results.

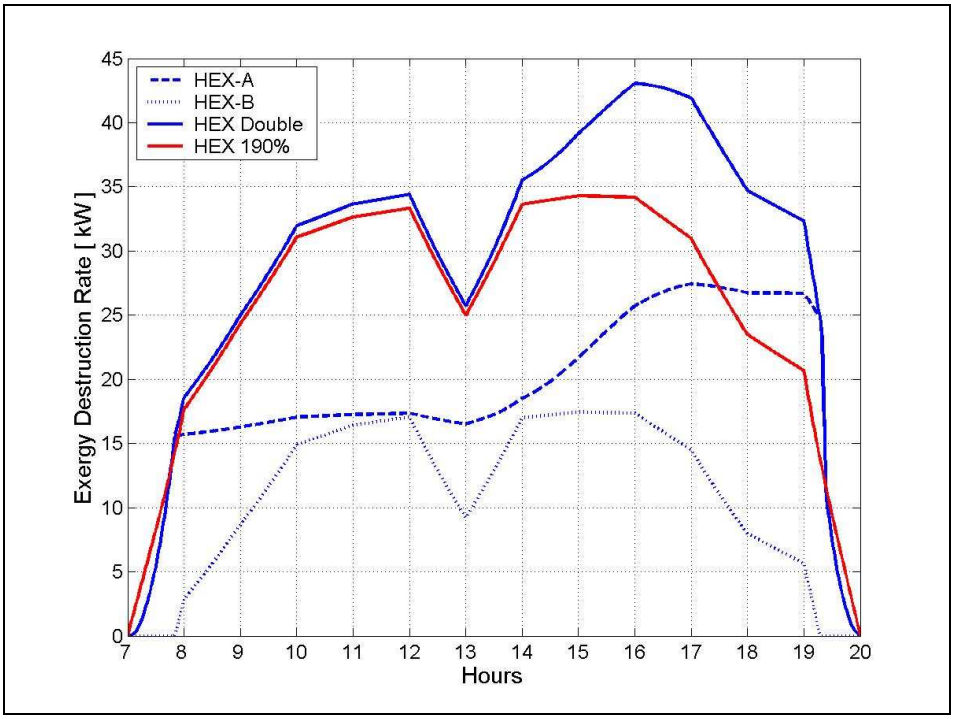

Figure 70 – Double system HEX exergy destruction compared to baseline system total exergy destruction rate referred to a heat exchange surface improved by 90%.

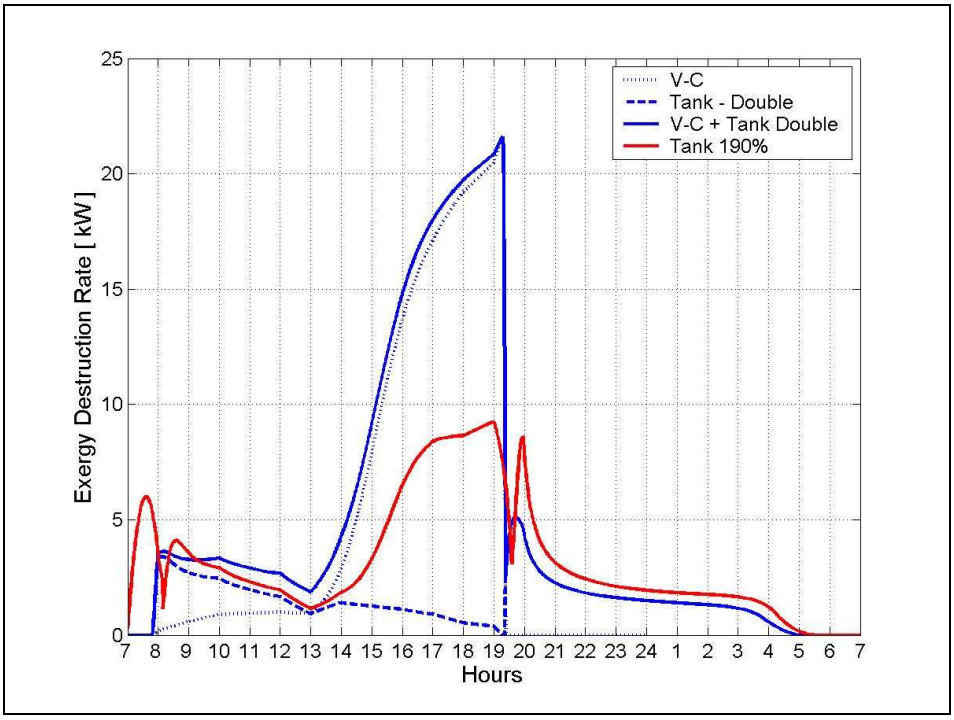

Figure 71 – Double system tank and operation mixings exergy destruction compared to baseline system total exergy destruction rate referred to a heat exchange surface improved by 90%.

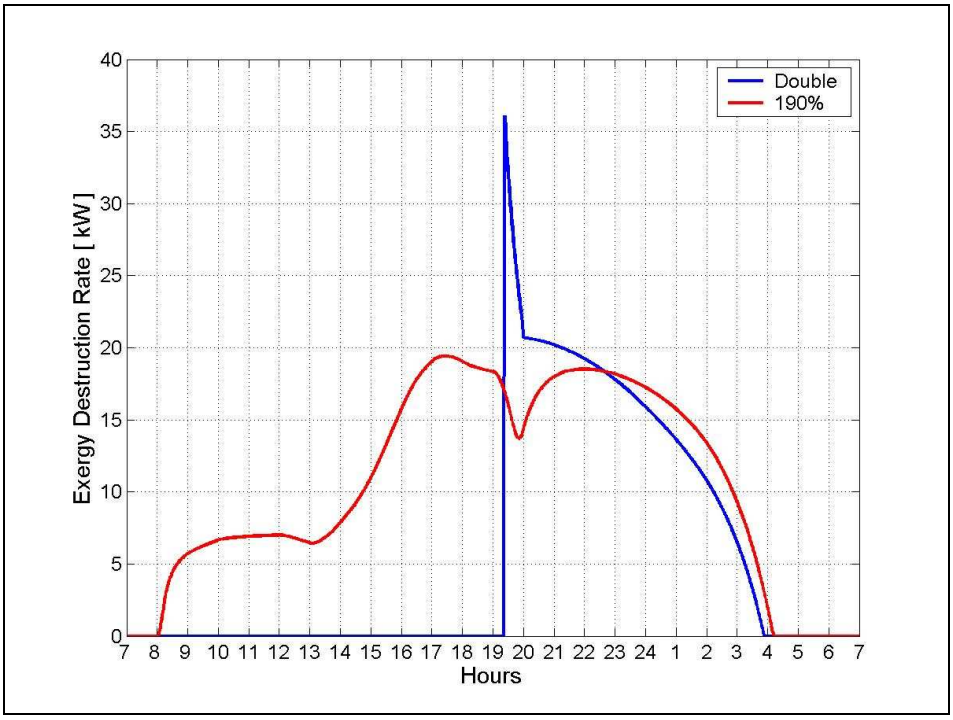

Figure 72 – Double system exergy destruction at the return temperature mixing node compared to baseline system total exergy destruction rate referred to a heat exchange surface improved by 90%.

The exergy destruction saving that is obtained during the operation phase at the return temperature control mixing node is dissipated within the mixing node V-C as well as at the HEX-A sections.

Note that the high peak of exergy destruction in the double system reported in Figure 72 depends on the necessity to undertake the restoration on duty process by delivering the fresh groundwater flow directly in the same direction as the hot stored water was previously supplied.

Finally we could observe that the attempt of the double system was to avoid the inefficiencies that occurred at the return temperature mixing node in order to control the return temperature to the limit value.
Even if the return temperature mixing node is cleaned up by exergy destruction, the alternative way to control the return temperature through V-C and HEX-A operation determine the same exergy destruction we would like to save.
That exergy lost consists in an obliged dissipation that lays within the thermal storage strategy and represents a minimum wastage that we could not avoid or optimize unless storage philosophy is denied.

5

CFD Analysis

Real tanks behavior is influenced by a combination of different regimes, from complete mixing to piston flow; moreover further effects could influence the tank response, as the heat exchange between sub-tanks through separating walls in a multi-connected configuration.
The fluid velocity and temperature fields comply with fluid dynamics laws that locally take into account viscous against pressure forces as well as buoyancy effects under laminar or turbulent assumption, depending on current inertial forces. All those parameters balance could allow complete mixing hypothesis to be more or less suitable.
A FLUENT 2D model is therefore been approached in order to perform a preliminary evaluation through CFD analysis of the range of validity of the full mixing assumption in simple tanks and multi connected tanks.

5.1. CFD Model Assumptions

The FLUENT model will be applied to the same system we took into account for the Matlab energy and exergy simulations. Hence, the groundwater thermal storage for HVAC purposes we talked about in chapter 2 is newly taken into account, referring to the same assumed office building and the same baseline regulation system which has been described from Figure 12 and Figure 13.
However, the CFD analysis introduces further variables on which the system performance could depend. Indeed, the analysis permit a preliminary calculation of temperature and velocity fields within the tank along the operation and restoration phases on a 2D simplified model. That way the full mixing or piston flow assumptions we did in the previous chapters is outdated in the current discussion. The tank could be no longer treated as a lumped model but its geometrical features will be relevant.

Given that the global volume V by 1200 m^3 is constant of the problem, two different geometrical configuration (Table 2) will be analyzed in the following paragraphs in order to infer the importance of the tank height on the storage efficiency. As a matter of fact, the most significant phenomenon that could be outlined by 2D CFD analysis is the effect of buoyancy forces resulting from the interaction between fluid layers at different temperature. The more a the tank is high, the more natural convection will be important.
According to this intention, the higher tank will be supposed to be combined to a heat rejection system in which the heat exchanger surface will be increased by about 30% with respect to the design value in order to enhance the temperature difference at the tank edges and consequently increase the buoyancy effect importance.

Case study	**Tank Volume**	**Height**	**Width**	**Length**	**HEX surface increasing percentage**
	m^3	m	m	m	%
1	1200	3	10	40	0
2	1200	6	8	25	30

Table 2 – CFD analysis case studies.

The 2D model of the tank supplies an approximate geometrical representation of the 3D phenomenon. Especially, flows inlet and outlet pipes will be actually represented as channels of unitary depth and the same height as the pipes design diameter (Table 3). Indeed, the temperature and velocity fields solution just around each connection is expected to be improper but the contribution of these regions is negligible with respect to the whole tank storage efficiency performance.

Connections	**Pipes internal diameter**
	mm
GW inlet	200
GW inlet	200
HEX discharge	300
HEX delivery	300

Table 3 – Inlet and outlet connection pipes model (see Figure 73)

Moreover, as it could be seen from Figure 73, tank edges are slightly modified at some connection sections so that the entrances and the exits do no provide sharp vertex that could cause fluid vortex formations and involve numerical problems of convergence.

Figure 73 – 2D tank geometrical model for the simple tank configuration (6m height)

Each case study has been developed for simple tank configuration as well as for the multi-connected pattern in order to infer buoyancy effect for each condition. Finally, four calculations have been carried out laying on the geometrical models described in Figure 74.

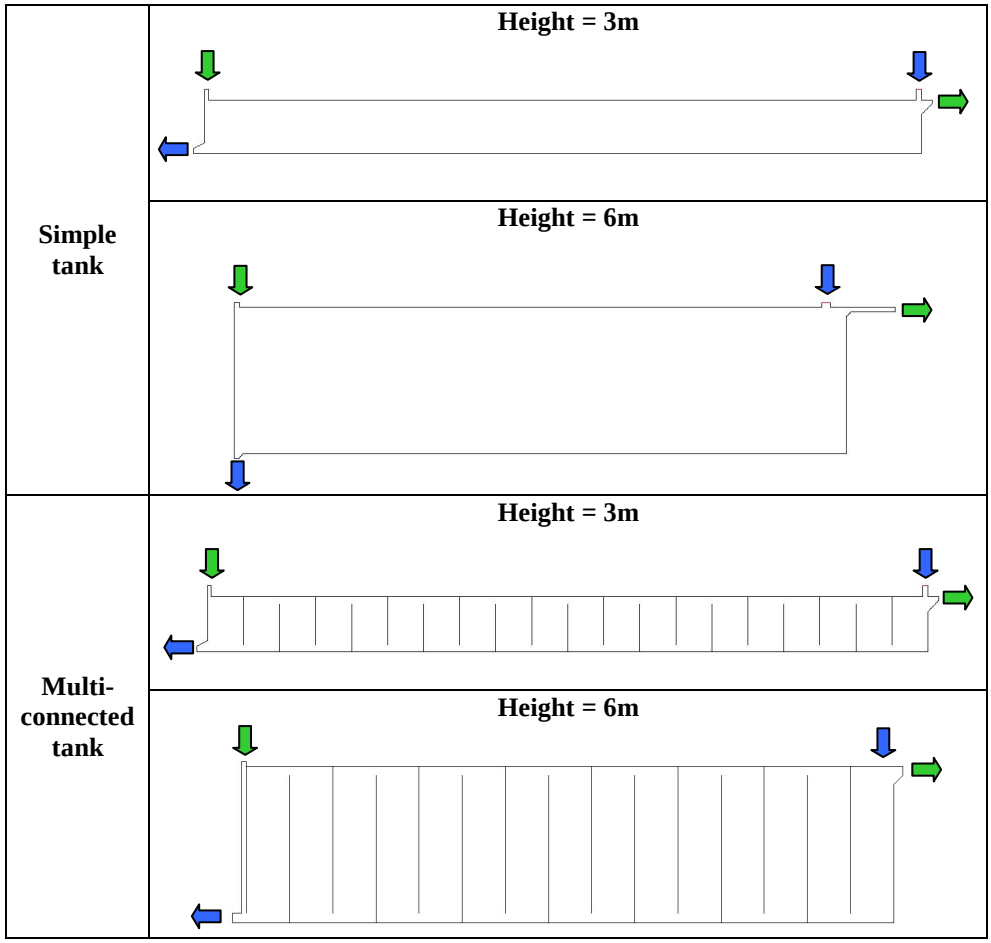

Figure 74– CFD calculations carried out through FLUENT.

The number of sub-tanks is 20 for the 3m height tank and 15 for the 6m height tank.
That is in accordance to Nakahara advices [4] and it depends on the smaller length of the 6m height tank with the aim to avoid that the single sub-tank length were not shorter than 1,5 m, under which there would be construction and mantainance concerns.
An alternative connecting holes arrangement has been adopted since it assures the best partitioning effect as it has been stated by Kitano, Iwata and Ichinose.
Both operation and restoration phases of the critical summer day will be investigated.
Then, each modeled tank undergoes the flow-rates required by the HVAC system at every given time and is subjected to the temperatures discharged by the heat exchanger along the system operation. During the restoration, the tank response will be simulated at every given time depending on the actual by-pass flow-rate requested to control the return temperature to the underground basin.
As a matter of fact, the CFD model will be combined to a system of routines modeling the HVAC system to which the tank is integrated. A dynamic simulation will be carried out in which tank boundary conditions will be up-dated at every time step depending on the HVAC system demands.

5.2. Mesh, Solver and Boundary Conditions

An unstructured, triangular mesh is chosen for all models. The mesh is refined close to connecting holes and around inlet/outlet pipes joints, where fields gradients are expected to be higher (
Figure 75)

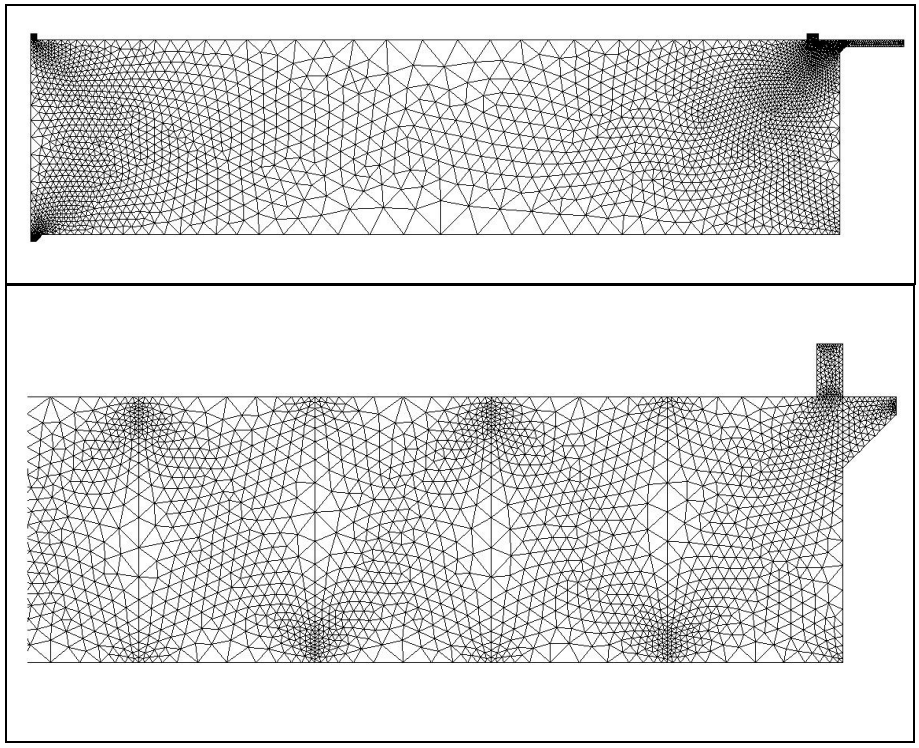

Figure 75 - Unstructured triangular mesh. Simple tank 6m height and multi-connected tank height 3m.

Navier-Stokes, Continuity and Energy equations are solved in FLUENT within the prepared models.
The tank heat capacity is very relevant, so the unsteady formulation of each equation must be considered.
Flow-rates passing through the tank as well as outlet temperatures of the heat exchanger varies at every given time depending on the HVAC system demands and their variation frequency is much more high then the tank response time constant. For that reason, steady state is never reached within the tank and the solution system must be compliant.
FLUENT Manual recommendations for unsteady buoyant flows have been adopted for the choice of the solver properties as well as for the solution algorithms of interpolation, equation discretization and pressure-velocity fields combination modeling.

For the buoyancy model, FLUENT concerns have not allowed to assume the Boussinesq hypothesis so a user defined relation between temperature and mass density has been stated

through a linear interpolation of actual water densities within the range of operating temperatures at atmospheric pressure (Table 4). Same way the dynamic viscosity has been modeled through a similar linear interpolation.

Temperature [°C]	15	40
Density [kg / m^3]	999.12	992.20
Dynamic viscosity [kg / ms]	0.0013	0.000655

Table 4 – Water density and viscosity properties at the top and bottom temperatures of the operating range

Buoyancy model is then completed by activating within the Navier-Stokes equations the gravity force term according to a gravity acceleration value by 9,81 m/s^2 and a vertical downward orientation. No direct relations are actually stated between pressure and the couple of thermodynamic variables temperature/density so that the static pressure field is determined by velocity field and gravity. In order to permit the unsteady equations to be properly solved at a given time in terms of temperature and velocity fields, the system of boundary conditions described in has been chosen. Two different assignment strategies have been followed in order to model either system operation period or restoration period.

	Boundary conditions	
Boundary region	**Operation phase**	**Restoration phase**
GW inlet	Constant mass flux along the inlet section: • Specified pressure • Specified temperature • Velocity: orientation normal to the boundary and value calculated by the system depending on adjacent faces temperatures/densities.	Constant mass flux along the inlet section: • Specified pressure • Specified temperature • Velocity: orientation normal to the boundary and value calculated by the system depending on adjacent faces temperatures/densities.
HEX discharge	Constant mass flux along the inlet section: • Specified pressure • Specified temperature • Velocity: orientation normal to the boundary and value calculated by the system depending on adjacent faces temperatures/densities.	No slip adiabatic walls

Table 5 Boundary condition assignments for operation phase

	Boundary conditions	
Boundary region	**Operation phase**	**Restoration phase**
HEX delivery	Constant mass flux along the inlet section: • Specified pressure • Specified temperature • Velocity: orientation normal to the boundary and value calculated by the system depending on adjacent faces temperatures/densities.	No slip adiabatic walls
GW outlet	Outflow: • Temperature equal to adjacent faces • Velocity: orientation normal to the boundary and value calculated by the system depending on adjacent faces temperatures/densities in order to cope with the mass flow-rate required by continuity	Outflow: • Temperature equal to adjacent faces • Velocity: orientation normal to the boundary and value calculated by the system depending on adjacent faces temperatures/densities in order to cope with the mass flow-rate required by continuity
Tank boundary walls	No slip adiabatic walls	No slip adiabatic walls
Internal partitioning walls (if applicable)	No slip, coupled to fluid walls with assigned concrete conductivity property by 1.28 W/mK and 15 cm thickness.	No slip, coupled to fluid walls with assigned concrete conductivity property by 1.28 W/mK and 15 cm thickness.
Crossing internal louvers	Interior	Interior
Water free surfaces	No shear adiabatic walls	No shear adiabatic walls

Table 6 Boundary condition assignments for operation and restoration phase

Temperatures and mass flow-rates to be applied to boundary regions have to be updated at each time step depending on the HVAC operation or in response to the modulated groundwater flow-rate that must be by-passed in order to keep the limit return temperature to underground basin.
A system of routines in C language have been prepared in order to implement this kind of service within FLUENT solution process. FLUENT requires that this kind of routine is written according to a specific syntax. Specific command codes should be included and

special functions must be provided in order to enable the access to the desired boundary region or to permit the needed repetitive operation. Such functions are called UDFs (User Defined Functions) and should be inserted within the proper software menus in order to be executed by FLUENT in the right order and at the right moment.

5.3. User Defined Functions (UD) implementation

Following treatments are valid for both multi-connected and simple tank models.
A group of UDFs has been written in order to translate Matlab routines into a C code that will be understandable for FLUENT.
The Matlab code has been suitably simplified into C in order to model only the summer critical operation.
Proper temperature and flow rate values will be assigned at each calculation iteration within the typical time step at boundary faces. Indeed, several iterations will be carried out within the given time-step in order to reach the solution convergence of unsteady equations.
Each iteration could be divided into the following main phases:

- Calculation parameters preparation
- Boundary conditions assignment
- Equation solution process
- Variables values assignment to mesh faces and edges representative points.

UDFs could actually operate at every listed phases. Although, the current problem requires that proper UDFs have to be hooked only to the first and the second process phases.

At the calculation parameters preparation phase, the HVAC simulation will be carried out in order to prepare the variable values to apply to boundary conditions.
In this phase, a suitable routine will import the actual building cooling load, it will calculate the proper combination factor and recover the inlet temperature from the previous time-step calculations results. An iterative sub-routine will be needed in order to determine the out of design point of work of VRV® external units. Thus, the out of design point of work of heat exchanger is also calculated through an another dedicated sub-routine. As a result, heat exchanger discharge temperature and the required tank-side flow-rate to allow the proper heat rejection will be available to the boundary conditions assignment phase.
Few dedicated routines will be prepared for the boundary conditions assignment in order to distribute the proper mass flux and temperature values to the representative points of boundary regions edges of the mesh.
A complex programming work has been necessary to implement such routines within the FLUENT syntax.
A user defined array of auxiliary variables could be defined in FLUENT for each representative point of an interior face as well of a boundary edges.
Every single case of this array is called User Defined Memory (UDM) and represents a memory case in which the operator could command to store auxiliary calculation parameters as well as variables which coul be directly calculated form the solution fields variables.
For the current problem, UDMs are used in order to temporary register calculation parameters, as they could be the calculated combination factor or the inlet temperature to external units value, in order to allow the variable passing from the sub-routines to the main routine, which is not permitted through the basic C code syntax.

DEFINE_ADJUST UDFs are the type of functions that must be used in FLUENT to manage the calculation parameters in the first phase of the calculation process. Then a DEFINE_ADJUST has been written to model the HVAC system simulation and merely represents the proper translation f Matlab code into C language. It includes two sub-routines that actually are the direct translation of HEAT_EXCHANGER.m and FIND_VRV.m Matlab routines.

DEFINE_PROFILE UDFs are the type of function that are requested to be hooked to FLUENT calculation process at the phase of boundary conditions assignment.
In Table 8 there is the list of UDFs that have been written in order to force FLUENT calculation at the first and the second phase of calculation process.

UDF TYPE	Purpose	Operation phase	Restoration phase
DEFINE_ADJUST	For UDM updating calling FIND_VRV.c and HEAT_EXCHANGER.c sub routines	Enabled	Inhibited
DEFINE_PROFILE_1	HEX discharge temperature assignment	Enabled	Inhibited
DEFINE_PROFILE_2	HEX delivery mass flux assignment	Enabled	Inhibited
DEFINE_PROFILE_3	GW inlet mass flux assignment	Enabled	Inhibited
DEFINE_PROFILE_4	GW outlet mass flux assignment	Enabled	Enabled

Table 7 – UDF system for groundwater storage tank modeling and UDFs activation state at operation phase or restoration phase.

Note that DEFINE_PROFILE_4 executes mass flow-rate assignment to a boundary region that should be modeled as an outflow. On the other hand, there is no mass flow-rate assignment to HEX discharge boundary region as it would have been.
Actually, in order to enhance convergence within FLUENT, a boundary condition permutation has been executed so that HEX discharge region has been modeled as an outflow and GW outlet as mass flow inlet. Especially, negative mass-flux has been applied to GW outlet region and a reverse flow is explicitly induced at HEX discharge inlet section.
For the same reason, the GW outlet mass flux assignment will be preserved for the restoration model and the outflow condition will be applied to the GW inlet

In Table 8 are listed the needed UDMs for the current calculation.

UDM	Value assigned	Served UDF
UDM_0	Individual external unit cooling capacity	From FIND_VRV.c(within DEFINE_ADJUST) to DEFINE_ADJUST
UDM_1	Individual external unit electric power consumption	From FIND_VRV.c(within DEFINE_ADJUST) to DEFINE_ADJUST
UDM_2	HEX required flow rate	From HEAT_EXCHANGER.c (within DEFINE_ADJUST) to DEFINE_PROFILE_2
UDM_3	HEX discharge temperature	From HEAT_EXCHANGER.c (within DEFINE_ADJUST) to DEFINE_PROFILE_1
UDM_4	GW available flow rate	From DEFINE_ADJUST to DEFINE_PROFILE_3/4

Table 8 – UDM description.

Direct groundwater inlet temperature will be constant by 15°C and will be assigned into mass flow inlet condition for the operation phase and as backflow temperature into outflow condition for the restoration phase.

Further ON_DEMAND UDFs have been written in order to initialize UDM for iteration as well as for final data extraction and management.

5.4. Results

The CFD analysis results are first described for the multi-connected tank configuration.
Temperatures and velocity fields are presented along the critical summer day both operation phase and restoration phase.
In Figure 76 , temperatures distribution within each sub-tank are reported at different times along the operation phase for the 6m height, 15 sub-tanks and 30% oversized heat exchanger configuration. The same representation is reported in Figure 78 for the 3m height tank with 20 sub-tanks and the design size of heat exchanger.
In both cases, tank partitioning determines a longitudinal near piston-flow effect along the tank and alternative connecting holes distribution allows an effective inhibition of temperature propagation.
However, in the case of the 6m height tank, the temperature field is not perfectly homogeneous within each sub-tank, due to the formation of a double dead-zone that is imputable to buoyant effect (Figure 77)
Given that connecting holes are alternatively distributed along the longitudinal direction at the top and at the bottom of the tank, the bottom to top connected sub-tanks are crossed by an arising flow and the top to bottom connected tank are crossed by a descendant flow. Arising flows are pushed by buoyancy and reversely the descendant flows are opposed by buoyancy. In both cases a multiple recirculation phenomenon takes place, as it could be seen from the velocity field analysis described in Figure 77.
In the case of bottom to top connected sub-tanks, the warm flow coming from the previous sub-tank tends to quickly rise up to the top connecting hole. At the sub-tank entrance the warm flow is squeezed against the bottom of the tank because of inertial effects due to the stream acceleration through the hole. Then the warm stream crashes against the separating wall (for example WALL 1 in Figure 77) and arises towards the connecting hole situated at the top flowing along the WALL 1. In a typical bottom to top connected sub tank, the stream acceleration through the alternate connecting holes engenders a pushing from below and pulling from above effect that squeezes the stream against WALL 1 and tends to exclude a dead zone from the crossing stream. The narrow stream running along the WALL 1 drags the adjacent fluid layers and determines the formation of a vortex in the top region of the bottom to top connected tank. However a second vortex also is engendered in the bottom region. Actually such a vortex do not appear in the CFD simulations in which buoyancy is removed. Thus, secondary recirculation could be motivated by natural convection within the dead zone situated just above the entrance connecting hole. The described phenomenon is then mirrored for the top to bottom connected tanks, where the main stream runs along the separating wall (for example WALL 2 in Figure 77), an inertial vortex is engendered at the bottom and an enclosed dead region lays just after the opposite separating wall (WALL 1). A secondary vortex takes place again in that region.
Hence, a sort of vortex classification could be done.

- A main inertial vortex occurs next to the outlet connecting hole
- A secondary buoyancy driven vortex occurs in the dead region next to the intake hole

It should be noticed that a configuration characterized by dead-zones and short-circuits implies that storage efficiency is damaged because the available water mass is not completed involved into the storage process. That is clearly represented in Figure 76 where at each very moment of the operation phase the warm stream crossing the tank leaves behind several cool water bags. Anyway, secondary vortexes formation permits that the fluid enclosed in the dead zones is partially mixed and reduces storage efficiencies concerns due to by-passes

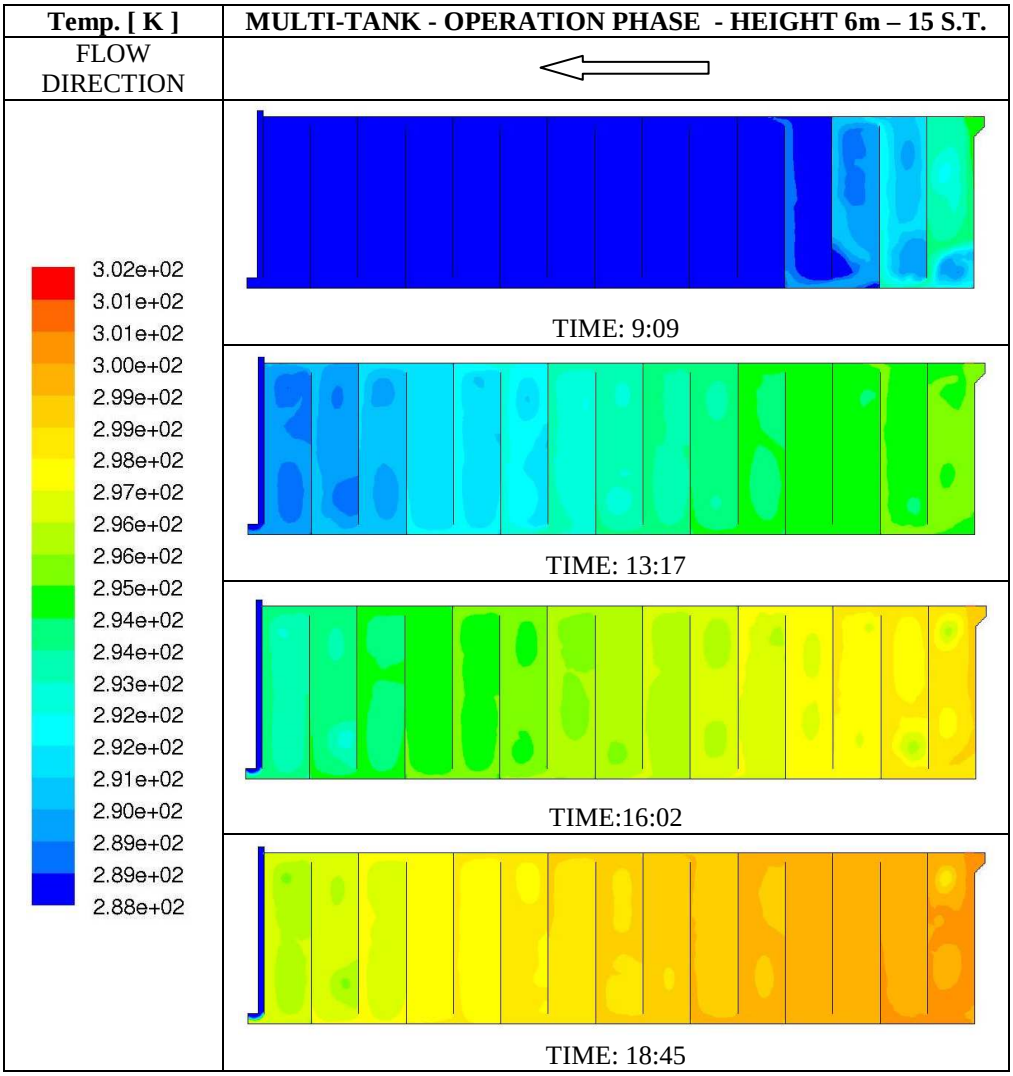

Figure 76 – CFD results describing the operation phase process within the tank for the multi-connected configuration 6m height in terms of temperature field.

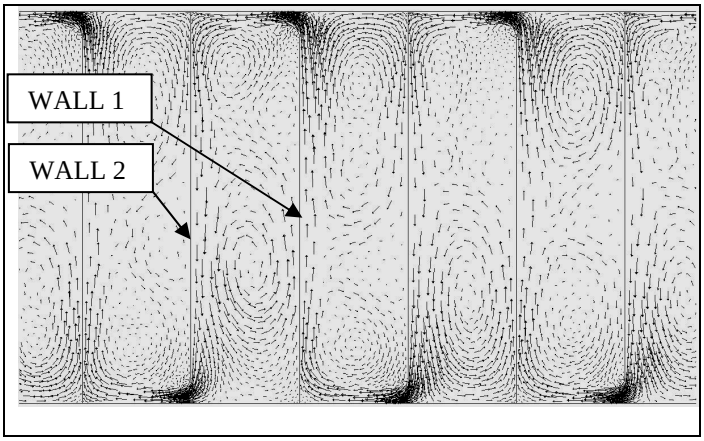

TIME:16:02 - Velocity range from 7 cm/s to 0 cm/s

Figure 77 – CFD results describing the typical velocity field during the operation phase process within sub-tanks.

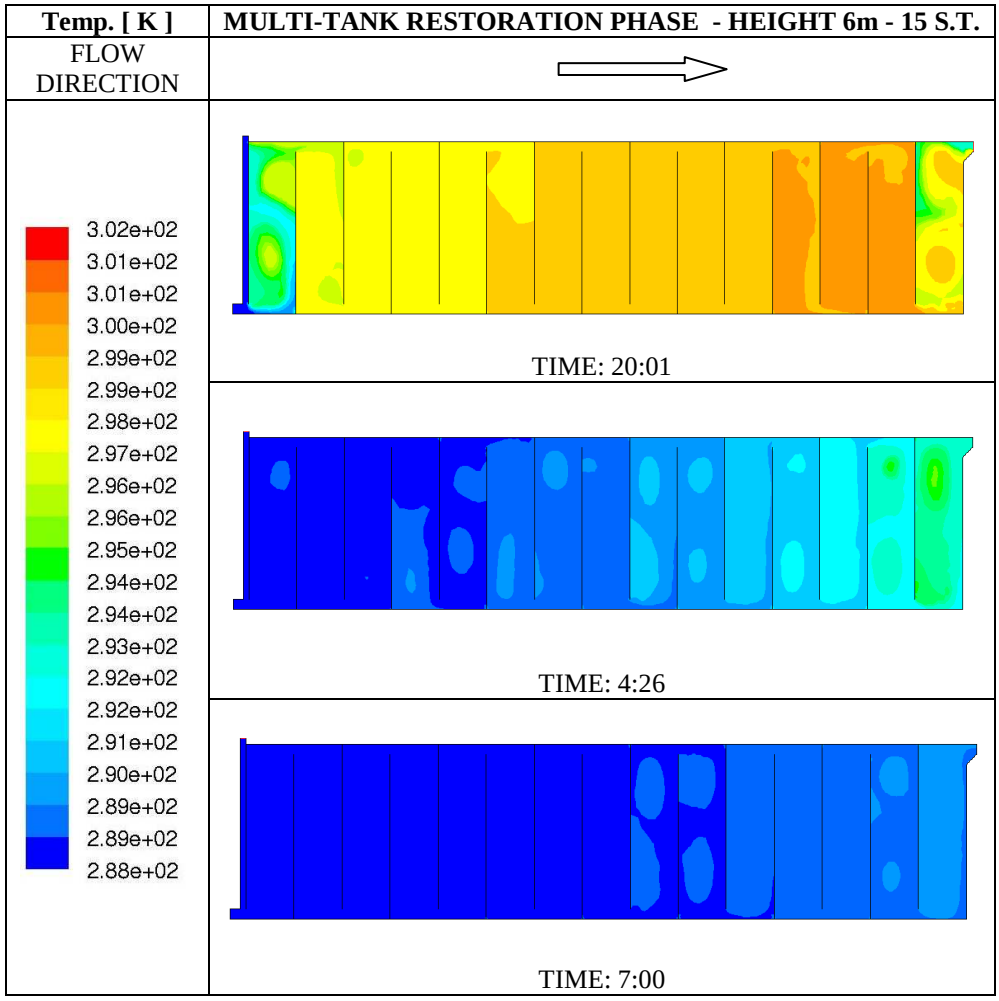

Figure 78 – CFD results describing the restoration phase process within the tank for the multi-connected configuration 6m height in terms of temperature field.

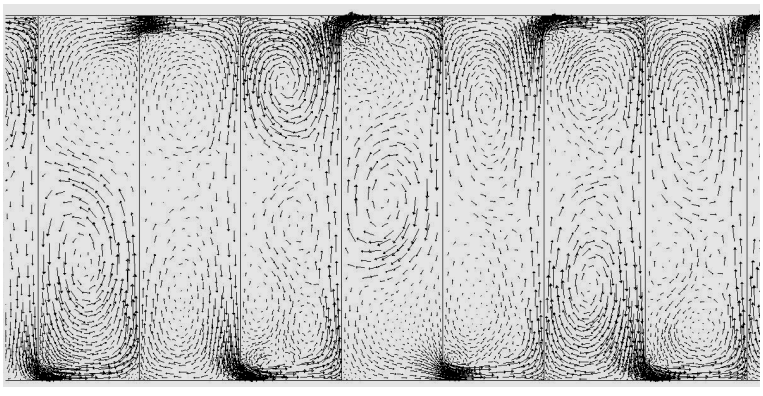

Figure 79 – CFD results describing the typical velocity field during the restoration phase process within sub-tanks.

In Figure 78 and Figure 79 the temperature and velocity fields are reported for the 6m high multi-connected tank.
At 20 o'clock the system have been just shut-off and several residual effects of the ending period of operation is still impressed within the tank. Actually, the first tank is slightly cooled and the last tank is already almost totally restored as the shut-off period starts. All other sub-tanks store almost all the exceeding heat that groundwater could not accept during the operation phase. The first tank is slightly cooled because at the end of the operation phase, the descendant building cooling loads caused the decreasing of the tank-side temperature difference of the heat exchanger so that HEX discharge temperature fell below the temperature values of the first tank water and cooled it. However, the last tank cooling is due to the restoration on duty phase, which is represented in Figure 16**.** It is a short period at the end of system operation in which heat rejection loads could be newly be satisfied by the available groundwater cooling capacity, so the stream reverses its crossing direction along the tank and restoration begins even if the HVAC is still turned on. Thus the last tank is cooled by groundwater during such a period. It should be noticed that the flow direction inversion causes that the warm water stored within the volume enclosed form the second sub-tank to the second last sub-tank is pushed towards the first sub-tank and then discharged towards the underground basin. Thus, the first sub-tank that was previously cooled by descendant cooling loads effects is now newly re-heated by that stream inversion.
That is the reason why the first sub tank is only slightly cooled at the shut-off period begin and the last sub tank is almost restored. Coming back to restoration phase during the system shut-off period, the same inertial short-circuits and dead-zones as well as inertial and buoyancy driven vortexes are engendered again. Although, buoyancy driven effects are slightly more relevant than the ones we saw for the operation phase. Indeed, it depends on the higher temperature difference between incoming groundwater at 15°C and stored water that lays at the beginning by about 23°C to 24°C in the last tank, yielding a delta by 8-9°C. Actually, during the operation phase the characteristic temperature difference for buoyancy forces evaluation equaled the tank-side heat exchanger temperature difference by about 5 to 6 °C. In Figure 80 and Figure 81 the temperature and velocity fields of the operation phase are represented for the multi-connected, 20 sub-tanks and 3m high tank.
As we saw for the higher tank, the temperature field is characterized by many dead zones that are excluded from the storage process. However many differences could be noted:

- In the sub-tanks where dead-regions are engendered, only one dead-region per sub-tank takes place, corresponding to a large vortex in the velocity field (Figure 81)
- In the fist few tanks, next to HEX thermal input, one vortex per tank is hosted, opposite in the last tanks only the bottom to top connected tanks (arising flow) host a vortex so that vortex distribution is actually alternate as the tanks connection is (Figure 80 and Figure 81). That implies dead-zones formation only where vortexes occur.
- In the tanks where a vortex takes place, it is engendered by a stream running along the separating wall to which the entrance hole belongs.

Moreover the following notes should be remembered:

- Tank height is lower than the 6m height tank case and tank-side temperature differences at heat exchanger edges are expected to be lower as well due to the lower heat exchange surface; so buoyancy is expected to be weaker.
- Connecting holes dimensions are preserved so they are longer with respect tank height. That implies that an inertial acceleration reduction through them is also expected.

Finally, it is clear that buoyancy has been weakened less than inertial effects so buoyancy driven vortexes occur in the arising flows and fully mixing occurs in the descendant flows, due to an equilibrium between stratification and pressure driven flow Figure 84.

In the case of 3m high tank restoration, the vortexes alternate distribution is even more clear Figure 82. It involves all the tank and imply a low number of short-circuits. A better storage efficiency is then expected for the 3m high tank than the 6m high one.

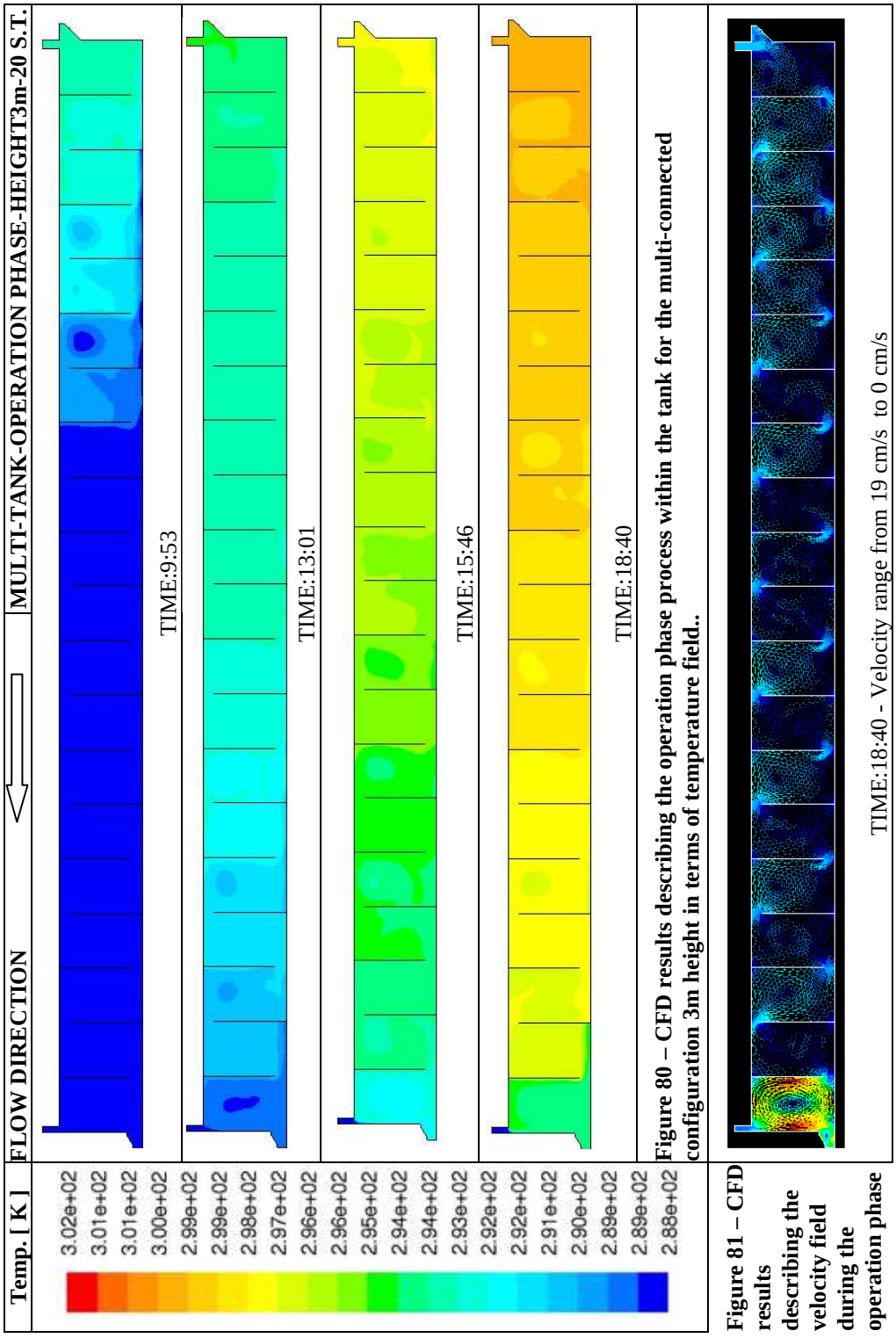

Figure 80 – CFD results describing the operation phase process within the tank for the multi-connected configuration 3m height in terms of temperature field..

TIME:18:40 - Velocity range from 19 cm/s to 0 cm/s

Figure 81 – CFD results describing the velocity field during the operation phase

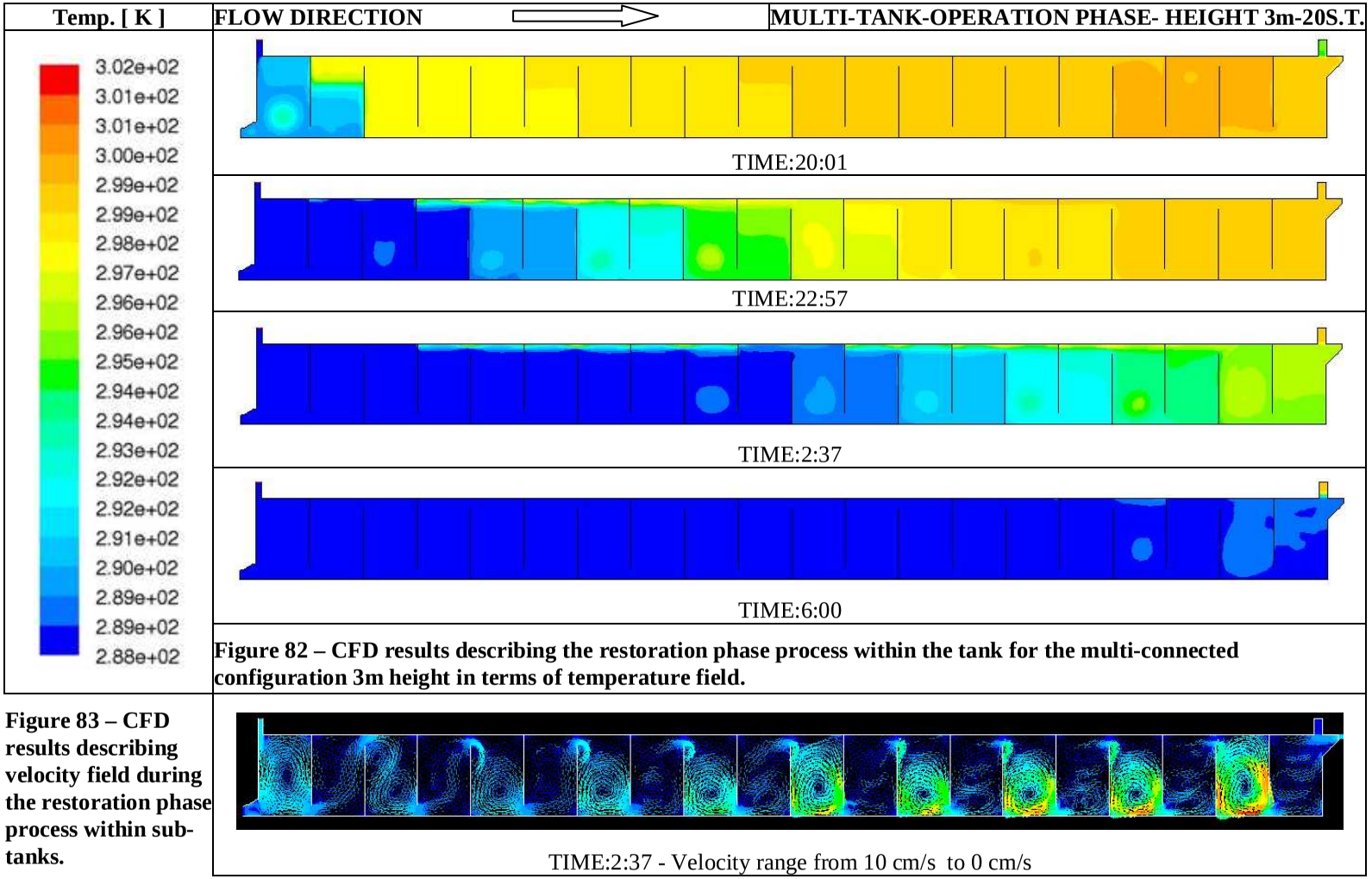

Figure 82 – CFD results describing the restoration phase process within the tank for the multi-connected configuration 3m height in terms of temperature field.

TIME:2:37 - Velocity range from 10 cm/s to 0 cm/s

Figure 83 – CFD results describing velocity field during the restoration phase process within sub-tanks.

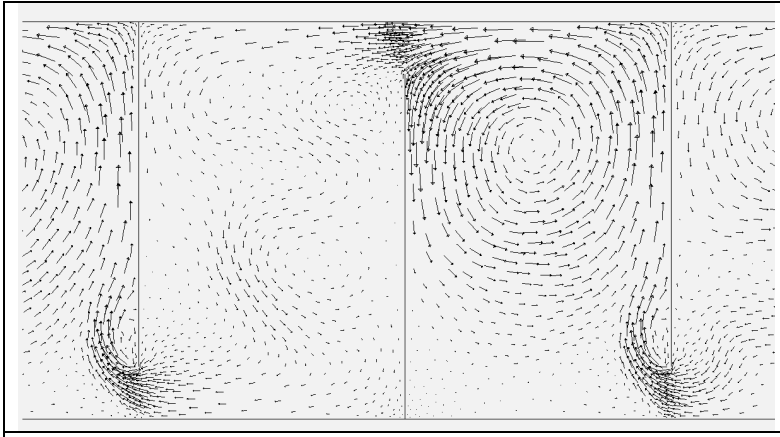

TIME:18:03 - Velocity range from 7 cm/s to 0 cm/s

Figure 84 – CFD results describing the typical velocity field during the operation phase process within sub-tanks.

The aspect ratio could be used as a geometrical characteristic of multi-connected sub-tanks. It is the ratio of tank height on sub-tanks length.

$$R = \frac{H}{L} n \qquad \textbf{Eq. 24}$$

It is a relevant factor to which stratified tank performances could be related.
Actually in the current work, the aspect ratio surely affect the number of vortex that could be engendered within sub-tanks.
The higher the aspect ratio is, the higher will be the number of vortexes that could arise within the tank.
In the 6m high multi-tank, a multiple recirculation was engendered because of both inertial and buoyancy effects.
In the 3m high multi-tank, a single vortexes was engendered in response to the inertial and buoyancy contingency.
The ratio between the tank height and the connecting holes cross-section length is significant as well.
In the following figures, it will be outlined the comparison between Matlab results an FLUENT simulations for the critical summer days in order to infer the simplified Matlab model reliability.
In Figure 85and Figure 86, it is reported the comparison between the 6 m tank and the 3m tank CFD simulations and the related one dimensional simulation ran through Matlab.
Note that the Matlab outputs differ because of the different heat exchanger model.
Following results could be inferred:

- In the case of 6m high tank, the inefficiencies involved by the short circuits/dead zone distribution determine a worse effect than fully mixing assumption. Actually, CFD the multi tank behaves as a fully mixed multi-connected tank whose globale volume V is reduced by 90% in terms of maximum first tank temperature (index of HVAC system energy efficiency) during the operation phase. Moreover, during the restoration phase, it behaves like a 13% oversized tank in terms of restoration time. So Matlab model is not enough accurate for such a case.
- In the case of 3m high tank, ther is a higher storage efficiency with respect fully mixing assumption. Actually, CFD the multi tank assures a restoration time that is almost equal to the one previewed by Matlab and Matlab energy consumptions

espectations are prudential. Then, the Matlab model is surely suitable for this kind of situation.

- The 3m high tank results in a global better performance in terms of storage efficiency and energy saving than the 6m high one.

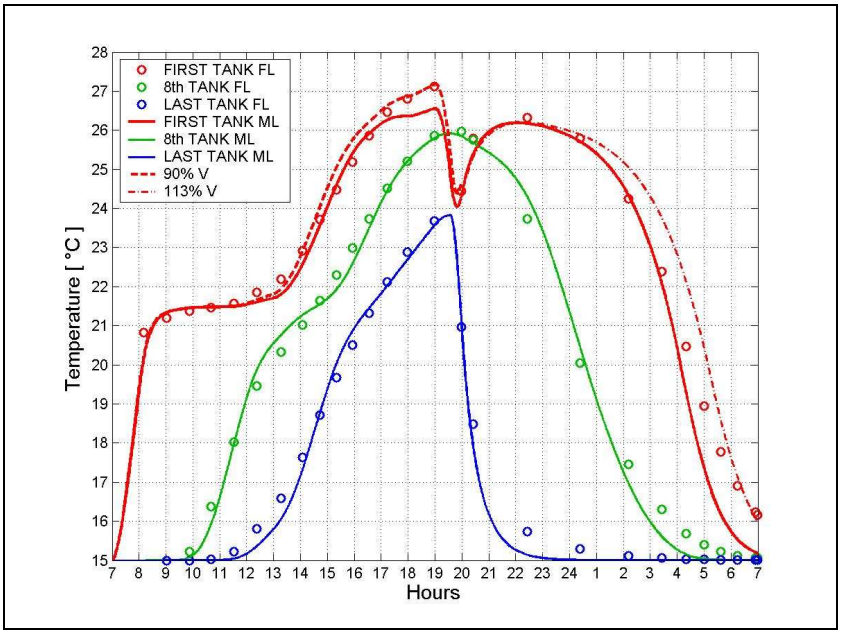

Figure 85 – Multi connected tank: 6m height, 15 sub-tank, oversized heat exchanger. Comparison between CFD results and one dimension Matlab model

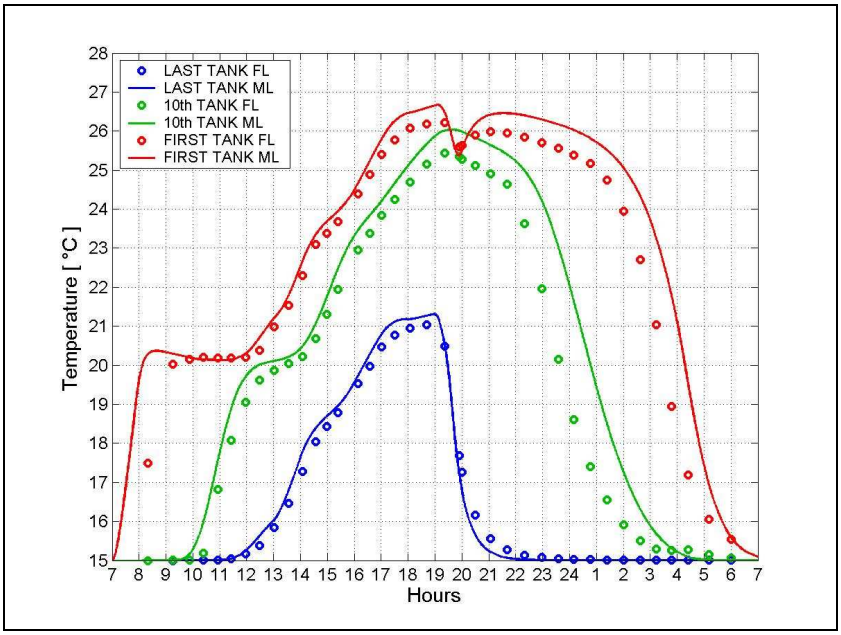

Figure 86 – Multi connected tank: 3m height, 20 sub-tank, design heat exchanger. Comparison between CFD results and one dimension Matlab model

Finally the simple tank configuration will be investigated for the two case studies proposed. Form Figure 87 to Figure 94, it is described the CFD analysis that has been carried out n order to investigate the two following tanks configurations along the critical summer day:

- Simple tank: 6m height, oversized heat exchanger by 30% with respect to design.
- Simple tank: 3m height, design heat exchanger.

CFD analysis gave similar results for the two hypothesis that are listed below:

- During operation phase the tank temperature fields is almost perfectly stratified (Figure 87 and Figure 91) , unless at he GW inlet section were a slight inertial and buoyant turbulence is caused by groundwater intake at 15°C within a heated mass water. (Figure 88 and Figure 92)
- During restoration phase a violent crash between fresh groundwater entering the tank and internal over-heated water occurs so that a buoyancy driven turbulence raids within the tank and remains by inertia almost all the process long (Figure 90 and Figure 94) Thus an almost fully mixing takes place during the shut-off period. Just at the end of the restoration phase, a cool layer of groundwater by-pass the above warmer mass of water causing a chocking of the heat exchange and strongly slowing the restoration process (Figure 89 and Figure 93).

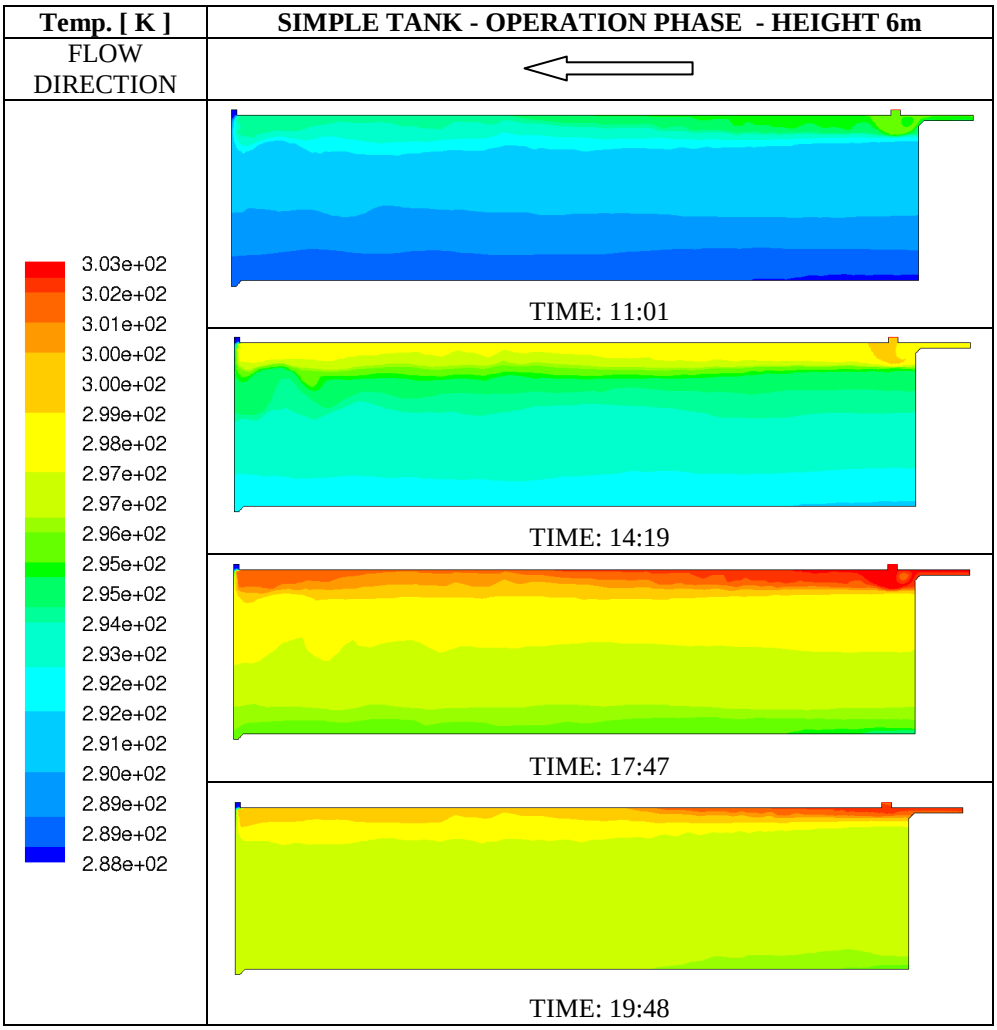

Figure 87 – CFD results describing the operation phase process within the tank for the simple-connected configuration 6m height in terms of temperature field.

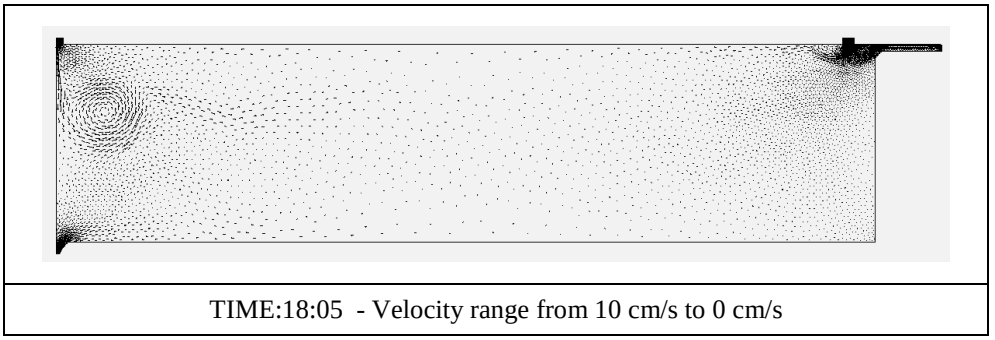

Figure 88 – CFD results describing the typical velocity field during the operation phase process within the simple tank.

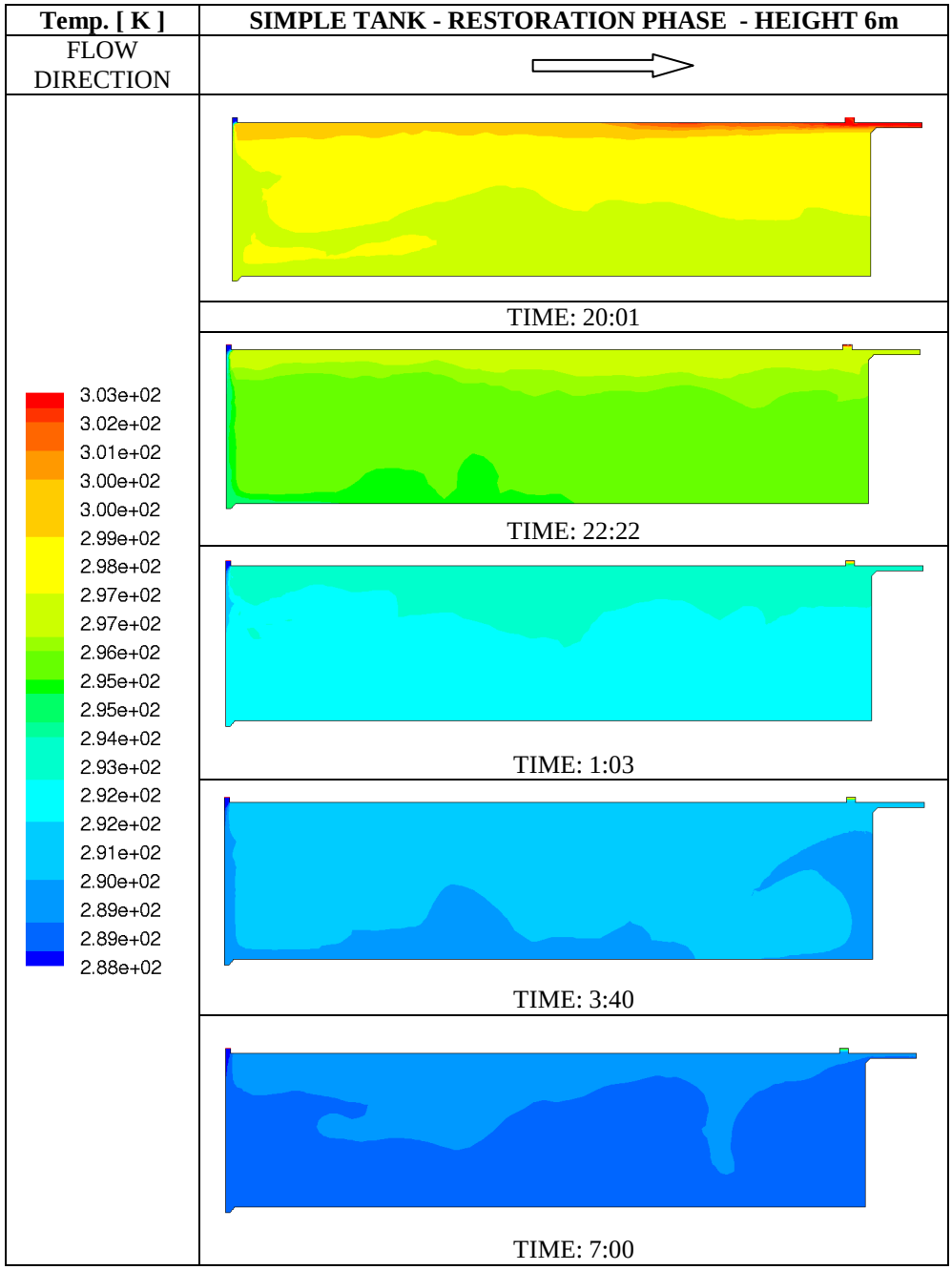

Figure 89 – CFD results describing the restoration phase process within the tank for the simple-connected configuration 6m height in terms of temperature field.

SIMPLE TANK - RESTORATION PHASE - HEIGHT 6m

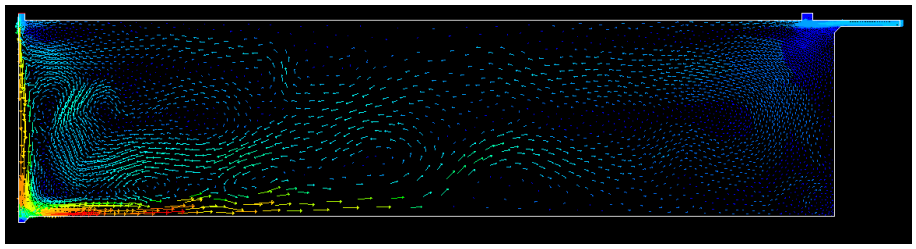

TIME: 20:05 - Velocity range from 10 cm/s to 0 cm/s

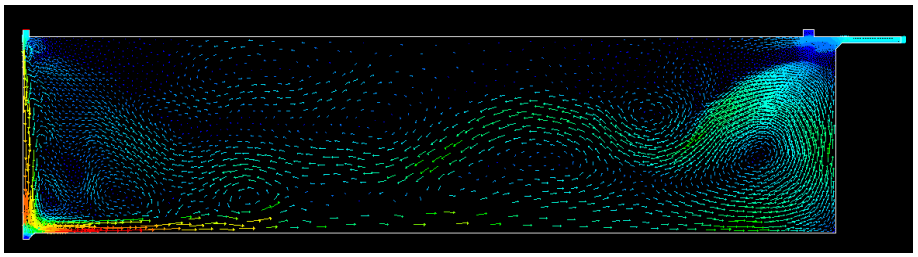

TIME: 23:58 - Velocity range from 15 cm/s to 0 cm/s

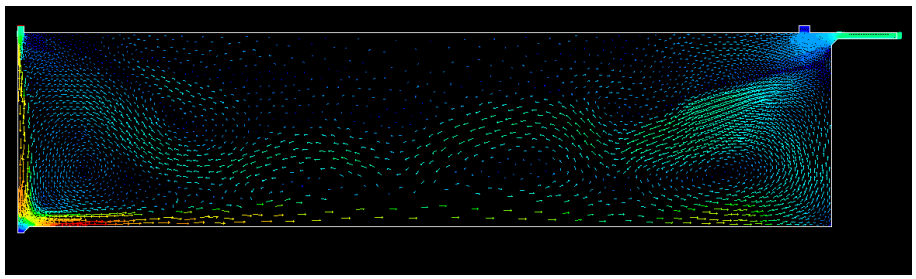

TIME: 4:11- Velocity range from 10 cm/s to 0 cm/s

Figure 90 – CFD results describing the velocity field during the restoration phase process within the simple tank.

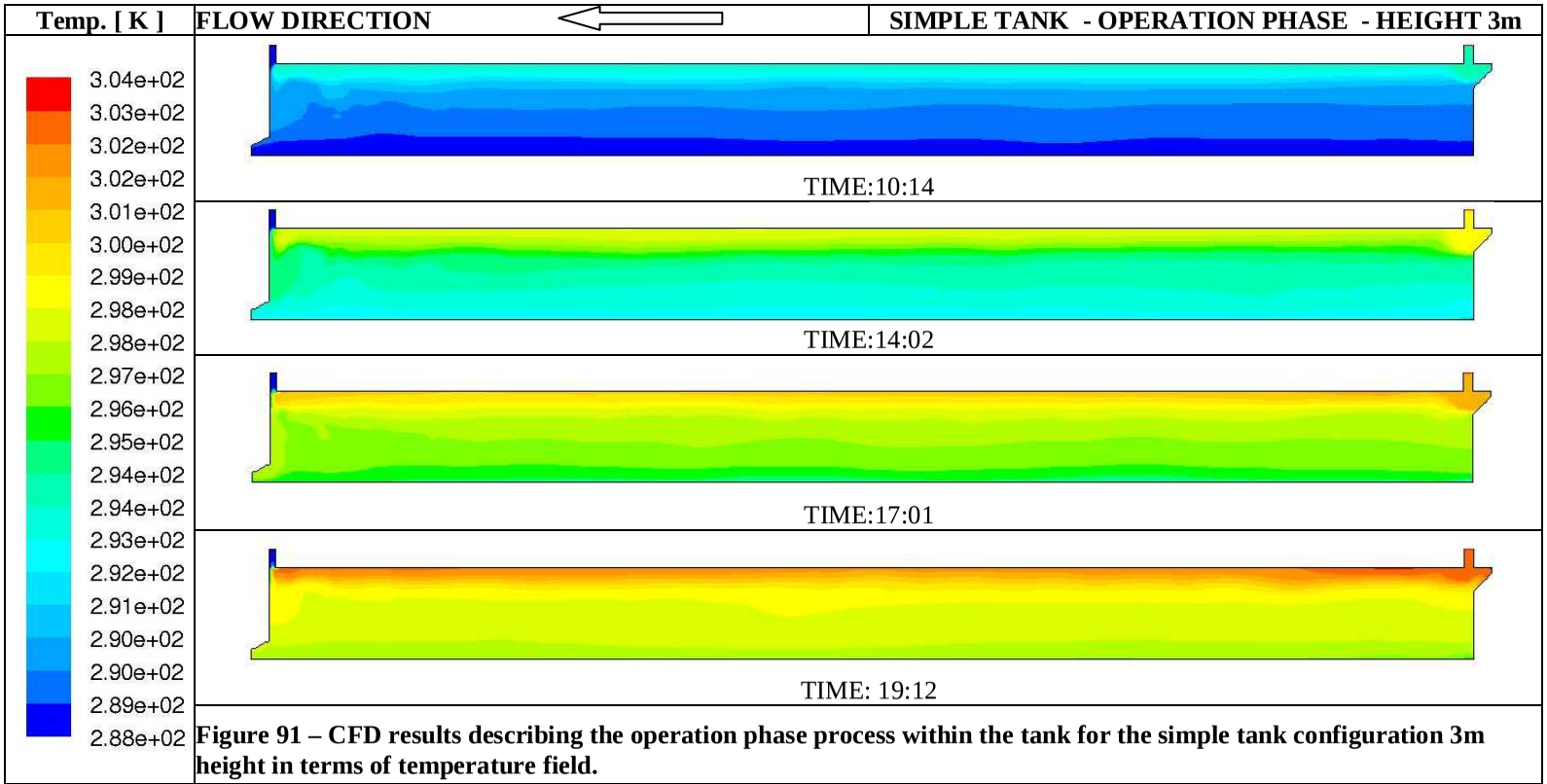

Figure 91 – CFD results describing the operation phase process within the tank for the simple tank configuration 3m height in terms of temperature field.

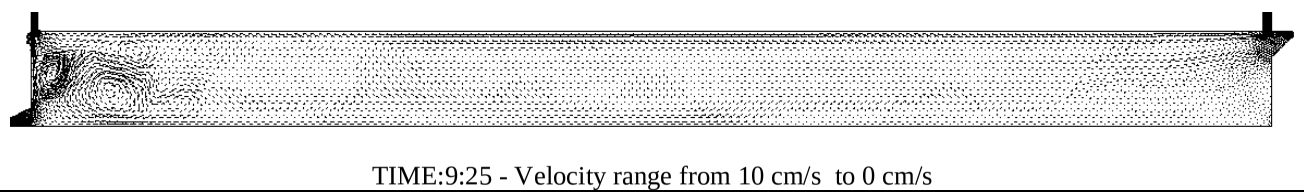

Figure 92 – CFD results describing the velocity field during the operation phase

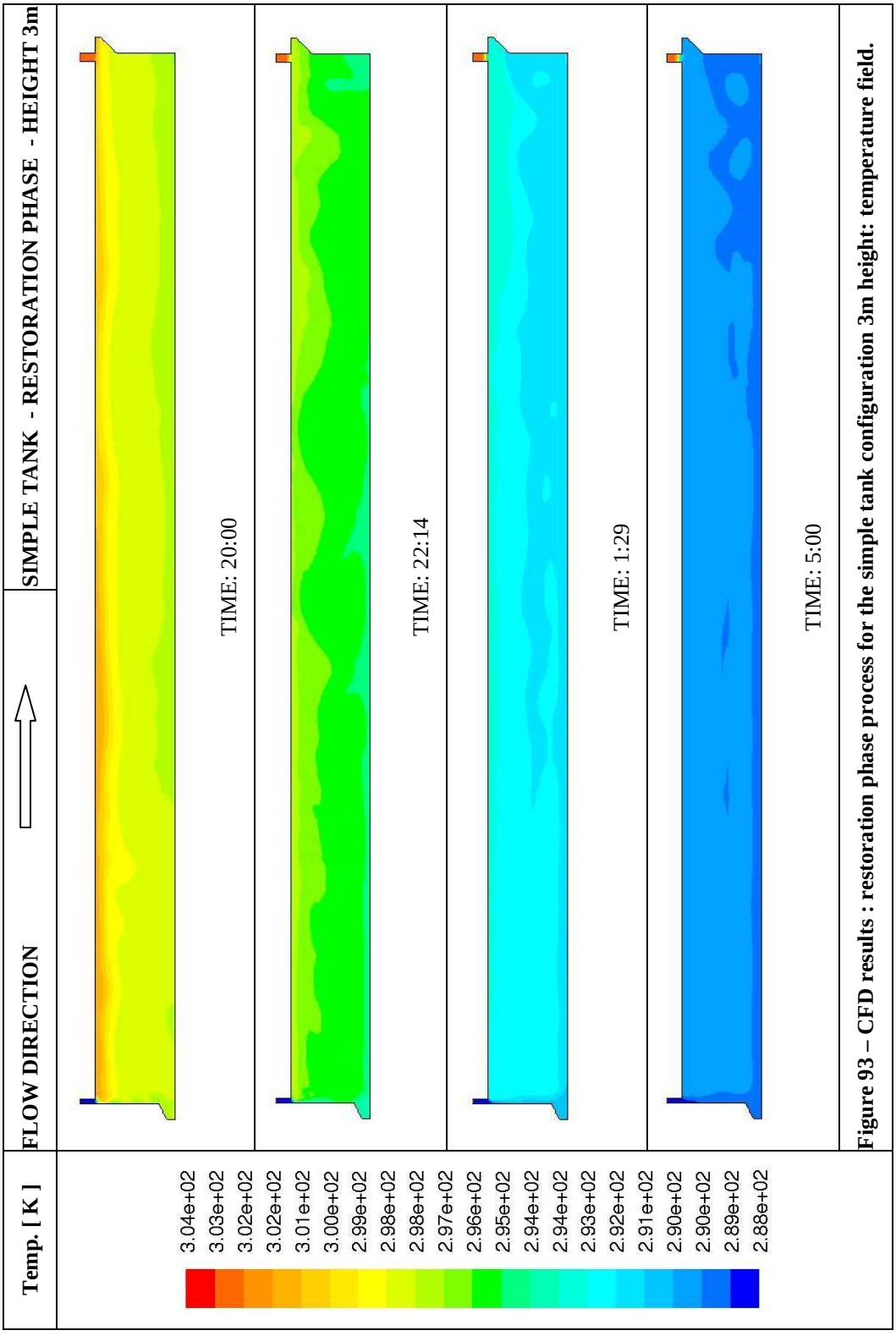

Figure 93 – CFD results : restoration phase process for the simple tank configuration 3m height: temperature field.

SIMPLE TANK - RESTORATION PHASE - HEIGHT 3m

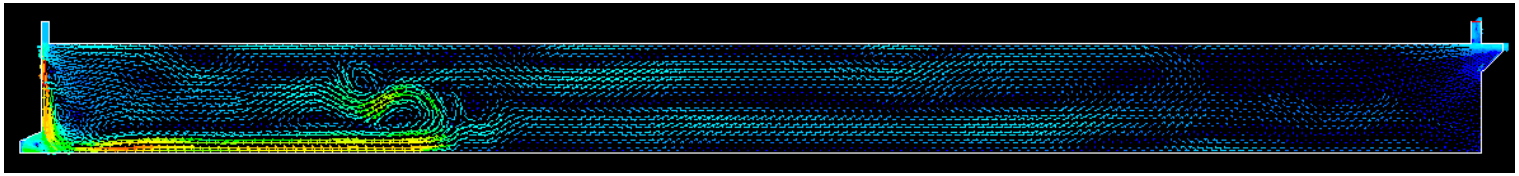

TIME: 20:00 - Velocity range from 9 cm/s to 0 cm/s

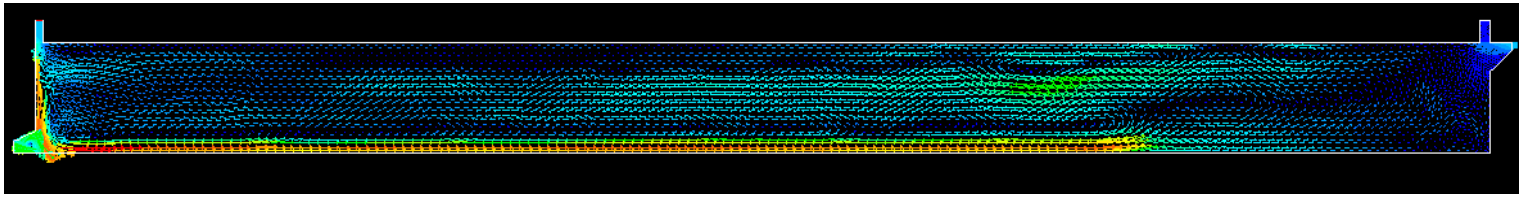

TIME: 20:18 - Velocity range from 10 cm/s to 0 cm/s

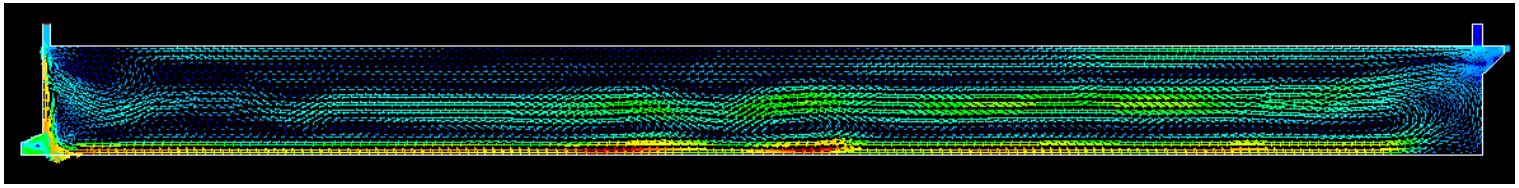

TIME: 21:26 - Velocity range from 10 cm/s to 0 cm/s

Figure 94 – CFD results describing the restoration phase process within the tank for the simple tank configuration 3m height in terms of velocity field.

In the following figures, it will be outlined the comparison between Matlab results an FLUENT simulations for the critical summer days in order to infer the simplified Matlab model reliability.
In Figure 95 and Figure 96, it is reported the comparison between the 6 m tank and the 3m tank CFD simulations and the related one dimensional simulation ran through Matlab.
It is possible to resume in the listed point the evidences from that comparison:

- 6m high simple tank and 3m high simple tank assures almost the same performance to the HVAC system all along the critical summer day
- Fully mixing assumption provide a poor preview of the tank behavior during the operation phase because of buoyancy predominance
- Fully mixing assumption is accurate for restoration phase as it is confirmed by CFD evidences (actually GW outlet temperature almost equals the average temperature).

Note that, during operation, CFD results denote a tank behavior that is similar to piston flow or tank partitioning due to stratification phenomenon.
Moreover, in **Errore. L'origine riferimento non è stata trovata.**, the 3m high tank presents an oscillating shape of delivery temperature to heat exchanger. That occurs because the shorter high with respect to the 6m high tank determines an influence of GW inlet turbulence at the delivery section. Such an oscillation the reflected to the heat exchanger behavior and could result in an undesired swinging response of the system.

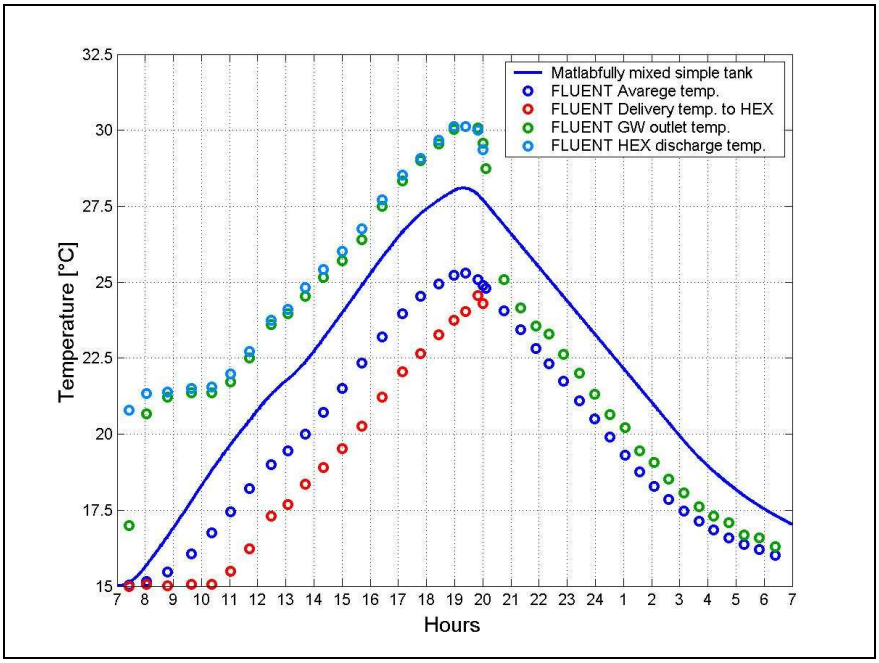

Figure 95 – Simple tank: 6m height, oversized heat exchanger. Comparison between CFD results and one dimension Matlab model

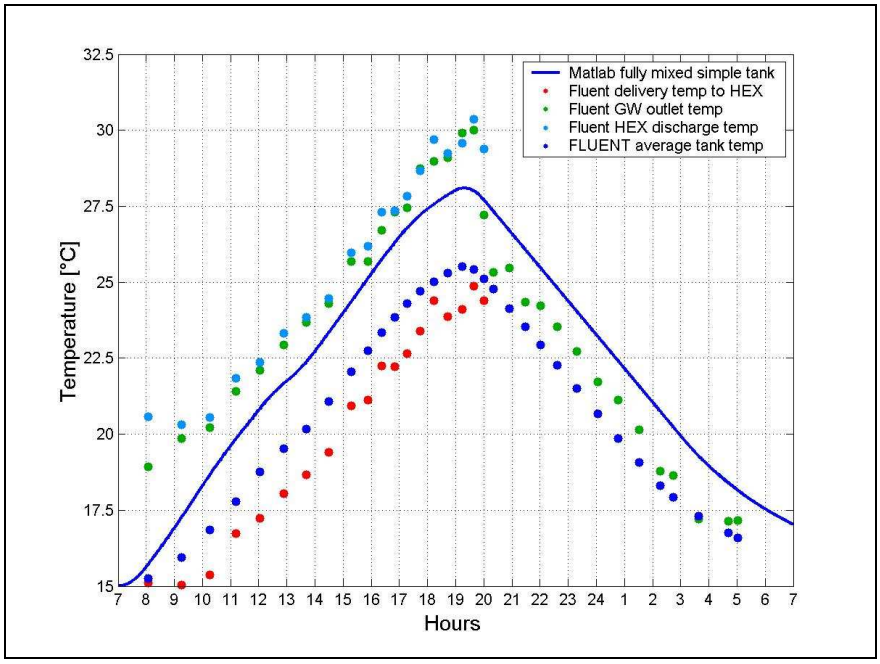

Figure 96 – Simple tank: 3m height, design heat exchanger. Comparison between CFD results and one dimension Matlab model

Finally a direct comparison between the simulated systems through CFD are compared in terms of average tank temperature along the critical summer day (Figure 97).

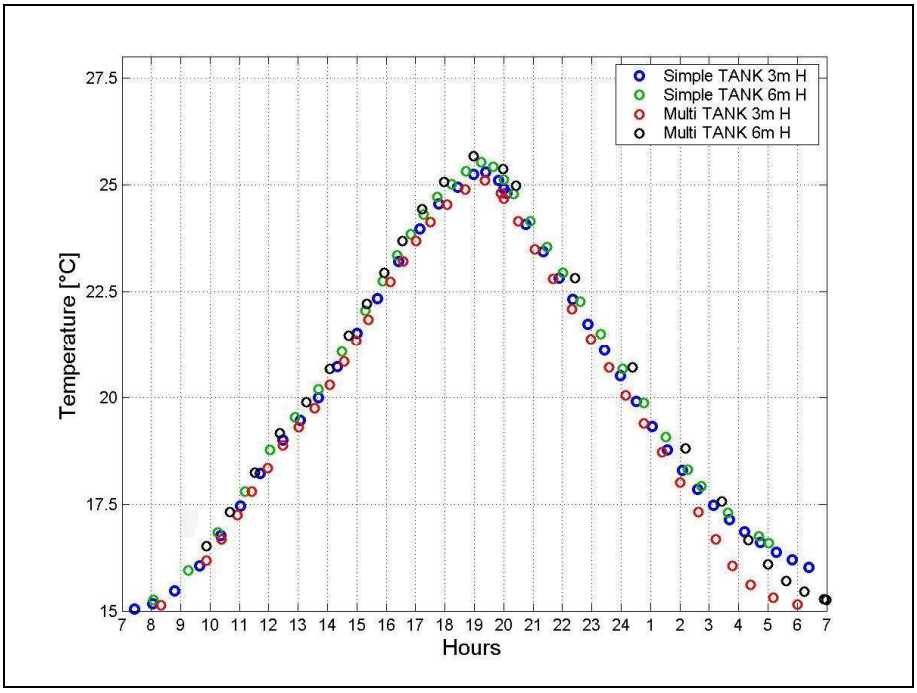

Figure 97 – Comparison between all CFD models investigated.

No significant differences are remarkable during the operation phase in terms of average tank temperature.
However, tank partitioning generally allows an important improvement in restoration time.
Aspect ratio and the ratio between connecting holes cross-section and tank height play an important role in multi-connected tanks performances. As a matter of fact, the 3m high tank and the 6m high tank occupy the best performance place and the worst one within the sample of cases investigated.
Tank height has a poor influence in tank performance in the simple tank configuration, whose performance is almost the same than multi-connected tank during operation but much more inefficient during restoration, especially at the end of the process.
Finally the CFD analysis confirm that tank partitioning is fundamental in order to assure the daily thermal storage strategy since the restoration efficiency is optimized.
However, further investigation is needed to infer a Matlab more reliable model for simple tank configuration

Conclusions

A numerical simulation has been carried out in order to model a groundwater thermal storage system for an office building conditioning service.
Heat storage is needed because of the limited availability of thermal source with respect to the real building demands all over the critical days in the winter as well as in the summer.
Unless a specific care is paid to the tank design, even if the global heat that the underground water basin could exchange is theoretically enough to fulfill the daily building necessity, thermal storage strategy could not be compliant because of the tank storage efficiency issues.
Complete mixing assumptions as well as perfect piston flow model have been stated in order to predict the tank storage efficiency.
Then tank partitioning has been taken into account with the aim of avoiding mixing diffusion across the tank.
Water tanks responses have been analytically investigated under a few regulation patterns for simple tanks as well as for multi-series-connected tanks under complete mixing hypothesis.
As a result, numerical approach is advisable in order to evaluate a thermal storage tank response connected to a real system.
A Matlab routine has then be developed to model a whole HVAC daily thermal storage system realized with variable refrigerant volumes reversible heat pumps which are supposed to be cooled by underground water.
A daily system operation phase has been separately examined with respect to the following temperature restoration phase.
The Matlab program can size required heat exchanger surfaces and the proper number of heat-pumps that are needed and can estimate their transient behavior in connection with a simple tank or multi-connected tank conditions under real climatic all over the year. Electric powers consumptions, actual heat fluxes exchanged with the tank and the underground basin, actual temperatures and flow rates at heat exchanger connections as well as within the tank are also monitored to figure out the problem with a detailed approach.
The winter and the summer critical behaviors have been investigated for a specific building and a particular tank volume. Tank partitioning ,at constant tank volume, has been argued to be outstandingly important for every critical situation.
In the summer, thermal storage strategy could be successfully executed under acceptable tank overheating, thanks to a remarkable restoration time reduction.
In the winter, the risk that the lowest heat pumps evaporation temperature is reached could be avoided, thanks to a proper time shift of temperature signal.

An advisable number of sub-tanks should be chosen in the range from 15 to 20 in order to comply with storage efficiency improvement and construction bounds.
Therefore, Matlab routine has been validated by a theoretical application to one of most significant experiments that Nakahara [4] developed in order to infer empirical results about thermal water storage for cooling purposes.
An annual simulation has been executed in order to infer compressors electrical energy saving due to tank partitioning under fully mixing assumption. A relevant saving has been inferred, however it should be confirmed by a more detailed study according to the CFD analysis results.
A quick design tool for multi-connected tanks, which takes into account storage efficiencies concerns, has been produced in order to get a fast verification of feasibility of a given heat rejection water thermal system for HVAC purposes under specified climatic and boundary conditions.
Moreover, an exergy analysis has been applied to the HVAC groundwater thermal system during the critical summer day. Exergy could be a powerful instrument for efficiency losses detection and systems improvement oriented to energy saving.
Exergy destruction rates have been calculated for either mixing than heat exchanging significant position in order to detect mutually influences between the system energy consumption and the tank storage efficiency.
A remarkable importance has been detected again in tank partitioning and a further treatment has been carried out with the aim of improving the whole system performances through a proper heat exchanger surface size as well as considering a more complex control management system.
Important exergy saving could be obtained by heat exchanger over-sizing.
All control systems oriented to keep the return to underground basin below the limit value by 20°C imply an exergy wastage that could not be avoided as long as thermal storage philosophy is mantained.
Finally, a 2D CFD simulation has been developed within FLUENT, in order to evaluate complete mixing assumption reliability and Matlab results consistency with fluid dynamics bi -dimensional concerns as buoyancy effects.
Matlab routines have been translated into C languages. So a specific group of user defined functions have been written in order to model proper boundary conditions and system parameters updating into a FLUENT unsteady model of the tank.
Four different simulations have been carried out for a specific volume of a tank in the summer critical day. Moreover, multi-connected pattern has been compared to a simple tank response.
Short-circuits are promoted within the multi-connected tank because of inertial and buoyancy phenomena. In the simple tank fully mixing does not occur during operation due to stratification effects. Actually, critical fluid dynamics have been detected has flow reverses within the simple tank passing from the operation phase to the restoration one, so that complete mixing is finally reached. At the end of the restoration phase in simple tank configuration, a by-pass cool layer of fluid is engendered at the bottom of the tank that chocks thermal exchange with the underground basin and strongly slows the restoration process.
Finally geometrical tank features, as aspect ratio and ratio between the connecting holes height and the tank height, are important on multi-connected tank performances.
On the other hand tank height plays a poor role in simple tank configuration, unless a probable concern regarding an induced oscillating effect on operation of HVAC system regulation equipments.
Tank partitioning implies a better heat exchange between the tank and the underground basin during the restoration phase so that it is fundamental in order to execute a successfully daily water thermal storage strategy. Although, no significant differences are outlined by CFD analysis during the operation phase between tank partitioning and simple tank.

Matlab predictions are acceptable for low multi-connected tanks but a threshold of aspect ratio exists over which the fully-mixing assumption does not return a reliable prediction.
Stratification occurs in the simple tank configuration during the operation phase, so a more accurate one-dimensional model should be developed within Matlab in order to better predict the simple tank response to operating HVAC systems under the usual geometrical configuration of storage tanks in building design and construction.
Indeed, further investigation is needed in order to detect a more detailed range of reliability of complete mixing assumption as well as multi-connecting suitability all over the allowable geometry shapes, crossing flow rates values and volumes capacities.

References

1. M.Yanagimachi, Heat storage system in Japan, Pt.1-Pt.2., *Special Bulletin International Day Program, ASHRAE Semiannua Meeting*, Atlantic City, NJ.JAN.26-30, 199, pp. 27-33,1975.

2. Y. Nakajima, Studies on thermal weighting of thermal storage tank, Pt.1-Pt.2., *Transactions of AIJ*, No. 199, pp. 37-47, No. 200, pp. 75-83, 1972.

3. H. Matsudaira and Y. Takana , Dynamic characteristics on a heat storage water tank Pt.1-Pt.2., *ASHRAE Transactions*, Vol. 85, Pt.1, 1979.

4. N. Nakahara, Water thermal storage tank, Pt.1-Pt.2-Pt.3, ASHRAE Transactions, Vol. 94, Pt.2, No. 3167, No. 3168, No.3169,1988

5. M. Yamaha, T.Ibamoto, Applications and technologies of cool storage in Japan

6. YH.H.Yau, B. Rismanchi, A review on cool thermal storage technologies and operating strategies, *Renewable and Sustainable Energy Reviews*, 16(2012) 787-797

7. I.Dincer, A.Rosen, Energetic, environmental, and economic aspects of thermal energy storage systems for cooling capacity, *Applied Thermal Engineering*, 21 (2001) 1105-1117

8. S.M. Hasnain, Review on sustainable thermal energy storage technologies, PART II: Cool thermal storage, *Energy Conversion Management*, Vol. 39, No 11, pp. 1139-1153, 1998

9. I.Dincer, On thermal energy storage systems and applications in buildings, *Energy and Building*, 34 (2002) 377-388

10. S. Shin, H. Kim, D. Jang, S. Lee, Y. Lee, H. Yoon, Numerical and experimental study on the design of stratified thermal storage system, *Applied Thermal Engineering*, 24(2004) 17-27.

11. J.D. Chung, Y. Shin, Integral approximate solution for the charging process in stratified thermal storage tanks, *Solar Energy*, 85 (2011) 3010-3016

12. W.P.Bahnfieth, A.Musser, Thermal performance of full-scale stratified chilled-eater thermal storage tank, *Ahrrae Transaction Vol 104, Pt.2 1998*

13. Y.Yu, K. Sagara, T. Yamanaka, H. Kotani, Y. Momoi, T. Kobayashi, T. Iwata, H. Kitora, Y. Taguchi, CFD Analysis on thermal storage performance of temperature–stratified water TES tank with new type diffuser, *9th International Conference on Sustainability Energy Technologies*, Shangai, China 24-27 August 2010

14. J.E.B. Nelson, A.R. Balakrishnan, S. Srinivasa Murthy, Experiments on stratified chilled-water tanks, *International journal of refrigeration*, 22 (1999) 216-234

15. S.Shin, H.Kim, D.Jang, S. Lee, Y. Lee, A numerical and experimental study on the mixing characteristics of stratified thermal storage, *Environ. Eng. Res.* Vol. 8, No 1, pp. 41-47, 2003, Korean Society of Environmental Engineers

16. H. Kitano, T. Iwata, K. Sagara, Study on modified model of temperature-stratified thermal storage tank under variable input condition

17. H. Kitano, T. Iwata, S.Ichinose, K. Sagara, Y. Ishikawa, Effect of connecting hole arrangement on mixing behavior in thermal Energy storage tank of multi-connected mixing type

18. N. Nakahara, The method of increasing efficiency in actual thermal storage operation., Journal of SHASE, vol. 50, No. 9, pp. 33-44, 1976.

19. M.Perrotta, Gestione ed ottimizzazione di vasche di accumulo termico per impianti di climatizzazione., *ATI Conference*, 2010.

20. A. Saito, Recent advances in research on cold thermal energy storage, *Internaltional journal of refrigeration*, 25 (2002)177-189

21. A.Mawire, M. McPherson, Experimental characterization of thermal energy storage system using temperature and power controlled charging, Renewable *Energy*, 33 (2008) 682-693

22. Y.P. Zhou. J.Y. Wu, R.Z. Wang, S. Shiochi, Y.M. Li, Simulation and experimental validation of the variable-refrigerant-volume (VRV) air-conditioning system in EnergyPlus, *Energy and buildings*, 40 (2008) 1041-1047

23. C.M. Tarawneh, K.O. Homan, Measurments of dendity profile evolution during stably-stratified filling of an open enclosure, *Heat and fluid flow*, 29 (2008) 1113 – 1124

24. L. Xinguo, Thermal performance and energy saving effect of water-loop heat pump systems with geothermal, *Energy Consversion Management*, Vol. 39,No. ¾, pp. 295-301, 1998

25. S. Kavanaugh, Ground-Coupling with water source heat-pumps

26. L.D. Cane, S.B. Clemes, A. Morrison, P.J. Hughes, Heat exchanger sizing for vertical closed-loop ground-source heat pumps

27. S. Pan, M. Zheng, N. Nakahara, Study on fault detection and diagnosis of water thermal storage HVAC systems,

28. N. Nakahara, S. Pan, M. Zheng, Y. Nishitani, Load prediction for optimal thermal storage – comparison of three kinds of model application

29. I.R. Otte, Integration of long and short term thermal storage